INDEX

Editorial

Dear reader:

"Change is the only constant thing", and Volume 32 of La Granja, Revista de Ciencias de la Vida, is an example of this change. This is our first special issue which addresses the problems of CO_2. At the same time, the Salesian Polytechnic University has changed its authorities after 11 years under the successful direction of Dr. Javier Herrán sdb., and now Dr. Juan Cárdenas Tapia sdb is the new Rector. This change not only guarantees continuity in the scientific quality of the University's publications, but also maintains the solidarity vision of the Salesian charisma.

On the other hand, it is known that many things will be different due to the global pandemic. In the face of the current uncertainty, spaces arise for reflection and creativity that can create new lifestyles and new opportunities. We have also been able to uncover limitations and the need to reaffirm the importance of research from universities as a transformative entity of society.

This special edition of La Granja, entitled "Carbon Frontiers: Valorization and Strategies for CO_2 Mitigation", aims to show the efforts made by various scientists from different agencies and research centers around the world in the fight to reduce CO_2 emissions, which is the most important greenhouse gas of anthropogenic origin produced mainly by the direct and indirect use of fossil fuels. In this sense, this special volume aims to highlight the different scientific contributions aimed at reducing and mitigating the consequences of greenhouse gas emission from various perspectives. From a broad point of view, this special edition envisages interdisciplinary and complementary points of view in addressing this problem, with multiple and diverse approaches aimed at contributing to the achievement of the Sustainable Development Goals (SDGs) of the United Nations Organizations (ONU)

This special edition is the first of its kind in the journal and has been an interesting challenge to visualize the various authors in other latitudes, as well as the journal itself, whose objective is to present novel research papers in multidisciplinary fields associated with the life sciences, with an emphasis on the efforts related to the mitigation of climate change. From Pakistan, Drs. Mehmood Ali and Saqib Jamshed Rind, both from the University of Engineering and Technology (Karachi-Pakistan), show how the use of bio-diesel blend derived from *Jatropha curcas* and Neem (*Azadirachta indica*), can contribute to an increase in combustion efficiency, decreasing CO emissions compared to mineral-based diesel, despite having slightly lower power-related results.

On the other hand, Dr. Leticia Citlaly López-Teloxa along with Dr. Alejandro Monterroso, from the Autonomous University of Chapingo, Mexico, show the impact of soil respiration and its contribution on CO_2 emissions into the atmosphere, as well as its evolution with regard to the change in land use. These researchers highlight the need to account for and show the negative impact on the delicate balance of soil respiration and its effect on the emission of large amounts of CO_2 into the atmosphere.

Likewise, Dr. Bence Mátyás from Dama Research Center in Hong Kong, along with colleagues from Hungary, India and Ecuador discuss the effect of the use of bio-fertilizers on the soil respiration process and its impact on CO_2 emissions. The results found by the team show that the use of bio-fertilizers is able to reduce carbon dioxide emissions compared to those produced in soils fertilized with commercial fertilizers.

Dr. Lucía Yánez-Iñiguez from University of Cuenca (Ecuador) and Dr. Esteban Zalamea-León and Dr. Antonio Barragán-Escandón, all from the same university, discuss the energy potential of urban forest waste as a potential route for electricity generation. The data estimated by the group indicate that this waste has the potential to generate approximately 476 MWh/year of electricity. This analysis is a small example of Ecuador's potential to leverage waste from an activity to be used as fuel for electricity generation, having an effect on the reduction of greenhouse gases resulting from the use of fossil fuels.

Finally, in this special issue, an analysis of the potential of the green roofs directed by Nelson López Machado and his team is presented, in an international research between Catholic University of Chile, Catholic University of Temuco, Universidad Central Lisandro Alvarado of Venezuela and the Polytechnic Salesian University of Ecuador.

The miscellaneous section presents a study of the impact of landfills conducted by Areli Machorro-Román and the research team from Universidad Popular Autónoma del Puebla, Autonomous University del Carmen and the National Polytechnic Institute. Likewise, Ketty Meza and the research team from Technical University of Manabí, Ecuador, present a study of plant pathologies on pitahaya.

Addressing novel techniques for the analysis of dermatophytosis in guinea pigs, Renzo Venturo and Siever Morales-Cautí, present their study from Scientific University of the South, Peru. Finally, Santiago Guerrero from Universidad Tecnológica Equinoccial del Ecuador, shows a vision from the academy of the COVID-19 pandemic faced globally.

The editorial board of the journal and the directives of Salesian Polytechnic University would like to thank all the authors who have participated in making this special edition possible, and by having contributed to the development of knowledge that allows the advancement and evolution towards sustainable societies in the near future. During this time of the global coronavirus pandemic, the editors reaffirm the need to reflect on this event and to seize this opportunity to further investigate in areas still little explored, to improve people's living conditions in global trends such as those included in this issue.

Sincerely,

Dr. Sabino Armenise
Universidad Rey Juan Carlos
Guest Editor

Dr. Fernando Bimbela
Universidad Pública de Navarra
Guest Editor

Dr. Ignacio de los Ríos Carmedano
Universidad Politécnica de Madrid
Editor in Chief

MsC. Sheila Serrano Vincenti
Universidad Politécnica Salesiana
Editor in Chief

Comparison of effects exerted by bio-fertilizers, NPK fertilizers, and cultivation methods on soil respiration in Chernozem soil

Comparación de los efectos ejercidos por los biofertilizantes, fertilizantes NPK y los métodos de cultivo sobre la respiración del suelo en el suelo de Chernozem

Bence Mátyás[1] , Daniel A. Lowy[1,2], Ankit Singla[3], Jesus R. Melendez[4]
and Zsolt Sándor[5]

[1] *Dama Research Center limited, 87-105 Chatham road South, Tsim Sha Tsui Kowloon, Hong Kong.*
[2] *VALOR HUNGARIAE, Ltd., 4 Nagysándor József Street, H-1054, Budapest, Hungary.*
[3] *Regional Centre of Organic Farming Department of Agriculture, Cooperation and Farmers Welfare, Ministry of Agriculture & Farmers Welfare, Government of India, Bhubaneswar, Odisha, India.*
[4] *Facultad Educación Técnica para el Desarrollo, Universidad Católica de Santiago de Guayaquil, Ecuador.*
[5] *Institute of Agrochemistry and Soil Science, University of Debrecen, Egyetem tér 1, 4032 Hungría, Debrecen, Hungary.*

*Corresponding author: bmatyas@edu.damaresearch.com

Abstract

Soil respiration is a significant indicator of soil microbial activity; global soil respiration and decomposition processes release yearly to the atmosphere a total of 220 billion tons of carbon dioxide. Therefore, studies on the whole- or one particular aspect of soil carbon cycle aiming at optimizing agricultural carbon dioxide emissions or improving carbon sequestration contribute to a sustainable agriculture practice. In this paper we present the effects of biofertilizer application (*Bacillus megaterium*, *Bacillus circulans*, and *Pseudomonas putida*) on soil respiration in chernozem soil. Experiments were performed at Látókép Experimental Station, belonging to the University of Debrecen, Hungary. Additionally, we compare our results with findings of prior studies related to commercial NPK fertilizer applications (in four doses: $N_{60}P_{45}K_{45}$; $N_{120}P_{90}K_{90}$; $N_{180}P_{135}K_{135}$; and $N_{240}P_{180}K_{180}$), and two different cultivation methods (ploughed, loosened, RTK in rows, and RTK between rows); these investigations were conducted at the same experimental station. Our results indicate lower tendency for soil respiration, when biofertilizers are applied as compared to commercial NPK fertilizers, which enables to decrease CO_2 emission in the environment. We also discuss a unit change in different alkali absorption-based methods (Oxitop and Witkamp) to facilitate comparability of recently acquired data with results of previous long-term fertilization experiments.

Keywords: Soil respiration, CO_2, biofertilizer, fertilizer, chernozem soil, soil respiration, Hungary, Ecuador.

Resumen

La respiración del suelo es un indicador importante de la actividad microbiana; los procesos de respiración y descomposición del suelo a nivel mundial liberan anualmente a la atmósfera un total de 220 mil millones de toneladas de dióxido de carbono. Por lo tanto, los estudios sobre los aspectos del ciclo del carbono del suelo para optimizar las emisiones de dióxido de carbono agrícola o mejorar el secuestro de carbono contribuyen una práctica agrícola sostenible. En este artículo se presentan los efectos de la aplicación de biofertilizantes (*Bacillus megaterium, Bacillus circulans,* y *Pseudomonas putida*) en la respiración del suelo, en el suelo chernozem. Los experimentos se realizaron en la Estación Experimental de Látókép, perteneciente a la Universidad de Debrecen, Hungría. Además, estos resultados se compararon con los hallazgos de estudios anteriores relacionados con aplicaciones comerciales de fertilizantes NPK (en cuatro dosis: $N_{60}P_{45}K_{45}$; $N_{120}P_{90}K_{90}$; $N_{180}P_{135}K_{135}$; y $N_{240}P_{180}K_{180}$), y dos métodos de cultivo (arado, aflojado, RTK en filas y RTK entre filas); estas investigaciones se llevaron a cabo en la misma estación experimental. Los resultados indican una menor tendencia a la respiración del suelo cuando se aplican biofertilizantes en comparación con los fertilizantes NPK comerciales, lo que permite disminuir la emisión de CO_2 en el medio ambiente. También se discutió un cambio unitario en los diferentes métodos basados en la absorción de álcalis (Oxitop y Witkamp) para facilitar la comparación de los datos adquiridos recientemente con los resultados anteriores de experimentos de fertilización a largo plazo.

Palabras clave: respiración del suelo, CO_2, biofertlizantes, fertilizantes, suelo chernozem, respiración del suelo, Hungría, Ecuador.

Orcid IDs:

Bence Mátyás: http://orcid.org/0000-0003-2694-1848

Daniel A. Lowy: http://orcid.org/0000-0003-2210-6757

Ankit Singla: http://orcid.org/0000-0002-0400-2885

Jesus R. Melendez: http://orcid.org/0000-0001-8936-5513

Zsolt Sándor: http://orcid.org/0000-0002-6969-5192

1 Introduction

Increase in CO_2 emissions is a contributor to global climate change (Gratani et al., 2016; Ashok et al., 2019). Unfortunately, carbon dioxide levels exceed the Earth's response rate to assimilate and process the emission within the carbon cycle (Lajtha et al., 2017). Metropolitan century has arrived in which a broad suite of sustainability challenges has to be addressed in both urban (Elmqvist et al., 2019) and rural areas (Lowy and Mátyás, 2020). If considering that over 50 % of the world's population is concentrated in urban areas, and it is expected that by year 2050 over two thirds will live in cities, the problem of mitigating the concentration of atmospheric CO_2 is considerable (Gratani et al., 2016). Furthermore, to satisfy increasing food needs of people living in urban areas, agriculture must become increasingly productive. Evaluated carbon emissions in all stages of the world's food system was firmly carried out by Vermeulen et al. (2012). Authors reported that food system (from fertilizer application and cultivation to food storage and packaging) is responsible for up to one-third of anthropogenic greenhouse gas emission (Thornton, 2012). Therefore, it is a proposed viable alternative and strategy based on absorbent materials from biomass (Moral et al., 2018) and sustainable agricultural solutions.

The global atmospheric concentration of carbon dioxide (CO_2), ranging from 278 to 391 ppm, nitrous oxide (N_2O), from 2.5 to 1803 ppb, methane (CH_4), from 270 to 342 ppb (Team et al., 2014) and fluorinated gases have shown continuous increase since pre-industrial times and have contributed significantly to global warming, as stated in 2007 by the Intergovernmental Panel on Climate Change (IPCC). Unfortunately, atmospheric greenhouse gas (GHG) concentrations continue to rise, and out of GHGs, CO_2 concentration is increasing at fast pace. For maintaining global warming below $2°C$ relative to pre-industrial levels, by 2050 the global anthropogenic GHG emissions should reduce by 40 %, relative to 2010. Also, it is envisaged the increase of existing biological carbon pools for carbon sequestration (Team et al., 2014).

Global trends allow the implementation of alternatives to mitigate CO_2 production and enable the conversion of algae biomass into biofuels and the use of biofuels for replacing fossil fuels (Eloka-Eboka and Inambao, 2017). Sequestration of CO_2 was evaluated in the context of fertilizers, the loading of $NaCl$ and $NaOH$, the intensity of light and its effects on algae-biomass growth, lipid productivity and CO_2 sequestration by Kumar et al. (2018). Agriculture contributes to three primary GHG emissions: CO_2, CH_4, and N_2O. Relevant to this topic is that soil can be regarded as a sink for CO_2 via carbon sequestration and its conversion into biomass products and soil organic matter (Johnson et al., 2007; Fekete et al., 2014). For example, a change from the use of conventional tillage practices to less intensive ones (e.g., no-tillage) has been proposed to mitigate CO_2 emission from agricultural soils. In Mediterranean areas, it is observed an increased carbon pool in the soil, when reducing or eliminating tillage (Álvaro Fuentes and Cantero Martínez, 2010). Xiao et al. (2020) reported results on addition of N-increased soil respiration (RS) by 7,1 % ($P < 0,05$) in all biomes. Positive SR response in farmland (27,0 %, $P < 0,05$) was significantly greater than in grassland and forest biomes, indicating that SR in anthropogenic ecosystems could be more sensitive to nitrogen enrichment. Nevertheless, it is still unclear, whether there is a similar pattern in SR response and of its components to the deposition of N in grasslands with a state of variable degradation (Zeng et al., 2018).

Recent experiments conducted with carbonate compounds in synthetic calcareous soil treated with biomass ashes, originating from a gasification power plant, showed that 16.5 g of CO_2 per kg of biomass ash were fixed. Without plant cultivation 19.7 g of CO_2 per kg of bottom biomass were fixed (López et al., 2018). This organic carbon fixation shows significant promise for carbon sequestration. Another important issue in soil carbon cycle is the extent of soil respiration (Kotroczó et al., 2018; Fekete et al., 2011), which is a reliable indicator of microbial activity proceeding in soil. Soil, plant, and animal respiration and decomposition with 28,56 % of CO_2 natural emissions are the second source of CO_2 after ocean atmospheric exchange. Both processes (respiration and decomposition) release carbon dioxide as a byproduct, equal to 220 billion tons of CO_2 freed by soil organisms over one year (Denman et al., 2007). Soil respiration processes typically take place in plant roots, bacteria, fungi, and soil animals to produce the energy needed for their survival. Also considered as soil respiration is the one going on

below-ground, decomposing buried organic matter (like roots, leaves, and animals). Carbon dioxide is released in both processes (Denman et al., 2007).

The increase in atmospheric nitrogen deposition (N) should also be considered, which impacts carbon (C) and the nutrient cycle in forest ecosystems. Findings by Peng et al. (2020) indicate that high N input increased the C content in the soil surface by reducing soil respiration. This occurred mainly by an improved stabilizing of soil organic matter, rather than reducing the microbial biomass of the soil.

Research conducted by Chen et al. (2020) established that extracellular enzymes involved in the C, N, and P cycle did not respond to the addition of N. Concentrations of extractable Ca^{2+} from the soil were reduced by adding N, while other extractable cations (Fe^{3+}, Al^{3+}, Mg^{2+}, K^+, and Na^+) were unaffected. Carbon contained by microbial biomass and the total abundance of microbes, bacteria, and fungi (phospholipid fatty acid and PLFA) was reduced by nitrogen addition, but the extracellular enzymes involved in the C, N, and P cycle did not respond to nitrogen addition. In forests, the buildup of microbial waste and its relationship with the accumulation of organic carbon in the soil has been affected by the addition of N and P, over a monitoring time frame of seven years. It produced changes in both the structure of the microbial community and the enzymatic activity induced by the deposition of N and P. All these can alter the accumulation and composition of microbial residues in tropical forests rich in nitrogen. The fungal ratio also underwent changes: bacteria population increased by the addition of P, or N and P, while the proportion of fungal residues, including bacterial residues, decreased upon adding of phosphorus. The latter may be related to an imbalance in the decomposition process of microbial waste.

Li et al. (2020) found that the stocks of C and N were related to the depth of the soil, duration of conversion and the precipitation, while the response of P was insensitive to these factors. Evidence was also provided that C, N, and P losses were correlated with physicochemical properties of the soil (pH, sand, silt, and clay). Changes in response ratios of C/N, C/P, and N/P indicated that soil C and N were more sensitive to grassland conversion, than phosphorus was.

Vast scientific research focuses on GHG emissions, based on evaluating different factors, such as soil types, cropping, irrigation, and fertilizer management (Glatzel et al., 2004; Kong et al., 2013; Singla et al., 2014; Singla and Inubushi, 2014). Different land uses impact significantly the production and consumption of GHGs (Baldock et al., 2012), including soil temperature (Rustad et al., 2001), soil moisture (Inubushi et al., 2005), aboveground plant biomass, and soil microbial biomass, SMB (Inubushi et al., 2005) and soil total carbon/nitrogen (C/N) ratio (Xu et al., 2008). Temperature changes may increase the decomposition rate of soil organic carbon, SOC (Powlson, 2005; Iqbal et al., 2010). Soil organic carbon returns to the atmosphere as CO2 via respiration, while soil organisms use organic materials as a source of energy and nutrients (Baldock et al., 2012). SMB encompassing microbial biomass carbon (MBC) and nitrogen (MBN) can serve as an early indicator of changes in soil properties (Glatzel et al., 2004). Given that soil respiration is important parameter of soil microbial activity, it can serve as an essential component of sustainable agriculture.

Aims of sustainable agriculture are to secure humankind's present food and textile needs, without compromising the resources of future generations. Involved in sustainable agriculture are: farmers, food processors, distributors, retailers, consumers, and waste managers. In addition, research scientists working in sustainable agriculture are guided by interdisciplinary approach. They combine a blend of disciplines, encompassing biology, chemistry, engineering, economics, and community development. They rely on project management and corporate social responsibility (Melendez et al., 2018a,b; Melendez and Gracia, 2019). All these groups seek to integrate three main objectives into their work: (i) a healthy environment, (ii) economic profitability, as well as (iii) social justice and fair trade (Francis and Porter, 2011).

Currently, many different microbial bio-fertilizers are available for agricultural use since they enhance plant growth and productivity. They improve soil fertility directly, by adding to the soil beneficial microbial inoculants, and indirectly, via stimulating soil microorganisms (El-Yazeid et al., 2007). Phylazonit is a bio-fertilizer brand released by Phylazonit Ltd., which contains an optimized

ratio of bacterial strains for soil injection (*Bacillus megaterium*, *Bacillus circulans*, and *Pseudomonas putida*). *Bacillus megaterium* is a cosmopolitan bacterium, which lives in an extended habitat, from soil to seawater, sediment, rice paddies, honey, fish, and dried food. It can easily grow in both simple and complex media, being mainly aerobic gram-positive, spore forming bacteria. *B. megaterium* is amongst the largest size known bacteria, with a cell length of up to 4 μm and a diameter of 1.5 μm. *B. megaterium* has at least up to 100-fold greater volume than *Escherichia coli* (De Vos et al., 2009; Vary et al., 2007; Bunk et al., 2010). Recently, it has become increasingly popular in the field of biotechnology for its recombinant protein production capacity. For the purpose of intra- and extracellular protein synthesis, several vectors were constructed and commercialized (Mo-BiTec GmbH, Germany). *B. megaterium* is also used in industry, where it produces biotechnologically relevant substances that grow on cheap substrates, and are non-pathogenic (they do not produce endotoxins associated with an outer membrane), unlike *E. coli*. Therefore, *B. megaterium* opens an avenue toward challenging biotechnological approaches (Vary et al., 2007; Bunk et al., 2010).

Bacillus circulans is a gram-positive rod that is motile by flagella. Cell size is in the range of 2.0-4.2 μm x 0.5-0.8 μm. *B. circulans* is a facultative anaerobic organism, so that it can make ATP (adenosine triphosphate) by aerobic respiration, when oxygen is present, but it also can switch to anaerobic respiration, when oxygen is absent. It can grow in the range of pH 6-9, but pH 7 is optimal for its evolution in an optimum temperature range of 30-37$°C$. This bacterium produces endospores, which allow bacteria to lie dormant for extended periods of time in harsh living conditions, but under favorable conditions they can reactivate themselves into vegetative stage. *B. circulans* bacteria are reported as plant growth promoting rhizobacteria (Gordon et al., 1973). *Pseudomonas putida* is a rod-shaped, flagellated, gram-negative bacterium found in most soil and water habitats, where oxygen is present. It grows optimally at 25-30$°C$. Given that *Pseudomonas putida* promotes plant development, it is used in bioengineering research to develop biopesticides and to the enhance plant health. The root surface, rhizosphere allows bacteria to prosper from the root nutrients; *P. putida* induces plant growth and protects plants from pathogens (Espinosa-Urgel et al.,

2000).

Recently, changes in several physical-chemical (Bautista et al., 2017; Jakab, 2020) and microbial soil properties (Mátyás et al., 2015; Sándor et al., 2020b) have been investigated in the region. Mátyás et al. (2016) examined the effect of different NPK doses on soil microbial activity and microbial biomass. Sándor et al. (2020b) explored how different cultivation methods affected soil respiration and enzymatic activity. In this study, the effects of a Phylazonit biofertilizer on soil respiration were addressed and compared to the extent of CO_2 emission caused by commercial chemical NPK fertilizers, biofertilizers, and different cultivation methods.

2   Materials and Methods

This investigation was conducted on a calcareous chernozem soil, in a multifactorial experiment at Látókép Experimental Station, the Center of Agricultural Sciences, the University of Debrecen. This station is in Eastern Hungary, 15 km away from the city of Debrecen. The area is known for the aeolain loess of Hajdúsag area, its geographical coordinates being $47°33'55{,}36''N; 21°28'12{,}27''E$. Annual yield fluctuations are primarily determined by the moisture content of soil in the month of July, and the water supply in May (Brebbia and Bjornlund, 2014). Experiments were performed from March to April 2016. The soil in the area can be classified as loamy and nearly neutral. Phosphorus supply of the soil is medium, while its potassium content is medium or good (Brebbia and Bjornlund, 2014).

Experimental plots were set up randomized in 4 replications per each measurement, in two sets. First set corresponds to measurements carried out on April 5, 2016, and the second on April 19, 2016. $15L/ha$ of Phylazonit were injected according to the manufacturer's specifications. Concentration of bacteria was $109/cm^3$. Phylazonit contains an optimized ratio of bacteria strains, *Bacillus megaterium*, *Bacillus circulans*, and *Pseudomonas putida*. Soil moisture content was measured gravimetrically by drying soil samples at 105$°C$ for 24 h, according to the protocol described in Klimes Szmik (1970). pH was determined potentiometrically in distilled water, for soil/water ratio of 1:2.5 (w/w), according to Buzás (1988), by using a glass electrode attached

to a Model Seven2Go Advanced Single-Channel Portable pH Meter (Mettler, Toledo), suited for pH and conductivity measurements. Silt and clay fraction were determined according to Buzás (1988). Physical-chemical and microbial soil properties and enzymatic activities are reported in the supporting material.

The experimental design for soil respiration was completely randomized, treatments were setup in incubators at 25°C for 180 h, in dark. These were placed in laboratory bottles (250 mL) equipped with a tight screw cap, 0.1 M NaOH (10 mL), and then a sterile gauze pad was filled with soil sample (10 g), and placed inside the bottle. After 2, 3, and 10 days, respectively, the amount of CO_2 absorbed by the residual alkali solution was determined by potentiometric titration with aqueous 0.1 M HCl solution, using phenolphthalein as the indicator. CO_2 outputs were calculated by Equation 1, as described by Witkamp (1966).

$$mg(CO_2) = V * M * 22 \qquad (1)$$

Where $mg(CO_2)$ is the mass of captured CO_2 (mg), V is the volume of HCl used in titration against saturated KOH solution (mL), M is the molarity of HCI ($mol\ L^{-1}$). Results are interpreted for respiration of 100 g soil samples over 10 day period, so the unit in Witkamp method is: $mg\ CO_2 \cdot (100g)^{-1} \cdot (10\ \text{day})^{-1}$.

Moisture multiplication factors of control samples are 1.40, and 1.26 for treated samples, respectively. Factor of KOH solution was 1.09,- while HCl solution had a factor of 0.93. An induced method was also used, in which 0.10 g glucose was added to the soil samples. Each treatment was replicated in quadruplicate. In addition, experimental results were compared to the findings of prior studies conducted at the same experimental station. In previous experiments, effects of commercial fertilizer doses of $N_{60}P_{45}K_{45}$; $N_{120}P_{90}K_{90}$; $N_{180}P_{135}K_{135}$; and $N_{240}P_{180}K_{180}$ (Mátyás et al., 2015) and of different cultivation methods (ploughed, loosened, RTK in rows, and RTK between rows) (Sándor et al., 2020a) on physical, chemical, and microbiological soil properties were assessed on the long term, in fertilization experiments that spanned over 30 years. Two methods for determining soil respiration were also compared, the Witkamp and Oxitop incubations (Bautista et al., 2017). Student's t-test was applied for statistical analysis, using SPSS (version 26) to reveal possible relevant differences in control and treated (biofertilizer) samples.

3   Results and discussion

Typically, induced methods are applied in studies related to microbial activity to reveal differences between various treatments. In this case, without induced method (added glucose) differences between control and treated samples are obvious. Differences can be observed between control and treated samples, starting the 2nd day of incubation (Table 1).

Table 1. Average results of soil respiration in incubation over 2, 3, and 10 days (mg $CO_2 \cdot 100g^{-1} \cdot 10\ \text{day}^{-1}$). Control = absolute control that does not stand for either biofertilizer treatment or induced method. Control + glucose = no biofertilizer was added, but induced method was applied. Treated = bio-fertilzer was applied. Treated + glucose= biofertilizer was added, and induced method was applied.

	Soil moisture content (%)	pH (H₂O)	Silt and clay fraction (%)	Soil respiration (mg $CO_2 \cdot 100g^{-1} \cdot 10\ \text{day}^{-1}$)		
				2nd day	3rd day	10th day
Control				85.2	77.4	143
Control + glucose	20.11-21.02	6.9	37.5	148.5	173.5	259.9
Treated				130.1	84.9	141.1
Treated+ glucose				137.3	194.8	265.7

Raw data (results in repetitions and factors) are provided in Supporting Material. Nevertheless, there is a decrease in soil CO_2 production in treated samples, starting the 2nd and 3rd days of incubation. This depletion in CO_2 production was assessed in all experiments, performed in quadruplicate. It is assumed that the phenomenon originates from the presence in soil of CO_2 consuming microbes or methanotrophs, which utilize the CO_2 produced periodically. This assumption is verified by a prior study (Bautista et al., 2017). However, this finding isunusual, because such bacteria are typically present in seawater and paddy soils, rather than in well ventilated chernozem soils with optimal moisture content (between 20.11 and 21.02 wt %) (Table 1). Values radically increased from the third to the seventh day of incubation. By the 10th day, there are no more notable differences between control and treated samples (Table 1); furthermore, no statistically significant differences were found between control and treated (Phylazonit) samples (at significance level 0.05).

In Figure 1, the results obtained on CO_2 emission dynamics were compared to findings reported previously in the scientific literature. In prior studies (Bautista et al., 2017; Sándor et al., 2020b), samples were collected from both irrigated and non-irrigated plots. Considering that soil moisture content strongly affects CO_2 production, it is assumed that results coming from prior studies had similar soil moisture content to the ones of the current research. Accepted range was: 19-21 wt % (within the optimal range on this soil type). In a prior study the effect of the same biofertilizer on soil respiration was examined at the same experimental station (Bautista et al., 2017). However, authors applied a different alkaline absorption method; they used Oxitop bottles, and their results were expressed in another unit, namely: CO_2 mL/L. To compare study findings obtained with different methodologies, the followings were considered:

(i) the amount of CO_2 in Oxitop bottles is calculated from the oxygen consumed by decomposition process that involves oxygen, carbon, and

carbon dioxide participating in the respiration process (Oxitop manual).

(ii) formation of a CO_2 molecule requires one C atom and one O_2 molecule.

To compare prior study findings with these, all results are expressed in $CO_2 \cdot (100 \text{ g})^{-1} \cdot (10 \text{ day})^{-1}$ according to Equation 2.

$$\text{ResultsOxitop}(ml/L) = 11,136363 * \text{Witkamp}CO_2(mgCO_2) \tag{2}$$

In studies conducted by Mátyás et al. (2015) and Sándor et al. (2020b) CO_2 values are expressed in $CO2 \cdot (100 \text{ g})^{-1} \cdot (10 \text{ day})^{-1}$, so there was no need for unit change. Generally, titration is carried out only after 10th day of incubation (comparable to the before mentioned prior studies). Additionally, in the present study the soil CO_2 production was measured along the entire incubation process; this is the reason why results are also shown for 2nd and 3rd days of incubation.

It can be stated that the highest NPK dose ($N_{240}P_{180}K_{180}$) causes the most intensive soil respiration as compared to bio-fertilizer application or different cultivation methods. Differences are observed between different cultivation methods; highest CO_2 values belong to samples from RTK in rows. Soil respiration values measured by two methods (Witkamp and Oxitop) are of the same order of magnitude, although Witkamp-based values are greater on each incubation day. Apart from the extremely high values of CO_2 measured by Witkamp's method on the second day of incubation, the increase in CO_2 from day 3 to day 7 is remarkable in the framework of both methods: Witkamp and Oxitop. During the incubation period, the increase of soil respiration was 60,17 %, within Witkamp's method, and 54,87 %, when Oxitop bottles were used. This pattern is notable if considering that experiments were performed quadruplicate, hence they are statistically relevant. These results validate a modern method (Oxitop) with a well-established, proven method (Witkamp).

4 Conclusions

This study indicates a lower tendency for soil respiration when bio-fertilizers are used, as compared to commercial NPK fertilizers. Hence, by means of bio-fertilizers CO_2 emissions can decrease to the environment. Nevertheless, long term experiments and field trials are needed for better understanding
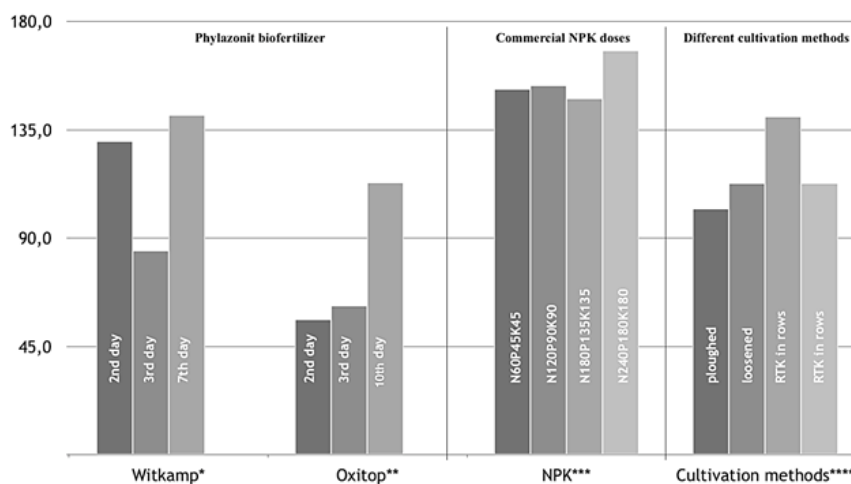
Figure 1. Soil respiration results after 2, 3, and 10 days of incubation ($mg\ CO_2 \cdot (100\ \text{g})^{-1} \cdot (10\ \text{day})^{-1}$), collated from own measurements and prior study findings. *own results related to effect of Phylazonit on soil respiration by the Witkamp method; **effect of Phylazonit on soil respiration by Oxitop bottles (Bautista et al., 2017); ***commercial NPK fertilizers in doses of $N_{60}P_{45}K_{45}$; $N_{120}P_{90}K_{90}$; $N_{180}P_{135}K_{135}$; and $N_{240}P_{180}K_{180}$ (Mátyás et al., 2015); ****different cultivation methods: ploughed, loosened, RTK in rows, and RTK between rows (Sándor et al., 2020b,a) on soil respiration.

and possibly reveal statistical differences between bio-fertilizers and chemical fertilizers-treated soil.

With the unit change in CO_2 results obtained in this study by two different alkali absorption-based methods (Oxitop and Witkamp) the aim is to contribute to improving comparability of scholarly studies, which apply different methodologies to determine soil respiration. This is particularly useful for examining changes in microbiological soil properties over long-term fertilization experiments, where even 30 years old results are being compared with new findings. Unit change applied and discussed here allows to compare studies based on different methods, allowing the adoption of new methods offered by the evolving technology. Data acquired by new methods can be incorporated with studies performed by traditional methods over the past decades.

Competing interests

No competing interests were disclosed.

Grant information

References

Álvaro Fuentes, J. and Cantero Martínez, C. (2010). Potential to mitigate anthropogenic co2 emissions by tillage reduction in dryland soils of spain. *Spanish J. Agricultural Research*, 8(4):1271–1276. Online: https://bit.ly/2Sjmq14.

Ashok, J., Falbo, L., Das, S., Dewangan, N., Visconti, C., and Kawi, S. (2019). *An Economy Based on Carbon Dioxide and Water*, chapter Catalytic CO2 Conversion to Added-Value Energy Rich C1 Products. Springer Nature Switzerland AG. Online:https://bit.ly/35c7Uh2. Springer, Cham.

Baldock, J., Wheeler, I., McKenzie, N., and Mcbratney, A. (2012). Soils and climate change: Potential impacts on carbon stocks and greenhouse gas emissions, and future research for australian agriculture. *Crop and Pasture Science*, 63:269. Online:https://bit.ly/3cP30Js.

Bautista, G., Mátyás, B., Carpio-Peñaherrera, I., Vilches, R., and Pazmino, K. (2017). Unexpected re-

Scientific paper / Artículo científico
CARBON FRONTIERS

Mátyás, B., Lowy, D., Singla, A., Melendez, J.R., and Sándor, Z.

sults in chernozem soil respiration while measuring the effect of a bio-fertilizer on soil microbial activity [version 2; referees: 2 approved]. *F1000 Research*, 6:Online:https://bit.ly/3bNavAh.

Brebbia, C. A. and Bjornlund, H., editors (2014). *Sustainable Irrigation and Drainage V: Management, Technologies and Policies*, volume 185. Wit Press.

Bunk, B., Schulz, A., Stammen, S., MünchH, R., Warren, M., Rohde, M., Jahn, M., and Biedendieck, R. (2010). A short story about a big magic bug. *Bioengineered Bugs*, 1:85–91. Online:https://bit.ly/2xZe8Vt.

Buzás, I. (1988). *Manual of Soil and Agrochemical Analysis*. INDA 4231 Kiadó., Budapest, 1 edition.

Chen, J., Xiao, W., Zheng, C., and Zhu, B. (2020). Nitrogen addition has contrasting effects on particulate and mineral-associated soil organic carbon in a subtropical forest. *Soil Biology and Biochemistry.*, 142:107708. Online:https://bit.ly/2VJxQxs.

De Vos, P., Garrity, G., Jones, D., Krieg, N., Ludwig, W., Rainey, F., Schleifer, K.-H., and Whitman, W., editors (2009). *Bergey's Manual of Systematic Bacteriology*, volume 3 of *The Firmicutes*. Springer-Verlag, New York. Online:https://bit.ly/2YcaDFL.

Denman, K., Brasseur, G., Chidthaisong, A., Ciais, P., Cox, P., Dickinson, R., Hauglustaine, D., Heinze, C., Holland, E., Jacob, D., Lohmann, U., Ramachandran, S., Da Silva Dias, P., Wofsy, S., and Zhang, X. (2007). *Climate Change: The Physical Science Basis. Contribution of Working Group I to the Fourth Assessment Report of the Intergovernmental Panel on Climate Change*, chapter Couplings Between Changes in the Climate System and Biogeochemistry. Cambridge University Press, Cambridge, United Kingdom and New York, NY, USA. Online:https://bit.ly/2KHwhtF.

El-Yazeid, A., Abou-Aly, H., Mady, M., and Moussa, S. (2007). Enhancing growth, productivity and quality of squash plants using phosphate dissolving microorganisms (bio phosphor) combined with boron foliar spray. *Research J. Agricultural Biological Science*, 3(4):274–286.

Elmqvist, T., Andersson, E., and Frantzeskaki, N. (2019). Sustainability and resilience for transformation in the urban century. *Nature Sustainability*, 2:267–273. Online:https://bit.ly/2SfrH9S.

Eloka-Eboka, A. C. and Inambao, F. L. (2017). Effects of co_2 sequestration on lipid and biomass productivity in microalgal biomass production. *Applied Energy*, 195:1100–1111. Online:https://bit.ly/2VL34UF.

Espinosa-Urgel, M., Salido, A., and Ramos, J. (2000). Genetic analysis of functions involved in adhesion of pseudomonas putida to seeds. *J. Bacteriology*, 189(9):2363–9.

Fekete, I., Kotroczó, Z., Varga, C., Nagy, P., Várbíró, G., Bowden, R., Tóth, J., and Lajtha, K. (2014). Alterations in forest detritus inputs influence soil carbon concentration and soil respiration in central-european deciduous forest. *Soil Biology and Biochemistry*, 74:106–114.

Fekete, I., Kotroczó, Z., Varga, C., Veres, Z., and Tóth, J. (2011). The effects of detritus input on soil organic matter content and carbon dioxide emission in a central european deciduous forest. *Acta Silv. Lign. Hung*, 7:87–96.

Francis, C. A. and Porter, P. (2011). Ecology in sustainable agriculture practices and systems. *Critical Reviews in Plant Sciences*, 30(1-2):64–73. Online:https://bit.ly/3f01aXT.

Glatzel, S., Basiliko, N., and Moore, T. (2004). Carbon dioxide and methane production potentials of peats from natural, harvested and restored sites, eastern québec, canada. *Wetlands*, 24:261–267. Online:https://bit.ly/35iVGmW.

Gordon, R., Haynes, W., and Pang, C. (1973). *The genus Bacillus. U.S. Department of Agriculture Agricultural Handbook*, chapter Bacterial Endospores. Bacterial Endospores. Number 427. Cornell University, Washington, D.C.

Gratani, L., Catoni, R., Puglielli, G., Varone, L., Crescente, M., Sangiorgio, S., and Lucchetta, F. (2016). Carbon dioxide (co_2) sequestration and air temperature amelioration provided by urban parks in rome. *Energy Procedia*, 101:408–415. Online:https://bit.ly/3bRlWHm.

Inubushi, K., Sakamoto, K., and Sawamoto, T. (2005). Properties of microbial biomass in acid soils and their turnover. *Soil Science & Plant Nutrition*, 51:605 – 608. Online:https://bit.ly/3aLYn1l.

Iqbal, J., Hu, R., Feng, M., Lin, S., Malghani, S., and Ali, I. M. (2010). Microbial biomass, and dissolved organic carbon and nitrogen strongly affect soil respiration in different land uses: A case study at three gorges reservoir area, south china. *Agriculture, Ecosystems & Environment*, 137(3):294 – 307. Online:https://bit.ly/2SgW6Vg.

Jakab, A. (2020). The ammonium lactate soluble potassium and phosphorus content of the soils of north-east hungary region: a quantifying study. *DRC Sustainable Future*, 1(1):7–13. Online:https://bit.ly/3faLbGO.

Johnson, J., Franzluebbers, A., Weyers, S., and Reicosky, D. (2007). Agricultural opportunities to mitigate greenhouse gas emissions. *Environmental pollution*, 150(1):107–24. Online:https://bit.ly/2zAokE1.

Klimes Szmik, A. (1970). A talajok fizikai tulajdonságainak vizsgálata. *Talaj és trágyvizsgálati módszerek*, 48:83–161.

Kong, Y., Nagano, H., Katai, J., Vago, I., Olah, A. Z., Yashima, M., and Inubishi, K. (2013). co_2, n_2o and ch_4 production/consumption potentials of soils under different land-use types in central japan and eastern hungary. *Soil Science and Plant Nutrition*, 59(3):455–462. Online:https://bit.ly/35g0ae3.

Kotroczó, Z., Fekete, I., Tóth, J., Tóthmérész, B., and Balázsy, S. (2018). Effect of leaf- and root-litter manipulation for carbon-dioxide efflux in forest soi. In *VII Alps-Adra Scientific Workshop*, Stara Lesna, Slovakia.

Lajtha, K., Bowden, R., Crow, S., Fekete, I., Kotroczó, Z., Plante, A., Simpson, M., and Nadelhoffer, K. (2017). The detrial input and removal treatment (dirt) network: Insight into soil carbon stabilization. *Science of The Total Environment*, (640-641):1112–1120. Online:https://bit.ly/2Yhi0vA.

Li, S., Xu, J., Tang, S., Zhana, Q., Gao, Q., Ren, L., Shao, Q., Chen, L., Du, J., and Hao, B. (2020). A meta-analysis of carbon, nitrogen and phosphorus change in response to conversion of grassland to agricultural land. *Geoderma*, 363:114149. Online:https://bit.ly/2VN09uO.

Lowy, D. and Mátyás, B. (2020). Sea water activated magnesium-air reserve batteries: Calculation of specific energy and energy density for various geometries. *DRC Sustainable Future*, 1(1):1–6. Online:https://bit.ly/3bOifSG.

López, R., Díaz, M. J., and González-Pérez, J. A. (2018). Extra co_2 sequestration following reutilization of biomass ash. *The Science of the total environment*, 625:1013—1020. Online:https://bit.ly/3f2Tu7d.

Melendez, J. and Gracia, G. (2019). Theoretical perspective of corporate social responsibility in the managerial scenario: Shared implications between the company-stakeholders. *Revista Espacios*, 40(10):1–14. Online:https://bit.ly/35fjCau.

Melendez, J., Perez Pupo, I., García Vacacela, R., and Piñero Pérez, P. (2018a). Strategic factors in the context of project management: Management perspectives. *Revista Espacios*, 39(39):10–16. Online: https://bit.ly/2W5zKaF.

Melendez, J. R., Zoghbe Nuñez, Y. A., Malvacias Escalona, A. M., Almeida, G., and Layana Ruiz, J. (2018b). Theory of constraints: A systematic review from the management context. *Revista Espacios,*, 39(48):1–14. Online:https://bit.ly/2VKomSs.

Moral, A., Reyero, I., Alfaro, C., Bimbela, F., and Gandía, L. (2018). Syngas production by means of biogas catalytic partial oxidation and dry reforming using rh-based catalysts. *Catalysis Today*, 299:280–288. Online:https://bit.ly/2W7lGNL.

Mátyás, B., Horváth, J., Kátai, J., and Tállai, M. (2016). Comparative analysis of certain soil microbiological characteristics of the carbon cycle. *Acta Agraria Debreceniensis*, 69:137–141.

Mátyás, B., Tállai, M., Kátai, J., and Horváth, J. (2015). The impact of fertilisation on a few microbiological parameters of the carbon cycle. *Acta Agraria Debreceniensis*, 64:45–50. Online:https://bit.ly/3f2Cka4.

Peng, y., , Song, S.-y., Li, Z.-y., Li, S., Chen, G.-t., Hu, H.-l., Xie, J.-l., Chen, G., Xiao, Y.-l., Liu, L., Tang, Y., and Tu, L.-h. (2020). Influences of nitrogen addition and aboveground litter-input manipulations on soil respiration and biochemical properties in a subtropical forest. *Soil Biology and Biochemistry*, 142:107694. Online:https://bit.ly/2yTYWZw.

Powlson, D. (2005). Climatology: Will soil amplify climate change? *Nature*, 433:204–205. Online:https://bit.ly/2y8HeBG.

Rustad, L., Campbell, J., Marion, G., Norby, R., Mitchell, M., Hartley, A., Cornelissen, J., and Gurevitch, J. (2001). A metaanalysis of the response of soil respiration, net nitrogen mineralization, and aboveground plant growth to experimental ecosystem warming. *Oecologia*, 126:543–562. Online:https://bit.ly/2W7Ynn1.

Singla, A. and Inubushi, K. (2014). Effect of biochar on ch_4 and n_2o emission from soils vegetated with paddy. *Paddy and Water Environment*, 12:239–243. Online:https://bit.ly/2zGxv63.

Singla, A., Sakata, R., Hanazawa, S., and Inubushi, K. (2014). Methane production/oxidation potential and methanogenic archaeal diversity in two paddy soils of japan. *Int. J. Ecol. Environ. Sci.*, 40:49–55. Online:https://bit.ly/3aO6A5d.

Sándor, Z., Tállai, M., Kincses, I., László, Z., Kátai, J., and Vágó, I. (2020a). Correction for .ᵉffect of various soil cultivation methods on some microbial soil properties". *DRC Sustainable Future: Journal of Environment, Agriculture, and Energy*, 1(1):21–22. online: https://bit.ly/2VNJZBr.

Sándor, Z., Tállai, M., Kincses, I., László, Z., Kátai, J., and Vágó, I. (2020b). Effect of various soil cultivation methods on some microbial soil properties. *DRC Sustainable Future: Journal of Environment, Agriculture, and Energy*, 1(1):14–20. online: https://bit.ly/2VNJZBr.

Team, I., Pachauri, R., and Meyer, L. (2014). Synthesis report. contribution of working groups i, ii and iii to the fifth assessment report of the intergovernmental panel on climate change. Technical report, IPCC:Climate Change, Geneva, Switzerland. Online:https://bit.ly/2zIGcwR.

Thornton, P. (2012). Recalibrating food production in the developing world: Global warming will change more than just the climate. Technical report, CCAFS Policy Brief No. 6. CGIAR Research Program on Climate Change, Agriculture and Food Security.

Vary, P., Biedendieck, R., Fuerch, T., Meinhardt, F., Rohde, M., Deckwer, W.-D., and Jahn, D. (2007). Bacillus megaterium – from simple soil bacterium to industrial protein production host. *Applied microbiology and biotechnology*, 76:957–67. Online:https://bit.ly/35cpguc.

Vermeulen, S. J., Campbell, B. M., and Ingram, J. S. (2012). Climate change and food systems. *Annual Review of Environment and Resources*, 37(1):195–222. Online:https://bit.ly/2YeNgvh.

Witkamp, M. (1966). Decomposition of leaf litter in relation to environment, microflora, and microbial respiration. *Ecology*, 47:194–201. Online:https://bit.ly/35lix11.

Xiao, H., Shi, Z.-H., Li, Z., Wang, L., Jia, C., and Wang, J. (2020). Responses of soil respiration and its temperature sensitivity to nitrogen addition: A meta-analysis in china. *Applied Soil Ecology*, 150:103484. Online:https://bit.ly/35f0I3x.

Zeng, W., Chen, J., Liu, H., and Wang, W. (2018). Soil respiration and its autotrophic and heterotrophic components in response to nitrogen addition among different degraded temperate grasslands. *Soil Biology and Biochemistry*, 124:255–265. Online:https://bit.ly/35dR41e.

ABYA YALA | UNIVERSIDAD POLITÉCNICA SALESIANA

ENGINE PERFORMANCE AND EMISSION ANALYSIS USING NEEM AND JATROPHA BLENDED BIODIESEL

RENDIMIENTO DEL MOTOR Y ANÁLISIS DE EMISIONES UTILIZANDO BIODIÉSEL DE NEEM Y JATROPHA

Mehmood Ali[1]* and Saqib Jamshed Rind[2]

[1] *Department of Environmental Engineering, NED University of Engineering and Technology. Karachi, Karachi City, Sindh 75270, Pakistan.*

[2] *Department of Automotive Marine Engineering, NED University of Engineering and Technology. Karachi, Karachi City, Sindh 75270, Pakistan.*

*Corresponding author: mehmood@neduet.edu.pk

Abstract

This paper presents the production of biodiesel from indigenous species of Jatropha curcas and Neem (*Azadirachta indica*) oils, then its engine performance and emission characteristics of B10 blends measured at 1000 rpm. Biodiesel production yields were found 90% and 68% by weight from Jatropha curcas and Neem (*Azadirachta indica*), respectively. Three prepared biodiesel blends were 10% Neem biodiesel (NB10), 10% Jatropha biodiesel (JB10) and 5% Jatropha + 5% Neem biodiesels (NJB10). The engine emission test showed less carbon monoxide production from NB10 (94 ± 2.15 ppm), followed by JB10 (100 ± 2.44ppm) and NJB10 (121 ± 3.65ppm) as compared to diesel (135 ± 2.18ppm). However, the carbon dioxide emissions were found higher due to the better combustion characteristics of biodiesel blends as NB10 (3.21%), JB10 (3.06%) and NJB10 (2.53%) than diesel (2.13%) by volume. The reduced amounts of sulphur dioxide (SO_2) emissions were found with blended biodiesel fuel in comparison to mineral diesel. Nitrogen dioxide (NO_2) emissions were 5 ppm from diesel at $73°C$ exhaust temperature, while it was increased by using blended biodiesel, to 8 ppm with NB10 due to higher exhaust temperatures $85,33°C$. The measured engine power and torque produced from the blended biodiesel samples were slightly lower than the conventional diesel by 12% and 7.7%, respectively. The experimental results showed that an engine performance and emission characteristic of Neem biodiesel (NB10) was better as compared to other biodiesel blends.

Keywords: Biodiesel, *Jatropha curcas*, Neem (*Azadirachta indica*), engine emissions, engine performance.

Resumen

Este documento analiza la producción de biodiésel a partir de especies autóctonas de aceites de Jatropha curcas y Neem (*Azadirachta indica*), junto con el rendimiento del motor y las características de emisión de mezclas B10 a 1000 rpm. Los rendimientos de la producción de biodiésel fueron 90 % y 68 % en peso de Jatropha curcas y Neem (*Azadirachta indica*), respectivamente. Las tres mezclas preparadas de biodiésel fueron 10 % Biodiésel de Neem (NB10), 10 % de biodiésel de Jatropha (JB10) y 5 % de Jatropha + 5 % de Biodiésel de Neem (NJB10). La prueba de emisiones del motor mostró menos producción de monóxido de carbono con NB10 (94 ± 2,15 ppm), seguida de JB10 (100 ± 2,44 ppm) y NJB10 (121 ± 3,65 ppm) en comparación con el diésel (135 ± 2,18 ppm). Sin embargo, las emisiones de dióxido de carbono fueron más altas debido a las mejores características de combustión de las mezclas de biodiésel como NB10 (3,21 %), JB10 (3,06 %) y NJB10 (2,53 %) comparado con el diésel (2,13 %) por volumen. Las cantidades más bajas de emisiones de dióxido de azufre (SO_2) se observaron con el combustible de biodiésel mezclado, en comparación con el diésel mineral. Las emisiones de dióxido de nitrógeno (NO_2) fueron de 5 ppm de diésel a 73°C de temperatura de escape, mientras que se incrementó a 8 ppm mediante el uso de biodiésel mezclado con NB10 debido a las altas temperaturas de escape de 85,33°C. La potencia y la carga del motor producidos a partir de las muestras de biodiésel mezclado fueron ligeramente inferiores al diésel convencional en un 12 % y un 7,7 %, respectivamente. Los resultados experimentales mostraron que el rendimiento del motor y la emisión del biodiésel de Neem (NB10) era mejor en comparación con otras mezclas de biodiésel.

Palabras clave: Biodiésel, *Jatropha curcas*, Neem (*Azadirachta indica*), emisiones del motor, rendimiento del motor.

Orcid IDs:

Mehmood Ali: http://orcid.org/0000-0002-1804-2677
Saqib Jamshed Rind: http://orcid.org/0000-0003-4881-0419

1 Introduction

The climate change and global warming issues are caused by greenhouse gas emissions (GHG's) such as carbon dioxide, methane and nitrous oxide in the atmosphere due to the human induced activities by burning fossil fuels used in transportation and energy generation sector (Climate Change Indicators, 2015). The two most common liquid biofuels for transportation (i.e. bioethanol and biodiesel) can replace the petroleum derived gasoline and diesel fuels, producing harmful gas emissions with detrimental impacts on the environment. Bioethanol and biodiesel are alternative fuels produced almost entirely from vegetable oil seed crops, having environmental benefits. The biggest difference between biofuels and petroleum feedstocks is the concentration of oxygen content, which makes biofuels environmental friendly with complete combustion producing carbon dioxide instead of carbon monoxide, causing harmful impact on the health of humans (Chauhan and Shukla, 2011).

Biodiesel as a biodegradable and an alternative fuel, getting more importance due to the depletion of crude oil reserves and its environmental benefits (Berchmans and Hirata, 2008). In fact, biodiesel fuel is a form of renewable fuel which can be obtained from various feed stocks including edible and non-edible oil seed crops. While it can be produced from non-edible oils example; mahua, neem, karanja and Jatropha curcas to avoid conflict with the edible food crops (Masjuki Kalam, 2013). The use of biodiesel fuel in diesel engine does not require engine modifications, it gives significant reduction in emissions of oxides of sulfur (SO_x), carbon monoxide (CO) and particulate matter (PM) with other benefits such as higher flash point and lower aromatic content in the exhaust gases due to the complete combustion of fuel (Ali and Shaikh, 2012).

In previous research investigation, methyl ester of Pongamia, Jatropha and Neem were produced by transesterification reaction and the experimental study carried out to test the emission characteristics of different blends ($B10, B20$, and $B40$) in comparison with petroleum diesel. The blended fuel samples showed lower smoke, carbon monoxide and unburned hydrocarbons (HC) emissions as compared to petroleum diesel (Rao et al., 2008). Another investigation showed that the exhaust emissions from neem biodiesel B30 were having lower smoke opacity (5 %) than with regular diesel fuel (55 %) at maximum brake power (5 kW). Similarly, the carbon monoxide (CO) is one of the intermediate products formed during the combustion reaction of hydrocarbons in the engine cylinder, and it was observed that the amount of CO produced decreases with increase in load on the engine for diesel and various blends of neem biodiesel. It was noticed that unburned hydrocarbons (HC) emission increases with respect to the increased engine load for diesel and blends of neem biodiesel due to more fuel consumption at high engine loads, with incomplete combustion. However, it was found that HC emissions decrease with increase in percentage of biodiesel in the blends, due to availability of more oxygen percentage leading to complete combustion of fuels (Mall, 2015).

The Pakistan's major portion of energy production is met by burning crude petroleum oil derived fuels, which are non-renewable resources. Currently the country is facing an electricity shortfall between 6,000 to 7,000MW (Yuosafzai, 2018). The Pakistan's oil import bill increased from US $ 7.4 billion in 2015-16 to US $ 9.1 billion in fiscal year 2016-17 as a result of increase in international crude oil prices and increase in import of petroleum products. Therefore, it is being assumed that the demand of petroleum crude oil will have an increasing trend in future for power generation and transportation sector in the country (Pervaz, 2018). However, for the sustainable future through the renewable energy, it is necessary to reduce the dependency on imported crude oil. These steps would not only help to save valuable foreign exchange of the country but also it would help in mitigating climate change and global warming issues (Ali, 2016).

Moreover, the Alternative Energy Development Board of Pakistan (AEDB) took an initiative under its National Biodiesel Program to minimize quantity of diesel consumption (10 % by volume) of the total diesel usage by the year 2025 with alternative biodiesel fuel (Ahmed et al., 2015). The past research studies have conducted limited investigation on Neem and Jatropha curcas blended biodiesel fuels related to engine performance and emission characteristics. Therefore, the aim of this research study was to characterize the produced biodiesel from Neem and Jatropha curcas oils, follo-

wed by engine performance and emission characteristics of Neem and Jatropha curcas blended biodiesel fuel samples in order to comply with AEDB target to use 10 % blended biodiesel by the year 2025 in Pakistan.

2 Materials and methods

The *Jatropha curcas* non-edible vegetable seed oil was obtained from Arid Zone Research Institute, Pakistan Agricultural Research Council, Umerkot, while neem oil (*Azadirachta indica*) was extracted with a mechanical oil expeller from locally available oil seeds. All the experiments were conducted in the Department of Environmental Engineering and the Department of Automotive Marine Engineering, NED University of Engineering & Technology, Karachi, Pakistan. The temperature and humidity in the laboratory were measured as $28 \pm 1°C$ and 45 % RH with (Temperature Humidity Meter Digital Thermometer, China).

2.1 Acid value test

For both non-edible oils, the free fatty acid (FFA) content % and acid value test were measured by following the standard titration method (The American Oil Chemists' Society Official Method Ca 5a-40) mentioned in literature (Berchmans and Hirata, 2008). According to the literature if vegetable oils have FFA content more than 1 % by weight, it will produce soap and a low yield of biodiesel product. Therefore two step reactions (i.e. acid esterification and base catalyzed transesterification) are usually adopted to reduce the oil FFA to produce biodiesel (Berchmans and Hirata, 2008).

2.2 Two-step (acid esterification and base catalyzed transesterification)

A two-step process, acid-catalyzed esterification process and base-catalyzed transesterification process were conducted according to the literature (Berchmans and Hirata, 2008). The first step was carried out with 0.60 w/w methanol to oil ratios in the presence of 1 % w/w H_2SO_4 (BDH, England) as an acid catalyst in 1 hr reaction at $50°C$ using a hot plate heater with magnetic stirrer operating at 400 rpm (Wise stir, MSH-20A, Daihan Scientific, Korea). After reaction, the mixture was allowed to settle for 2

hrs and the methanol water mixture collected at the top layer was removed with the help of pipette. The second step was base catalysed transesterification using 0.24 w/w methanol (BDH, England) to oil and 1,4 % w/w *NaOH* (Merck, Germany) to oil as alkaline catalyst to produce biodiesel at $65°C$ for 2 hrs reaction time using a hot plate heater with magnetic stirrer with a mixing speed of 400 rpm (Berchmans and Hirata, 2008). The two layers were formed after the reaction i.e. biodiesel (upper layer) and bottom layer glycerine were separated out in a separating funnel (1L). The biodiesel phase and glycerine phase were washed with 10 % by volume of warm distilled water at $70°C$ and then dried in a conventional oven (YCO-N01, Gemmy Industrial Corp., Taiwan) for 1 hr at $80°C$ (Ali et al., 2018). The amount of biodiesel and glycerine produced after separation and drying were collected in a pre-weighted beaker (50 mL) and the quantity was measured by weight in grams with the help of a weight balance (AB 304-S, Mettler Tolendo, Switzerland).

2.3 Physicochemical properties of biodiesel produced

The following physicochemical properties of biodiesel produced were measured and the results are presented as mean ± standard deviation, for sample size (n=3).

2.3.1 Density:

Density of the extracted oil and the biodiesel produced were measured in g/mL with density meter (DA-130N, Kyoto Electronics Manufacturing Co. Ltd, Japan).

2.3.2 Kinematic viscosity:

Kinematic viscosity in mm^2/sec of the vegetable oils (Jatropha curcas and Neem oils) and its blended biodiesel samples were measured by using Kinematic/ Dynamic viscometer (VDM-300, AS Lemis, EU).

2.3.3 Calorific value:

The calorific value in MJ/kg of Jatropha curcas, Neem oils and its blended biodiesel samples were determined with an oxygen bomb calorimeter (IKA C200, Germany) according to the ASTM D2015 standard method.

2.3.4 Flash point:

The flash point of Jatropha and Neem biodiesel and blended fuel samples were measured with a flash point tester (AD 0093-710, SCAVINI, Italy) according to the ASTM D93 standard method.

2.4 Methyl esters (oleic acid) content

The oleic acid composition in the Jatropha and Neem oil samples were determined using GC-FID (GC-2014, Shimadzu, Japan) equipped with flame ionization detector at the Institute of Chemical Engineering Technology, University of the Punjab, Lahore.

2.5 Biodiesel-diesel blending ratios

Each fuel sample (1 L =1000 mL) was prepared by mixing biodiesel produced with the conventional diesel procured from the company operated fuel station of Pakistan State Oil (PSO) in the following ratios as shown in Table 1 as per the requirement of AEDB to blend the conventional diesel with 10 % biodiesel fuel.

2.6 Engine emissions and performance testing protocol

The prepared fuel samples emission characteristics were measured with operating a diesel engine, having specifications mentioned in Table 2, at a constant speed of 1000 rpm at the Department of Automotive & Marine Engineering, NED University. The gaseous emissions concentration measurement of carbon dioxide (CO_2), carbon monoxide (CO), oxides of nitrogen (NO_X), sulphur dioxide (SO_2) and oxygen content (O_2) were measured using flue gas analyzer (340, Testo Instruments Ltd, Germany). The gas emission results are presented as (mean $\pm$ standard deviation) for sample size n=3.

Engine performance was measured for 100 % diesel fuel, NB10 neem biodiesel, JB10 Jatropha biodiesel and NJB10 (mixed neem and Jatropha) biodiesel. The engine performance was studied at a constant speed of 1000 rpm following the procedures mentioned in the literature (Calder et al., 2018). After the engine reached its stabilized working condition, external restraining load torque (10 %) was fitted with a water brake dynamometer connected with a servo controller installed on the water load release to control engine load. The corresponding engine brake power was calculated using the equation 1, where torque is measured in N-m and engine speed in revolution per minute.

$$\text{Brake Power}(hp) = \frac{\text{Torque} \times \text{Engine Speed}}{5252} \quad (1)$$

2.7 Estimation of potential of biodiesel production to meet local requirement

The production of biodiesel from neem oil crop and waste cooking oil was calculated based on the marginal land available in the country to meet local diesel demand per annum.

Table 1. Fuel samples prepared blending ratios.

Sample	Mineral diesel (mL)	Neem biodiesel (mL)	Jatropha biodiesel (mL)
Diesel fuel	1000	-	-
NB10	900	100	-
JB10	900	-	100
NJB10	900	50	50

3 Results and Discussion

3.1 Biodiesel and glycerol yield

The measured quantity of biodiesel and glycerol produced from Jatropha curcas oil were found 90 % (36.28 g/ 40 g oil) and 11 % (4.36 g / 40 oil), respectively. While the quantity of biodiesel and glycerol produced from Neem oil were found 68 % (27.49 g/ 40 g oil) and 30 % (12.50 g / 40 oil), respectively.

Table 2. Engine specifications used in this study.

Engine make	Rotronics, France
No. of cylinders	2
Volume of cylinders	380 cc
Maximum speed	2700 rpm
Maximum power output	2.0 kW
Bore	62 mm
Stroke	72 mm
Type	4 stroke, direct injection, air cooled
Compression ratio	8.5:1

3.2 Physical and chemical properties of fuel

The Jatropha curcas and Neem biodiesel fuel properties were determined following the ASTM standards and procedures as summarized in Table 3 and then were compared with the international biodiesel standard (ASTM D 6751). It was interesting to note that kinematic viscosity of Neem biodiesel was found lower i.e. 2.91 mm^2/sec as compared to Jatropha biodiesel 4.18 mm^2/sec. The reduced kinematic viscosity is good in terms of biodiesel fuel quality, but the Neem biodiesel yield was 24.33% less in contrast to Jatropha biodiesel yield.

3.3 Methyl oleate content results

The methyl oleate concentration in% by weight was measured with GC-MS analysis and the results showed methyl oleate concentration in Jatropha oil (41.12% wt) and Neem oil (50.77% wt), respectively. The results showed Neem oil has value comparable to Jatropha oil, having more favorable property with longer biodiesel storage time with good oxidation stability and decreased cold filter plugging point during winters, keeping the biodiesel in liquid phase for proper atomization. Furthermore, it is recommended to measure the complete free fatty acids profile of both vegetable oil samples.

Table 3. Physicochemical properties of vegetable seed oils and its biodiesel produced.

Parameters	Jatropha Curcas	Neem (Azadirachta indica)	Test method	ASTM D 6751 Biodiesel standard
Density of oil (g/cm^3)	0.877	0.914	ASTM D1298	-
Kinematic viscosity of oil (mm^2 /sec) at 40°C	44.5	33.37	ASTM D 445	-
Biodiesel yield (g)	36.28	27.49	-	-
Density of biodiesel (g/cm^3)	0.884	0.875	ASTM D1298	$0.86 - 0.90$*
Kinematic viscosity of biodiesel (mm^2 /sec)	4.18	2.91	ASTM D445	$1.9 - 6.0$
Glycerine yield (g)	4.36	12.5	-	-
Calorific value of biodiesel (MJ/kg)	38.96	39.67	ASTM D240	-
Flash point (°C) of biodiesel	120	130	ASTM D93	130°C (minimum)

*According to European biodiesel standard EN 14214

3.4 Engine emissions test results

The gas emissions profile of different biodiesel fuel blends were plotted to compare the difference between their emission characteristics. Figure 1 shows the percentage of oxygen content present in the exhaust flue gas emissions and it was observed that the mineral diesel (17.12 ± 0.05%) has more oxygen content as compared to biodiesel blended fuel samples. The possible reason could be due to high temperature and high oxygen content present in

biodiesel fuel, the excess oxygen present in biodiesel was used in the production of nitrogen oxides (NO_x). Generally excess oxygen does not react with nitrogen in the engine cylinder, but it reacts with atmospheric nitrogen at high exhaust temperatures (Nair et al., 2017). Similarly, the exhaust temperature profile of flue gas from the diesel engine operating on different fuel blends (see Figure 2) showed higher temperatures were obtained from biodiesel blend fuel combustion as compared to the diesel fuel. This is due to the presence of oxygenated property of biodiesel, with complete combustion, resulting in higher exhaust temperatures (i.e. 14% and 8.75% from neem and jatropoha blended biodiesel fuels higher than mineral diesel). A previous research study on palm biodiesel showed 5.6% higher exhaust gas temperature than petroleum diesel. The improved combustion characteristic of biodiesel with higher cylinder temperature is due to the effect of excess oxygen content present in its composition (Arunkumar et al., 2018).
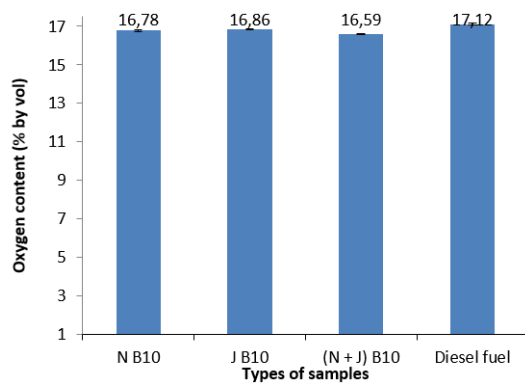
Figure 3 depicts the emission of carbon monoxide (CO) from different fuel samples, showing less CO emissions from biodiesel blended fuels (such as NB10= 94 ± 2.15, JB10= 100 ± 2.44 and NJB10=121 ± 3.65 ppm) as compared to the mineral diesel (135 ± 2.18 ppm). As the previous literature, the main reason for higher CO emissions from mineral diesel combustion is due to its incomplete combustion (Nair et al., 2017). Therefore, the presence of higher percentage of oxygen in biodiesel leads to more complete combustion process resulting in lower emissions of CO (Dincer, 2008). In the results of carbon dioxide (CO_2) emissions were found higher from biodiesel blended fuel samples as compared to the mineral diesel fuel (see Figure 4). Neem biodiesel NB10 showed higher CO_2 emissions in contrast to Jatropha biodiesel JB10. The CO emissions were reduced for Neem biodiesel blend (NB10) by 30.37% volume as compared to mineral diesel. The CO emission value was found close with an average reduction for Neem B10 by 26% volume, as mentioned in literature (Nair et al., 2017).

Figure 1. Oxygen content in exhaust emissions.
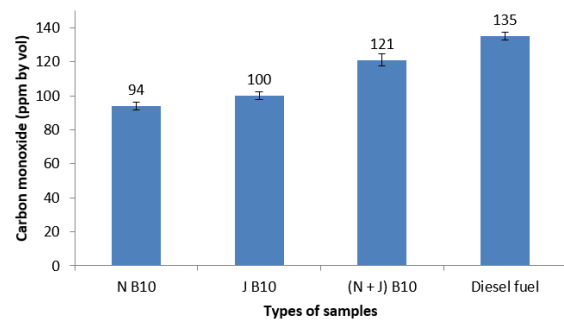
Figure 3. Carbon monoxide content in exhaust emissions.

Figure 2. Exhaust temperatures with different fuel blends.
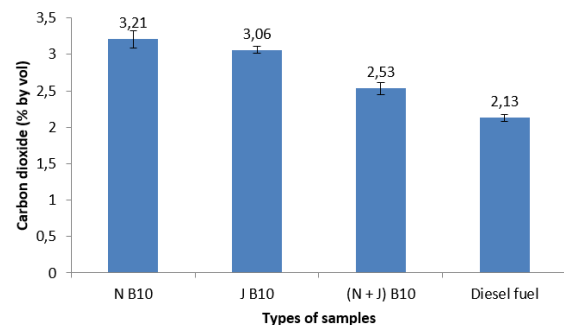

Figure 4. Carbon dioxide content in exhaust emissions.

Figure 5 shows the nitrogen dioxides (NO_x) emissions from the combustion of different blended

fuel samples. It was observed that NO_x emissions were higher from biodiesel blended fuel samples as compared to mineral diesel (i.e. 37.5% from NB10 and 28.57% from JB10, respectively). It was also observed by the past research studies showing 20% increase in NOx emissions from neem B10 as compared to neat diesel fuel (Nair et al., 2017). Higher temperature results from combustion of biodiesel, produces NO_x with a reaction between excess percentage of oxygen content present in biodiesel blended fuel emissions and atmospheric nitrogen. The emissions of sulphur dioxide (SO_x) are presented in Figure 6, the results showed reduction of SO_x emissions by over 38.46% from NB10 and 34.61% from JB10, respectively as compared to mineral diesel. It is an advantage using biodiesel blended fuel, since low sulphur content for mitigation of air pollution causes global warming and acid rain issues.
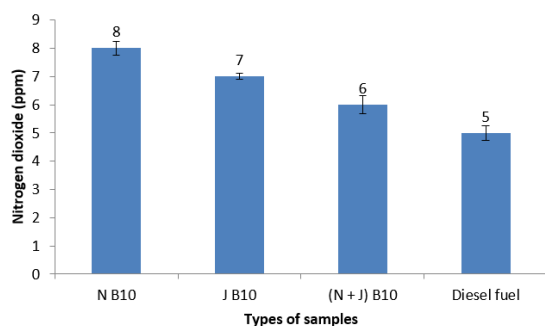

Figure 5. Nitrogen dioxide content in exhaust emissions.

3.5 Engine torque and brake power measurements

The variation of brake power of different blended fuel samples (mineral diesel, NB10, JB10 and NJB10) at a constant 1000 rpm engine speed is presented in Table 4. The results showed slightly less power generated from blended biodiesel fuel as compared to petroleum diesel, due to its lower calorific value (38 to 39 MJ/kg) in comparison to mineral diesel (42MJ/kg) and it is also endorsed by the literature (Chakrabarti and Ali, 2008). In addition, it was observed that engine torque and power generated by Neem biodiesel NB10 were higher compared with the Jatropha biodiesel JB10. It was due to higher calorific value of the Neem biodiesel (39.67 MJ/kg), in contrast to the Jatropha biodiesel (38.96

MJ/kg). The mineral diesel combustion produced higher torque during engine testing against different biodiesel blends due to its greater calorific value (42 MJ/kg) (Chakrabarti and Ali, 2008). The results indicated that B10 have closer engine performance to mineral diesel due to its kinematic viscosity comparable to mineral diesel (Chakrabarti and Ali, 2009). The power generated by Neem biodiesel NB10, Jatropha JB10 and mixed Neem / Jatropha biodiesel NJB 10 were found 7.7%, 16.4% and 12% lower compared to mineral diesel.
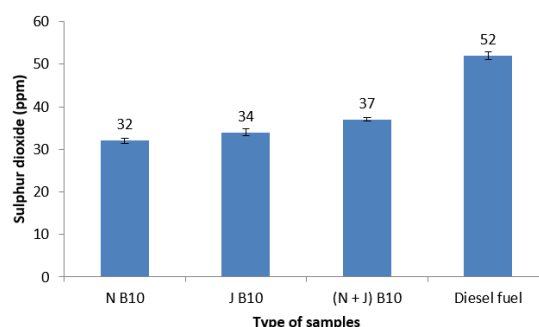
Figure 6. Sulphur dioxide content in exhaust emissions.

3.6 Estimation of production of biodiesel to meet local requirement

Neem (*Azadirachta indica*) seed contains approximately 20-35% by weight oil content and it produces about 2670 kg of oil/ hectare (Aransiola et al., 2019). According to the literature, Pakistan has arid/ semi-arid and marginal land approximately 350,000 acres (141640 hectares) that can be used to grow non-edible crops for biodiesel production (Ali, 2016). Table 5, shows the production of neem oil in the country is 378178.8 kgs per annum (i.e. 0.3781 million tonnes) obtained by multiplying 2670 kg of oil /hectare with the marginal land area 350,000 hectares. It is assumed that 90% by weight of neem oil produced per annum is converted into biodiesel, it comes to 0.3402 million tons, while 10% by weight is converted into its by-product glycerine (i.e. 0.0378 million tons). Moreover, according to the previous literature (Qamar et al., 2020) Pakistan has a capacity of producing 468,842 tonnes (0.4688 million tonnes) of biodiesel annually using waste cooking oil (WCO).

Table 4. Showing engine torque and its corresponding brake power at a constant speed (1000 rpm).

Samples	Engine Torque (N-m)	Engine Brake power (hp)
Diesel fuel	2.854	0.543
NB10	2.634	0.501
JB10	2.387	0.454
NJB10	2.514	0.478

Table 5. Estimation of local production of biodiesel per year.

	Statistics of local production per year	
(1)	Demand of petro-diesel per year (million tons)	6.764
(2)	Demand of blended biodiesel (B10) per year (million tons)	0.6764
(3)	Neem oil production per year (million tons)	0.3781
(4)	Estimated Neem biodiesel production per year (million tons)	0.3402
(5)	Estimated WCO biodiesel production per year (million tons)	0.4688
(6)	Quantity of biodiesel (B10) production per year (million tons)	0.1326

The total demand of high speed diesel in the country per annum is 6.674 million tonnes (DAWN, 2019) and if blended biodiesel (B10) is used in the country, the quantity of biodiesel required will be 0.6764 million tons per year to comply with AEDB requirement of using B10 blended biodiesel. To meet the required quantity of biodiesel, the difference between column (2) minus the estimated quantities of neem biodiesel (column 4) and waste cooking oil biodiesel (column 5) gives a surplus quantity of biodiesel production that meets consumers demand (0.1326 million tons) in the country per year, without competing with the vegetable cooking oils obtained from edible seed crops.

4 Conclusions

The indigenous Jatropha and Neem vegetable seed oils can be converted into biodiesel, and then blended biodiesel (B10) can be used as an alternative fuel in diesel engines to meet the target set by Alternative Energy Development Board. The emission of carbon monoxide (CO) from different fuel samples showed less CO emissions from biodiesel blended fuels.

The amount of CO_2 concentration showed increasing trend in exhaust emissions with respect to increasing biodiesel quantity in the fuel mixture, converting more CO into CO_2. NO_x emissions were found higher with increasing ratio of biodiesel fuel with mineral diesel. Results indicated that B10 have closer engine performance with mineral diesel, this is mainly due to their comparable kinematic viscosities. Less engine power being generated was observed by neem biodiesel NB10, Jatropha JB10 and mixed neem / Jatropha biodiesel NJB10 i.e. 7.7 %, 16.4 % and 12 %, respectively as compared to the mineral diesel.

The estimated production of biodiesel in the country from Neem seed oil crops and waste cooking oil is was found producing a surplus quantity of biodiesel (0.1326 million tons per year) to meet local demand of using B10 fuel in the future.

Acknowledgments

providing laboratory facilities. Furthermore, special gratitude to Arid Zone Research Institute (Pakistan Agricultural Research Council, Umerkot, Pakistan) for providing the Jatropha curcas vegetable seed oil for experimental work. The authors are also grateful to the Institute of Chemical Engineering Technology, University of the Punjab, Lahore, Pakistan for GC-MS analysis of vegetable seed oils.

References

Ahmed, M., Jan, H., Sultana, S., Zafar, M., Ashraf, M., and Ullah, K. (2015). *Biernat, Biofuels - Status and Perspective*, chapter Prospects for the Production of Biodiesel in Pakistan, pages 1–25. Intech.

Ali, M. (2016). Biological process- fuel. December 15, 2019,.

Ali, M., Naqvi, B., and Watson, I. (2018). Possibility of converting indigenous salvadora persica l. seed oil into biodiesel in pakistan. *International Journal of Green Energy*, 15(7):427–435. Online:https://bit.ly/3kF2uTc.

Ali, M. and Shaikh, A. (2012). Emission testing of jatropha and pongamia mixed biodiesel fuel in a diesel engine. *NED University Journal of Research Thematic Issue on Energy*, pages 43–52.Online:https://bit.ly/33WgamR.

Aransiola, E., Ehinmitola, E., Adebimpe, A., Shittu, T., and Solomon, B. (2019). *Azad, Advances in Eco-Fuels for a Sustainable Environment*, chapter Prospective ecofuel feedstocks for sustainable production., pages 43–87. Woodhead Publishing, London.

Arunkumar, M., Murali, G., Vikky, S., Thangadurai, R., and Tamilarasi, M. (2018). Performance study of a diesel engine with exhaust gas recirculation (egr) system fuelled with palm biodiesel. *International Journal of Thermal Engineering*, 6:1–9. Online:https://bit.ly/2DRVUrm.

Berchmans, H. and Hirata, S. (2008). Biodiesel production from crude jatropha curcas l. seed oil with a high content of free fatty acids. *Bioresource technology*, 99(6):1716–1721. Online:https://bit.ly/3gN9r1W.

Calder, J., Roy, M., and Wang, W. (2018). Performance and emissions of a diesel engine fueled by biodiesel-diesel blends with recycled expanded polystyrene and fuel stabilizing additive. *Energy*, 149:204–212. Online:https://bit.ly/3kGYe5m.

Chakrabarti, M. and Ali, M. (2008). Engine emissions testing of indigenous biodiesel/diesel fuel blends in pakistan. *NED Univ. J. Res*, 5(2):1–9. Online:https://bit.ly/3agMEci.

Chakrabarti, M. and Ali, M. (2009). Performance of compression ignition engine with indigenous castor oil bio diesel in pakistan. *NED university Journal of research*, 6(1):10–20. Online:https://bit.ly/2Cowdyo.

Chauhan, S. and Shukla, A. (2011). *Environmental Impacts of Production of Biodiesel and Its Use in Transportation Sector*, chapter Environmental Impact of Biofuels, pages 1–13. InTech., Croatia.

Climate Change Indicators (2015). Climate change indicators: Greenhouse gases. Online:https://bit.ly/33Q426H. Retrieved May 30, 2020.

DAWN (2019). High speed diesel (hsd) sales to 6.764 m tonnes. Online:https://bit.ly/3itfJEu. Retrieved May 30, 2020.

Dincer, K. (2008). Lower emissions from biodiesel combustion. *Energy Sources, Part A*, 30(10):963–968. Online:https://bit.ly/3kE8RG1.

Mall, A. P. (2015). Performance and emission testing of neem oil methyl ester (biodiesel). *nternal Combustion Engine. International Journal of Innovative Research in Science, Engineering and Technology*, 4(11):11101–11111. Online:https://bit.ly/31LRoD5.

Nair, J., Kaviti, A. K., and Daram, A. K. (2017). Analysis of performance and emission on compression ignition engine fuelled with blends of neem biodiesel. *Egyptian Journal of Petroleum*, 26(4):927–931. Online:https://bit.ly/3alfYyH.

Pervaz, M. A. (2018). Pakistan energy yearbook 2017. Technical report, Ministry of Energy (Petroleum Division), Hydrocarbon Development Institute of Pakistan, Islamabad.

Qamar, M., Liaquat, R., Jamil, U., Mansoor, R., and Azam, S. (2020). Techno-spatial assessment of waste cooking oil for biodiesel production in pakistan. *SN Applied Sciences*, 2:1–16. Online:https://bit.ly/2FkmH0h.

Rao, T., Rao, G., and Reddy, K. (2008). Experimental investigation of pongamia, jatropha and neem methyl esters as biodiesel on ci engine. *Jordan Journal of Mechanical and Industrial Engineering*, 2(2):117–122. Online:https://bit.ly/3gVkO87.

Yuosafzai, F. (2018). 7000mw shortfall triggers extra unscheduled loadshedding. February 2019.

CO_2 MITIGATION STRATEGIES BASED ON SOIL RESPIRATION

ESTRATEGIAS DE MITIGACIÓN DE CO_2 A PARTIR DE LA RESPIRACIÓN DEL SUELO

Leticia Citlaly López-Teloxa[1]* and Alejandro Ismael Monterroso-Rivas[2]

[1] *Department of Crop Science, Universidad Autónoma de Chapingo. Km 38.5 carretera México-Texcoco, Chapingo, 56230, Estado de México, Mexico.*
[2] *Department of Soil, Universidad Autónoma de Chapingo. Km 38.5 carretera México-Texcoco, Chapingo, 56230, Estado de México, Mexico.*

*Corresponding author: citlaly_lo@hotmail.com

Abstract

Soil, in addition to storing, provides CO_2 to the atmosphere emitted by soil respiration, mainly due to biotic and abiotic factors, as well as soil management. The objective of the research was to evaluate soil respiration in different uses and quantify its CO_2 emissions at two different times of the year, as well as estimate its storage to make a balance to establish strategies that allow with the climate change mitigation. The CO_2 emission was measured every 30 min by using a closed dynamic chamber placed on the soil and integrated with an infrared gas analyzer, as well as temperature and moisture of the soil with sensors. Three land uses (agroforestry, forestry and agricultural) and two seasons of the year (summer and winter) were analyzed for 24 continuous hours at each site. Positive correlation between environmental temperature and soil respiration was found. The agricultural system stores low carbon content in the soil (50.31 t C ha^{-1}) and emits 9.28 t of C ha^{-1} in the highest temperature season, in contrast to a natural system that emits 3.98 t of C ha^{-1} and stores 198.90 t of C ha^{-1}. The balance sheet reflects the need to know $CO2$ emissions to the atmosphere from soils and not just storages. Having scientific support from the ground to the atmosphere is an important step in decision-making that will contribute to climate change mitigation.

Keywords: Agricultural, C storage, land use change, agroforestry, forestry.

Resumen

El suelo, además de almacenar es fuente de CO_2 a la atmósfera emitido por la respiración del suelo, principalmente por factores bióticos y abióticos, así como del manejo del suelo. El objetivo de la investigación fue evaluar la respiración del suelo en diferentes usos y cuantificar las emisiones de CO_2 en dos momentos diferentes del año, así como estimar el almacén de este para hacer un balance que permita establecer estrategias que ayuden con la mitigación del cambio climático. Mediante una cámara dinámica cerrada colocada en el suelo e integrada con un analizador de gas

infrarrojo se midió la emisión de CO_2 cada 30 min, así como la temperatura y la humedad del suelo con sensores. Se analizaron tres usos del suelo (agroforestal, forestal y agrícola) y dos temporadas del año (verano e invierno) durante 24 horas continuas en cada en sitio. Se encontró que existe correlación positiva entre la temperatura ambiental y la respiración del suelo. El sistema agrícola almacena bajo contenido de carbono en el suelo (50,31 t C ha^{-1}) y libera hasta 9,28 t de C ha^{-1} en la temporada de mayor temperatura, en contraste con un sistema natural que emite 3,98 t de C ha^{-1} y almacena 198,90 t de C ha^{-1}. El balance refleja la necesidad de conocer las emisiones de CO_2 a la atmósfera por los suelos y no sólo los almacenes. Contar con soporte científico desde la respiración del suelo a la atmosfera es un paso importante para la toma de decisiones que contribuyan a la mitigación del cambio climático.

Palabras clave: Agrícola, almacén de C, cambio de uso de suelo, agroforestería, forestal.

Orcid IDs:

Leticia Citlaly López-Teloxa: http://orcid.org/0000-0002-0258-325X
Alejandro Ismael Monterroso-Rivas: http://orcid.org/0000-0003-4348-8918

1 Introduction

The soil can act as a source and sink of atmospheric carbon dioxide (CO_2) (Sainju et al., 2008). The constant increase in CO_2 to the atmosphere is the main factor of climate change, as well as the increase in temperatures and change in precipitation patterns (Liebermann et al., 2020). One of the main sources of CO_2 emissions is soil, also known as soil respiration (SR), which is also one of the crucial components within the carbon cycle in terrestrial ecosystems (Murcia-Rodríguez and Ochoa-Reyes, 2008). It is well known that small changes in SR can influence the concentration of atmospheric carbon and caloric balance (Kane et al., 2005; Murcia-Rodríguez and Ochoa-Reyes, 2008). Understanding SR is an important step, as it helps determine whether an ecosystem behaves as a source of carbon or CO_2 sink ((Burbano, 2018; Singh et al., 2015). Unfortunately, the change in land use, which is defined as the change from soil cover to other use, and changes in management practices can have important C balance ratios, which is an important precursor to the increase in SR (Francioni et al., 2019; Wang et al., 2013).

In Mexico, (SEMARNAT-INECC, 2018), from 1990 to 2015 the increase in CO_2e was 208%, whereas in 2015 net emissions amounted to 503 473.80 Gg of CO_2e, of which 11 340 Gg of CO_2e correspond to deforestation for new farmland. Although soil processes play a key role in carbon flows in ecosystems, there is still little information on soil breathing dynamics. It is important to understand the impact of environmental changes on ecosystems and to identify the factors that control CO_2 emissions from the soil and their effects on emission rates (Ramírez and Moreno, 2008). The determination of SR can contribute to the development of better mitigation tools. In addition, it provides detailed information to promote co-activities between climate change mitigation and adaptation strategies, and will be based on soil management and conservation (Serrano et al., 2017).

For example, Araújo de Santos et al. (2019) reported that a crop of corn emits 0.99 μmol CO_2 m^{-2} s^{-1} and corn cropped with bean 1.00 μmol CO_2 m^{-2} s^{-1}. In addition, the application of different types and concentrations of fertilizer influence SR (Chi et al., 2020). Soil management influences SR, as according to Zsolt et al. (2020), conventional plowing methods favor the increase of SR. In turn, Costa et al. (2018) evaluated soil respiration in a preserved forest and cocoa SAF with and without management, finding that the first emits 45.03 mg CO_2-C m^{-2} h^{-1}, while SAF without management emits up to 125 mg CO_2-C m^{-2} h^{-1} and with management 41.8 mg CO_2-C m^{-2} h^{-1}. On the other hand, in a pine forest (*Pinus palustris Mill.*) the annual SR was evaluated in stands from 5 to 21 years old, 12.0 Mg C ha^{-1} and 13.9 Mg C ha^{-1}, respectively (ArchMiller and Samuelson, 2016). Tang et al. (2006) report SR in different mixed and pine forests 450.5±22.3, 381.8±18.2 and 250.9±20.2 mg CO_2-C m^{-2} h^{-1}, respectively, where they also report that it correlated with soil temperature and humidity. Hence, SR can be predicted in combination with soil temperature and water content; and the effects of Ts and Hs on soil respiration will vary depending on the location of the sampling (Zhao et al., 2013).

Therefore, the aim of this study was to evaluate soil respiration in different uses and quantify CO_2 emissions at two different times of the year, as well as to estimate the carbon store to establish balances to formulate strategies that contribute to climate change mitigation.

2 Materials and methods

2.1 Description of the area

2.1.1 Agroforestry and agricultural systems

Both systems cover an area of 0.05 ha (10 × 50 m) and are located between coordinates $19°49'N$ and $98°89'W$. They are located at 2250 masl in a predominantly temperate subhumid climate with summer rainfall, with an average annual temperature of $16.4°C$ and average annual precipitation of 618 mm. The floors are Vertisoles type. The systems belong to a farm that integrates various technologies and have an organic and agroecological production of vegetables, fruit and meat, such as fish, rabbit and sheep for approximately 20 years.

The agroforestry system (AS) consists of technology of crops in alleys with fruit trees of *Prunus persica* (peach), Pyrus communis (pears) and *Malus domestica* (apples) in the tree formation. The separation between tree and tree is 2.5 m. Annually

planted interspersed vegetables (*Beta vulgaris sp.* (chard), *Lactuca sativa* (lettuce) and *Cucurbita pepo* (pumpkin), (Ruta graveolens and *Avena sativa* (for grazing). The agricultural system of monoculture (ASM) consists of maize (*Zea mays*) planted in rows and with irrigation system. To start the growing cycle, the soil is tilled and periodically weeded manually.

2.1.2 Temperate forestry system

The temperate forest system (TFS) covers an area of 1640.48 ha, and it is located between coordinates $19°15'N$ and $98°37'O$ (Chávez-Salcedo et al., 2018).The dominant climates are semi-cold in the parts of higher altitude and temperate in the areas nearby; the average annual precipitation ranges from 800 mm to 1200 mm, the average annual temperature ranges from $6°C$ in the highest altitude areas to $14°C$ (Lomas-Barrié et al., 2005).

2.2 Soil respiration

SR was measured with a 8100A LICOR portable equipment and two cameras, one fixed and one quick tap (LI-COR Biosciences, 2015). The chambers are closed and have 20 cm of diameter, and are placed on PVC collars inserted into the floor at 3 cm depth at least 24 hours in advance (López-Teloxa et al., 2020). The experimental design consisted of installing two separate chambers at 5 m to achieve two simultaneous observations every half hour. The 8100A LICOR monitors changes in CO_2 concentration over time within the chamber through optical absorption spectroscopy in the infrared region (IRGA infrared gas analyzer). The camera measures for 90 seconds the concentration of CO_2 of which the first 30 seconds are deadband to stabilize and are not considered. Atmospheric CO_2 accumulated in the chamber is measured as CO_2 flow in micromoles per square meter per second (μmol m^{-2} s^{-1}) of dry air, which are subsequently converted to grams per hour (g CO_2 m^{-2} h^{-1}). The reported CO_2 flow is the result of soil CO_2 emission by autotrophic (plant roots) and heterotrophic (microorganisms) (Moitinho et al., 2015). The camera has sensors (model p/n8150-203 Soil Temperature Probe and 8100-204 Theta Soil Soil Soil Probe soil) that also allow to record soil temperature and humidity (St and Sh, respectively).

2.3 Organic carbon stored

To determine soil organic carbon (SOC) a total of 9 soil samples were analyzed for each of the 3 sites, having a total of 27 per season. Each sample was collected by the method of unchanged samples at three depths, 0-10, 10-20 and 20-30 cm with a drill composed of two radio rings 2.6 cm and a height of 2.9 cm, so the floor volume calculated by each ring is 63.98 cm^3 (Etchevers Barra et al., 2005). The collected samples were dried at room temperature and sifted with a 100 mm sieve. To obtain the DAP, the complete (dry) soil sample was weighed and stones and roots were separated and weighed. The percentage of organic carbon was determined with a total organic carbon analyzer (TOC-V, Shimadzu Labs) equipped with a solid sample module (model SSM-5000, Shimadzu Labs).

2.4 Experimental design

SR was determined in three land uses (TFS, AS and ASM) and in two seasons of the year, summer and winter. SR was determined for 24 hours at each site, thus having 3 sites, 144 h and 576 measurements per season. Daily meteorological registers [environmental temperature (Tamb) and precipitation (Prec)] were obtained with a portable weather station (The Crosse Technology Mod.C86234) placed at 1.5 m height and 1 m away from the measuring and sampling chamber. In addition, the data were corroborated with weather stations near the sampling sites: Estación Chapingo and Estación Avila Camacho operated by Cuenca Aguas del Valle de México Agency (OCAVM) and Estación Altzomoni operated by Sistema Monitor Nacional (https://smn.cna.gob.mx/es/estaciones-meteorologicas-automaticas-3), Mexico state.

2.5 Statistical analysis

The statistical analysis was done in 2 moments: 1) The variance analysis (ANDEVA) and the Tukey test were used to identify statistically significant differences ($p < 0.05$) in the values of respiration, temperature and soil humidity between the two seasons and the three uses of the soil. For more accuracy and reduced potential errors, the data was first standardized. 2) Pearson correlation analysis was used to identify correlation between soil respiration

from the three soil uses and climatic variables (St, Sh, Tamb and Prec).

3 Results

3.1 Area description

SR in all three land uses and both seasons are presented in Figure 1. SR in TFS fluctuates from 0.20 to 0.40 g CO_2 m^{-2} h^{-1}, in AS from 0.41 to 0.61 g CO_2 m^{-2} h^{-1} and in ASM from 0.67 to 0.99 g CO_2 m^{-2} h^{-1} in summer. Increases are seen at 08:00 hours, reaching maximums between 13:00 and 15:00 hours. SR in ASM is 35 % higher compared to AS. SR in a natural system such as TFS is 50 % lower compared to agricultural management, since this is mainly due to the mineralization of organic carbon in the soil that increases its decomposition rate by farming and soil structure is altered, increasing CO_2 as reported by Baah-Acheamfour et al. (2016). On the other hand, during winter, TFS fluctuates from 0.15 to 0.24 g CO_2 m^{-2} h^{-1}, in AS from 0.19 to 0.62 g CO_2 m^{-2} h^{-1} and in ASM from 0.23 to 0.60 g CO_2 m^{-2} h^{-1}. SR in natural systems is mainly due to the joint action of biotic and abiotic factors such as: type and age of vegetation, soil type and climatic variations (Hu et al., 2018).

Regarding temperature and humidity, Oertel et al. (2016) mention that these vary significantly with the depth and characteristics of the area, for example, exposure to light, shadow and wind. During summer, in the AS and ASM the environment temperature showed variation from 13.5 to 23.9°C and zero millimeters of rain reported. While in the forest, the variation was 6.9 to 13.3°C and 2.6 mm of rain throughout the day. AS and ASM present similar values and behaviors in SR throughout the season from 15.7 to 24.8°C and 15.3 to 23.5°C, respectively, with highs between 12:00 and 14:00 hours, time in which respiration has its peaks. On

the other hand, in the TFS, SR ranged from 8.12 to 11.97°C. In relation to Sh, in the AS it ranged from 0.16 to 0.20 m^3 m^{-3}, while the humidity in the SAM and SFT is similar, 0.36 to 0.40 m^3 m^{-3} and 0.37 to 0.53 m^3 m^{-3}, respectively. In ASM the increase of Sh is mainly due to the system being irrigated, which is carried out every day from 10:00 to 12:00 hour.

During winter, the environment temperature values are lower as expected, in AS and ASM the environment temperature ranged from 3.4 to 23.9°C and zero millimeters of rain. While in TFS the temperature ranged from 2.2 to 13.3°C and 1 mm of rain throughout the day. AS and ASM presented similar values and behaviors in the St throughout the day, from 3.1 to 20.3°C and 2.6 to 20.6°C, respectively, with highs between 13:00 and 14:00 hours. Unlike the first season, AS and TFS humidity records are similar 0.25 to 0.27m^3 m^{-3} and 0.22 to 0.23m^3 m^{-3}, respectively. Due to a fallow period, Sh in ASM presented the lowest recorded values of 0.15 to 0.16m^3 m^{-3}, along with the fact of the lack of precipitation during the period evaluated. In agricultural crops, SR correlates with physical characteristics of soil, soil temperature and humidity (Araújo de Santos et al., 2019).

Soil respiration had higher emissions in higher temperature periods, so it can be ensured that it is mostly correlated with it (Figure 1). On the other hand, due to irrigation, SR increases in dry soils by increasing microbial activities (Sainju et al., 2008). As for the COS, 198.9, 89.97 and 58.55 t ha^{-1} concentrations were found for TFS, AS and ASM, respectively, for summer, while for the following season the first two cases decreased their concentration to 171.36 and 76.50 t ha^{-1}, while ASM increased to 65 t ha^{-1}. However, the following order of concentration is generally presented for summer and winter ASM >AS >TFS, similar to López-Teloxa et al. (2017), who claimed that land use and management significantly influences the content of COS.

3.2 Statistical analysis

Table 1 summarizes the average SR, SOC, St and Sh values per season (summer and winter) and land uses (TFS, AS, and ASM). ANDEVA was performed following the three factors of the sampling protocol to determine the variability of soil parameters between the factors (season, land use and sampling

time) of the area (Table 2). SR and St values showed significant differences in season, land use and sampling time, as well as in their interactions. Hence, the variation in environmental temperature in each season, as well as soil disturbance due to different uses significantly influence the SR and St (Baah-Acheamfour et al., 2016; Murcia-Rodríguez
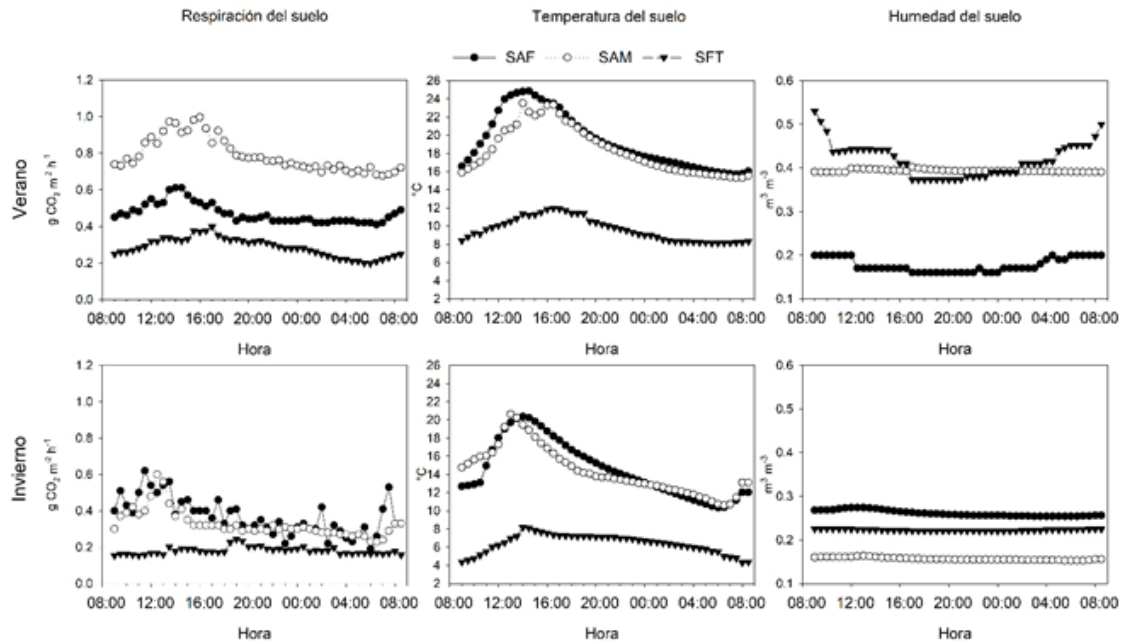
Figure 1. Variation of SR, St and Sh throughout the day in Summer and Winter.

and Ochoa-Reyes, 2008). In addition to the above, management practices significantly affect SR (Sainju et al., 2014). Despite the fact that environmental conditions such as temperature and precipitation normally have a dominant influence on the amount of SOC in the soil (López-Teloxa et al., 2017), no statistical differences were observed according to sampling seasons (p = 0.40), but they are observed according to the uses (p<0.05). Sampling seasons, land uses, measurement time and seasonal interaction with land use influence the variation of Sh (p<0.05).

Several studies have shown that there is correlation with SR and environmental variables as well as with their combined effect (Figure 2) (Murcia-Rodríguez et al., 2012; Ramírez and Moreno, 2008). As is the case of AS and ASM, where St and Tamb, have high positive correlation in SR (p<0.05), but there is inconclusive evidence on significance in TFS (p>0.05). In addition to the low temperatures in the TFS, the system is preserved with little or no soil disturbance unlike the AS and ASM. On the other hand, Sh presents positive correlation in ASM and TFS, this is consistent with other studies where it

was reported that the values of SR increases after precipitation or irrigation events (La Scala et al., 2001; Moitinho et al., 2015; Panosso et al., 2009), while it is negative for AS in all three cases p<0.05. The relationship between temperature and humidity content with SR results in complex interactions that depend on the relative limitation of these two variables on microbial and root activity, as well as on the diffusion of gases (Ramírez and Moreno, 2008). Since no precipitation data was reported during AS and ASM sampling for both seasons, Pearson's correlation is zero. While in the TFS the correlation is positive with the precipitation (p<0.05). SOC has a negative influence, i.e. it decreases by increasing SR, this occurs for AS and TFS while it is positive for ASM, the latter could be due to fertilizer in the area (Sainju et al., 2008). In short, SR is mostly influenced by environmental and soil variables, with soil temperature being most influential (Mukumbuta et al., 2019). This information is consistent with ArchMiller and Samuelson (2016); Han et al. (2018), Wang et al. (2013), and Wang et al. (2013), who say that SR increases exponentially with the increase in St.

Table 1. Respiration and CO_2 storing by land use and season of the year.

USE OF THE SOIL	SEASON	SR $g\ m^{-2}\ h^{-1}$	SOC $t\ ha^{-1}$	St $^{\circ}C$	Sh $m^3\ m^{-3}$
SFT	Summer	0.29±0.05a	198.9±31.4a	9.65±1.30a	0.42±0.04a
	Winter	0.18±0.02b	171.36±19.7a	6.36±1.04b	0.22±0.00b
SAF	Summer	0.47±0.05a	86.97±7.96a	19.32±3.05a	0.18±0.01a
	Winter	0.38±0.11b	76.5±7.78a	14.60±3.14b	0.26±0.007b
SAM	Summer	0.79±0.09a	58.55±11.65a	18.34±2.61a	0.39±0.002a
	Winter	0.32±0.07b	65.00±14.1a	14.40±2.64b	0.16±0.003b

Letters a and b indicate significant differences (Tukey test).
TFS-Temperate Forest System, AS-Agroforestry System, ASM-Agricultural Monoculture System.

Table 2. P-values resulting from multivariate variance analysis at a 95 % confidence level.

Factor	Variable			
	SR	SOC	St	Sh
Season	0.00	0.40	0.00	0.00
Soil use	0.00	0.00	0.00	0.00
Measurement time	0.00	N.D.	0.00	0.04
Season*Soil use	0.00	0.49	0.00	0.00
Season * Measurement time	0.00	N.D.	0.00	1.00
Soil use * Measurement time	0.01	N.D.	0.00	0.92

4 Discussion

As expected in a forest, lower emissions were observed compared to an agricultural system of up to 50 % less. Data is similar to that found by Campos (2014), who reports that up to 89.6 mg C $m^2\ h^1$ is emitted in a cloud forest while in an agricultural system with corn-potato-corn rotation 128.1 mg C $m^2\ h^1$ is emitted. Regarding the differences between summer and winter, a similar behavior is found, although ASM reduces its emission to a level similar to AS, but retains the tendency to be more emitting, since altered systems have higher CO_2 emissions especially in summer (Abdalla et al., 2018). The results of this study focus on the importance of soil respiration analysis in different uses, in order to offer multifunctional systems that ensure food security and diversity of environmental benefits.

Soil use and management practices can affect CO_2 emission into the atmosphere by modifying soil temperature and water content (Baah-Acheamfour et al., 2016). A commonly used practice in agricultural systems is tilling, which can make the soil dry; hence, it increases the temperature due to soil disturbance and decreases waste on the soil surface, which is consistent with Nouchi and Yonemura (2005) in a rice paddy with tillage, where the annual emission is 2845 g $CO_2\ m^{-2}$ per year while without tillage is 2198 g $CO_2\ m^{-2}$ per year.

The results obtained here show that there is a positive correlation between environmental temperature and CO_2 or SR emissions, which is consistent with Wang et al. (2013), who say that SR is lower at low temperatures. On the other hand, irrigation in soils that have remained directly exposed to the sun's rays for a long period of time increases SR, due to microbial breathing that is limited by water stress (Curtin et al., 2000)

The system and type of crop, as is the case with AS and ASM, differ in terms of SR, St and Sh, since there is greater soil coverage in AS than in a monoculture, in addition to fallow periods that affect the intensity of shadow and evapotranspiration (Sainju et al., 2008). Management practices, such as farming, can increase soil CO_2 emission by altering soil aggregates, reducing plant residues and oxidizing soil organic C by more than 47 % in 5 years, and zero farming practices and reduced crop intensity can increase SOC (Patiño-Zúñiga et al., 2009). This is a limitation of our results but they frame future research work to conduct further respiration

studies in different uses and soil management.

When it comes to carbon storing, the behavior is as expected, i.e., TFS retains more than ASM, while there are no differences for seasons. This is similar to López-Teloxa et al. (2017) where SOC concentration is higher in a forest with secondary vegetation

in contrast to temporary agriculture, 28.44 and 20.42 t ha^{-1}, respectively. Once the emission and storage of C was quantified, it allowed to raise a balance sheet (table 3). As found by Mukumbuta et al. (2019) who reported a balance of 1.2 t C ha^{-1} (SOC of 8 t C ha^{-1} and SR of 6.8 t C ha^{-1}) in pasture.
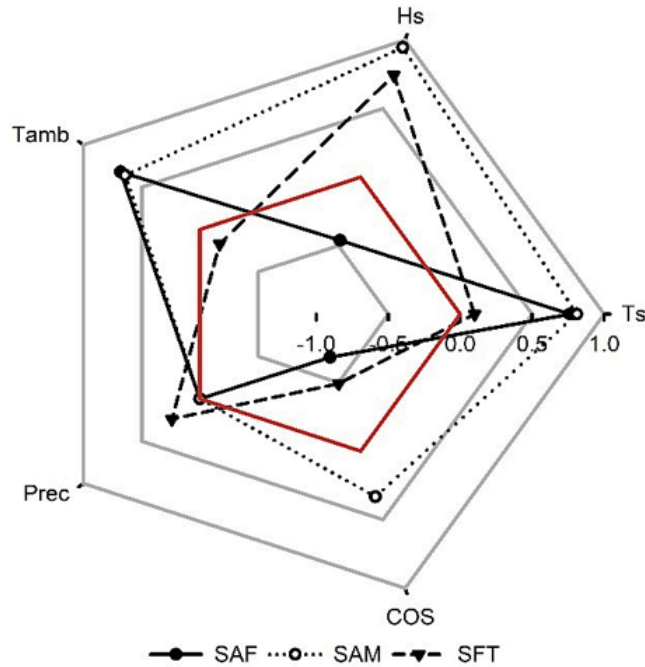

Figure 2. Correlation with environmental and SOC variables according to SR. Note: Variables close to the red line have no correlation.

An important factor that helps to understand the integral C balance of an agroecosystem is the close relationship between SR and SOC (Alberti et al., 2010). It is clear that an agricultural system preserves lower amounts of carbon in the soil, releasing up to 9.28 t of C ha^{-1} in the highest temperature season, in contrast to a natural system (3.98 t of C ha^{-1}). Therefore, agroforestry systems (table 3) are intermediate points that allow to ensure food and preserve as much possible). According to various authors such as Baah-Acheamfour et al. (2016) and Kwak et al. (2019) it is a land-use practice that, in addition to introducing trees and shrubs to farmland or livestock, helps to potentially mitigate CO_2 emissions from agricultural systems.

Finally, it should be remembered that according to IPCC (2013) the increase in temperature is unequivocal and an increase in temperature is expected worldwide (UNFCCC, 2015). Hence, soil can contribute to climate change mitigation as land use is systemized and the organic carbon of land is conserved (Burbano, 2018), adapting management and irrigation practices in different seasons of the year (Francioni et al., 2019; Chi et al., 2020). The actions carried out and adapted to each system offer beneficial solutions to face multiple environmental and social challenges (Tschora and Cherubini, 2020). Thus, the following studies should focus on the different soil management practices, seasons of the year and growing cycles, in order to deepen on the balance of SR and SOC.

Table 3. Balance of carbon emitted and stored from the soil.

USE OF THE SOIL	SEASON	C emitted t ha^{-1}	C stored t ha^{-1}			
			Depth (cm)			Total
			0 - 10	10 - 20	20 -30	
TFS	Summer	3.98	77.21	64.54	57.14	198.90
	Winter	1.91	66.59	58.30	46.46	171.36
AS	Summer	5.55	29.24	28.74	23.36	81.34
	Winter	4.36	25.88	24.41	20.85	71.14
ASM	Summer	9.28	14.94	14.99	20.39	50.31
	Winter	3.86	21.42	21.32	24.04	66.78

TFS=Temperate forestry system, AS=Agroforestry system, ASM=Agricultural system of monoculture.

5 Conclusiones

Studying storage-carbon emission dynamics in terrestrial ecosystems underpins the understanding of the problem and helps in the definition of better policies and care programs. The change in land use that increases soil organic carbon losses mainly in CO_2 should be avoided while promoting, for example, natural coverage or agroforestry production systems.

The increase in global temperature has impacted the carbon cycle, especially on its soil, which is exacerbated by deforestation and openness to new agricultural areas. It is believed that it is important to improve the knowledge of various multifunctional production systems that contribute to the reduction of CO_2 emissions and increase carbon stored in the soil.

This study made it possible to evaluate land uses that mostly contribute to mitigating the effects of climate change with the incorporation of agroforestry systems into the production system; in addition to the importance of year-round soil coverage, as fallow periods can be detrimental to both soil and CO_2 contribution to the atmosphere. It should be noted that the data obtained are the first reported from the evaluated areas, so it is important to continue the measurements throughout the year to characterize the behavior in SR of agroforestry systems. Having scientific support from SR (CO_2 emission) to the atmosphere is an important step in decision-making that will contribute to climate change mitigation.

References

Abdalla, K., Mutema, M., Chivenge, P., Everson, C., and Chaplot, V. (2018). Grassland degradation significantly enhances soil co2 emission. *Catena*, 167:284–292. Online:https://bit.ly/3kZk6co.

Alberti, G., Vedove, G., Zuliani, M., Peressotti, A., Castaldi, S., and Zerbi, G. (2010). Changes in co2 emissions after crop conversion from continuous maize to alfalfa. *Agriculture, Ecosystems and Environment*, 136(1–2):139–147. Online:https://bit.ly/3aFbSkZ.

Araújo de Santos, G., Moitinho, M., de Oliveira Silva, B., Xavier, C. V., Teixeira, D. D. B., Corá, J. E., and Júnior, N. L. S. (2019). Effects of long-term no-tillage systems with different succession cropping strategies on the variation of soil co2 emission. *Science of the total environment*, 686:413–424. Online:https://bit.ly/2DZQR8U.

ArchMiller, A. A. and Samuelson, L. J. (2016). Intra-annual variation of soil respiration across four heterogeneous longleaf pine forests in the southeastern united states. *Forest ecology and management*, 359:370–380. Online:https://bit.ly/34dI4uA.

Baah-Acheamfour, M., Carlyle, C. N., Lim, S., Bork, E. W., and Chang, S. X. (2016). Forest and grassland cover types reduce net greenhouse gas emissions from agricultural soils. *Science of the total Environment*, 571:1115–1127. Online:https://bit.ly/2Q9KYbr.

Burbano, H. (2018). El carbono orgánico del suelo y su papel frente al cambio climático. *Revista de Ciencias Agrícolas*, 35(1):82–96. Online:https://bit.ly/2QaRNte.

Campos, A. (2014). Trends in soil respiration on the eastern slope of the cofre de perote volcano (mexico): Environmental contributions. *Catena*, 114:59–66. Online:https://bit.ly/2Q6e7UY.

Chávez-Salcedo, L. F., Queijeiro-Bolaños, M. E., López-Gómez, V., Cano-Santana, Z., Mejía-Recamier, B., and Mojica-Guzmán, A. (2018). Contrasting arthropod communities associated with dwarf mistletoes arceuthobium globosum and a. vaginatum and their host pinus hartwegii. *Journal of Forestry Research*, 29(5):1351–1364. Online:https://bit.ly/3hexeIt.

Chi, Y., Yang, P., Ren, S., Ma, N., Yang, J., and Xu, Y. (2020). Effects of fertilizer types and water quality on carbon dioxide emissions from soil in wheat-maize rotations. *Science of The Total Environment*, 698:134010. Online:https://bit.ly/3aDtuxG.

Costa, E. N. D., Landim de Souza, M. F., Lima Marrocos, P. C., Lobão, D., and Lopes da Silva, D. M. (2018). Soil organic matter and co2 fluxes in small tropical watersheds under forest and cacao agroforestry. *PloS one*, 13(7):e0200550. Online:https://bit.ly/3g7JbhK.

Curtin, D., Wang, H., Selles, F., McConkey, B. G., and Campbell, C. A. (2000). Tillage effects on carbon fluxes in continuous wheat and fallow–wheat rotations. *Soil Science Society of America Journal*, 64(6):2080–2086. Online:https://bit.ly/3j0SJNt.

Etchevers Barra, J., Monreal, C. M., C., H., Acosta, M. M., Padilla, J., and R., L. (2005). *Manual para la determinación de carbono en la parte aérea y subterránea de sistemas de producción en laderas.*

Francioni, M., D'Ottavio, P., Lai, R.and Trozzo, L., Budimir, K., Foresi, L., Kishimoto-Mo, A., Baldoni, N., Allegrezza, M., Tesei, G., and Toderi, M. (2019). Seasonal soil respiration dynamics and carbon-stock variations in mountain permanent grasslands compared to arable lands. *Agriculture*, 9(8):165. Online:https://bit.ly/3l3lWZZ.

Han, M., Shi, B., and Jin, G. (2018). Conversion of primary mixed forest into secondary broadleaved forest and coniferous plantations: Effects on temporal dynamics of soil co2 efflux. *Catena*, 162:157–165. Online:https://bit.ly/3aEUBbu.

Hu, S., Li, Y., Chang, S., Li, Y., Yang, W., Fu, W., Liu, J., Jiang, P., and Lin, Z. (2018). Soil autotrophic and heterotrophic respiration respond differently to land-use change and variations in environmental factors. *Agricultural and Forest Meteorology*, 250:290–298. Online:https://bit.ly/2EfVHyq.

IPCC (2013). *Climate Change 2013: The Physical Science Basis. Contribution of Working Group I to the Fifth Assessment Report of the Intergovern-mental Panel on Climate Change.* Cambridge University Press, Cambridge, United Kingdom and New York, NY, USA. 1535 pp.

Kane, E. S., Valentine, D. W., Schuur, E., and Dutta, K. (2005). Soil carbon stabilization along climate and stand productivity gradients in black spruce forests of interior alaska. *Canadian Journal of Forest Research*, 35(9):2118–2129. Online:https://bit.ly/325LJrC.

Kwak, J. H., Lim, S. S., Baah-Acheamfour, M., Choi, W. J., Fatemi, F., Carlyle, C. N., Bork, E., and Chang, S. X. (2019). Introducing trees to agricultural lands increases greenhouse gas emission during spring thaw in canadian agroforestry systems. *Science of the Total Environment*, 652:800–809. Online:https://bit.ly/3h8WcJb.

La Scala, N., Lopes, A., Marques, J., and Pereira, G. T. (2001). Carbon dioxide emissions after application of tillage systems for a dark red latosol in southern brazil. *Soil and Tillage Research*, 62(3-4):163–166. Online:https://bit.ly/34kzDxx.

Liebermann, R., Breuer, L., Houska, T., Kraus, D., Moser, G., and Kraft, P. (2020). Simulating long-term development of greenhouse gas emissions, plant biomass, and soil moisture of a temperate grassland ecosystem under elevated atmospheric co2. *Agronomy*, 10(1):50. Online:https://bit.ly/2YhwCdr.

Lomas-Barrié, C. T., Terrazas-Domínguez, S., and Maga, H. (2005). Propuesta de ordenamiento ecológico territorial para el parque nacional zoquiapan y anexas. *Revista Chapingo. Serie Ciencias Forestales y del Ambiente*, 11(1):57–71. Online:https://bit.ly/31aHbRE.

López-Teloxa, L., Monterroso-Rivas, A., and Gómez-Díaz, J. (2020). Diseño de calibración para cuantificar emisiones de *co2* (respiración) en suelos durante intervalos horarios diurnos. Agrociencia, p. En prensa.

López-Teloxa, L. C., Cruz-Montalvo, A., Tamaríz-Flores, J. V., Pérez-Avilés, R., Torres, E., and Castelán-Vega, R. (2017). Short-temporal variation of soil organic carbon in different land use systems in the ramsar site 2027 'presa manuel ávila camacho'puebla. *Journal of Earth System Science*, 126(7):95. Online:https://bit.ly/3g9vajr.

Moitinho, M., Padovan, M. P., Panosso, A. R., Teixeira, D. D. B., Ferraudo, A. S., and La Scala, N. (2015). On the spatial and temporal dependence of co_2 emission on soil properties in sugarcane (saccharum spp.) production. *Soil and Tillage Research*, 148:127–132. Online:https://bit.ly/32cv0TL.

Mukumbuta, I., Shimizu, M., and Hatano, R. (2019). Short-term land-use change from grassland to cornfield increases soil organic carbon and reduces total soil respiration. *Soil and Tillage Research*, 186:1–10. Online:https://bit.ly/2YkdICK.

Murcia-Rodríguez, M., Ochoa-Reyes, M. P., and Poveda-Gómez, F. (2012). Respiración del suelo y caída de hojarasca en el matorral del bosque altoandino (cuenca del río pamplonita, colombia). *Caldasia*, pages 165–185. Online:https://bit.ly/2EhIHIz.

Murcia-Rodríguez, M. A. and Ochoa-Reyes, M. P. (2008). Respiración del suelo en una comunidad sucesional de pastizal del bosque altoandino en la cuenca del río pamplonita, colombia. *Caldasia*, 30(2):337–353. Online:https://bit.ly/2YjaCiy.

Nouchi, I. and Yonemura, S. (2005). Co~ 2, ch~ 4 and n~ 2o fluxes from soybean and barley double-cropping in relation to tillage in japan. *Phyton - Annales Rei Botanicae*, 45(4):327. Online:https://bit.ly/325LHAc.

Oertel, C., Matschullat, J., Zurba, K., Zimmermann, F., and Erasmi, S. (2016). Greenhouse gas emissions from soils—a review. *Geochemistry*, 76(3):327–352. Online:https://bit.ly/3ghU1lg.

Panosso, A. R., Marques, J., Pereira, G. T., and La Scala, N. (2009). Spatial and temporal variability of soil co2 emission in a sugarcane area under green and slash-and-burn managements. *Soil and Tillage Research*, 105(2):275–282. Online:https://bit.ly/3l5wHem.

Patiño-Zúñiga, L., Ceja-Navarro, J. A., Govaerts, B., Luna-Guido, M., Sayre, K. D., and Dendooven, L. (2009). The effect of different tillage and residue management practices on soil characteristics, inorganic n dynamics and emissions of n_2o, co_2 and ch_4 in the central highlands of mexico: a laboratory study. *Plant and Soil*, 314(1-2):231–241. Online:https://bit.ly/34mBrGx.

Ramírez, Á. and Moreno, F. (2008). Respiración microbial y de raíces en suelos de bosques tropicales primarios y secundarios (porce, colombia). *Revista facultad nacional de agronomía Medellín*, 61(1):4381–4393. Online:https://bit.ly/3iUf6ny.

Sainju, U. M., Jabro, J. D., and Stevens, W. B. (2008). Soil carbon dioxide emission and carbon content as affected by irrigation, tillage, cropping system, and nitrogen fertilization. *Journal of Environmental Quality*, 37(1):98–106. Online:https://bit.ly/326JtjX.

Sainju, U. M., Stevens, W. B., Caesar-TonThat, T., Liebig, M. A., and Wang, J. (2014). Net global warming potential and greenhouse gas intensity influenced by irrigation, tillage, crop rotation, and nitrogen fertilization. *Journal of Environmental Quality*, 43(3):777–788. Online:https://bit.ly/2CMyIL4.

SEMARNAT-INECC (2018). Sexta comunicación nacional y segundo informe bienal de actualización ante la convención marco de las naciones unidas sobre el cambio climático. techreport Online:https://bit.ly/31cO1Ge, SEMARNAT.

Serrano, E., Nuñez, M., and Valleter, E. (2017). Respiración de dióxido de carbono de suelo, en bosque tropical húmedo–gamboa panamá. *I+D Tecnológico*, 13(2):49–54. Online:https://bit.ly/2FziplG.

Singh, S. K., Thawale, P. R. and, S. J. K., Gautam, R. K., Kundargi, G. P., and Juwarkar, A. A. (2015.). Carbon sequestration in terrestrial ecosystems. *Hydrogen Production and Remediation of Carbon and Pollutants*, 6:99–131. Online:https://bit.ly/3j1DN1h.

Tang, X., Zhou, G., Liu, S., Zhang, D.-Q., Liu, S., Li, J., and Zhou, C. (2006). Dependence of soil respiration on soil temperature and soil moisture in successional forests in southern china. *Journal of Integrative Plant Biology*, 48(6):654–663. Online:https://bit.ly/31efc3o.

Tschora, H. and Cherubini, F. (2020). Co-benefits and trade-offs of agroforestry for climate change mitigation and other sustainability goals in west africa. *Global Ecology and Conservation*, 22:e00919. Online:https://bit.ly/3hrqPdb.

UNFCCC, editor (2015). *Decision 1/CP.21. The Paris Agreement.*, number Online:https://bit.ly/2YntEV3.

Wang, C., Han, Y., Chen, J., Wang, X., Zhang, Q., and Bond-Lamberty, B. (2013). Seasonality of soil co2 efflux in a temperate forest: Biophysical effects of snowpack and spring freeze–thaw cycles. *Agricultural and Forest Meteorology*, 177:83–92. Online:https://bit.ly/3g8wV0o.

Zhao, Z., Zhao, C., Yan, Y., Li, J., Li, J., and Shi, F. (2013). Interpreting the dependence of soil respiration on soil temperature and moisture in an oasis cotton field, central asia. *Agriculture, ecosystems and environment*, 168:46–52. Online:https://bit.ly/2Qbybp6.

POTENTIAL FROM FORESTRY WASTE FOR THE CONTRIBUTION TO THE URBAN ENERGY MATRIX

POTENCIAL DE LOS RESIDUOS FORESTALES PARA LA CONTRIBUCIÓN A LA MATRIZ ENERGÉTICA URBANA

Lucía Yánez-Iñiguez[1]*, Enma Urgilés-Urgilés[1], Esteban Zalamea-León[2] and Antonio Barragán-Escandón[3]

[1] *Faculty of Chemical Sciences, Universidad de Cuenca. Av. 12 de Abril, 010107, Cuenca, Ecuador.*
[2] *Faculty of Architecture and Urbanism, Universidad de Cuenca. Av. 12 de Abril, 010107, Cuenca, Ecuador.*
[3] *Research Group of Energy (GIE), Universidad Politécnica Salesiana. Calle Vieja, Cuenca 010105, Cuenca, Ecuador.*

*Corresponding author: irina.yanezi@ucuenca.edu.ec

Abstract

Nowadays, fossil fuels are the main source for energy supply in urban centers. Therefore, development of renewables from endogenous resources has become a strategy to reduce its consumption. Within that framework, this study case proposes a methodology to estimate the energy potential of urban forestry wastes in Cuenca-Ecuador city, which are obtained from maintenance activities at the public green areas, as an alternative energy source. It has been determined by laboratory analyses the average of the net calorific value of some biomass samples taken at the local area, and its result is about 0.38 tep/ton. From a statistical database, it has been calculated that forestry waste mass available per year in Cuenca city is 608.63 ton. Its energy potential is around 233.13 tep/year and the electrical generation efficiency is approximately 41 tep/year, corresponding to the average consumption of 110 local families. Finally, it is concluded that this energy source could rise significantly through the increase of maintenance activities of public green areas. Furthermore, it represents an alternative for the effective use of this kind of waste.

Keywords: Renewable energies, energy potential, endogenous resources, forestry wastes.

Resumen

Los combustibles fósiles son por ahora la principal fuente de abastecimiento energético de las ciudades. Una estrategia para reducir este consumo es el desarrollo de energías renovables desde recursos endógenos urbanos. Se propone una metodología para determinar el potencial energético que poseen los residuos forestales urbanos en la ciudad de Cuenca-Ecuador, obtenidos mediante las actividades de mantenimiento (poda) de las áreas verdes públicas, con el propósito de transformarlos en fuente energética. Mediante análisis en laboratorio de muestras tomadas en el medio

local, se determina que el poder calorífico inferior promedio que posee la biomasa es de 0.38 tep/ton. A partir de ello, con una base de datos estadísticos se calcula que en la ciudad de Cuenca se dispone de 608.63 ton de masa forestal anualmente. Ésta cuenta con un potencial energético de 233.13 tep/año y una eficiencia para la producción de energía eléctrica de aproximadamente 41 tep/año, que permite cubrir el consumo promedio de 110 familias. Se concluye que esta fuente de energía puede crecer significativamente con el incremento de las actividades de mantenimiento de las áreas verdes públicas y además constituye una estrategia para el aprovechamiento secundario de esta clase de residuos.

Palabras clave: Energías renovables, potencial energético, recursos endógenos, residuos forestales.

Orcid IDs:

Lucía Yánez-Iñiguez: http://orcid.org/0000-0002-1602-3464
Enma Urgilés-Urgilés: http://orcid.org/0000-0001-5511-7570
Esteban Zalamea-León: http://orcid.org/0000-0001-5551-5026
Antonio Barragán-Escandón: http://orcid.org/0000-0003-2254-2524

1   Introduction

The diversification of Renewable Energy (RE) sources is key to sustainable supply systems, especially when urban waste can be leveraged (Arrese and Blanco, 2016). Energy self-supply from endogenous resources is essential to reduce the need for energy imports into cities (Barragán et al., 2019). The energy matrix in Cuenca-Ecuador mostly depends on fossil fuels, whose extraction methods and processes transformation are an important environmental issue (Bristow and Kennedy, 2013). Forest biomass within an energy context refers to the set of renewable elements of organic origin or their derivatives, whose energy comes from solar radiation that is transformed into chemical energy during the photosynthesis process conducted by plant species (Manzano et al., 2012). This chemical energy can be used directly from combustion processes or transformed by thermal methods (gasification) or biological methods (bioethanol production), according to the final requirement of use (Yaman, 2004).

Forest waste from urban pruning operations can be used as a RE for the production of electricity from thermal processes (Pérez et al., 2010). One of the advantages of residual forest biomass is the lack of an ecological or agricultural value, unlike other types of non-arboreal plant waste (Barragán, 2018). Maintaining the Green Public Areas (GPA) is also a need for the urban development, which generates a continuous production of the resource. In five cities in South Korea (Seoul, Daegu, Daejaeon, Gwangju, Busan)the energy Potential (EP) of the biomass from urban forest products has been analyzed in order to establish adequate management for its conversion to energy; obtaining maximum and minimum capacities of 2 625 753 tep/year and 76 760 tep/year, respectively (Kook and Lee, 2015). In General Pueyrredón (Argentina), the usable potential energy of the pruning of public spaces has been assessed, determining that these can meet about 4.37% of the city's electricity consumption (Roberts et al., 2015). However, each locality has its own conditions, either by quantity or by the characteristics of the vegetation (Barragán, 2018). Additionally, the type of energy consumption, the sizing and the supplying also differ, which means great variability in each of the researches in this area.

In analyzing these case studies, it has been established that the determination of the EP requires the knowledge of the Lower Calorific Power (LCP) of the species that make up the forest waste, the annual production mass and the percentage of efficiency that the resource has for the power generation. In the city of Cuenca, the Municipal Public Company of Toilet for Cuenca (EMAC EP), is responsible for the maintenance of the GPAs of the city. These are distributed in three categories: parks, riverbanks and parterres (Ortiz, 2018), which constitutes these spaces in sources to obtain the aforementioned renewable resource.

2   Materials and methods

2.1   General aspects of the area under study

The study area comprises the GPAs: parks, parterres and riverbanks (Figure 1), of Cuenca, located in the province of Azuay in the south-central region of Ecuador. The city center has an area of about 72 km^2 and a population of 391 657 inhabitants (INEC, 2016). Cuenca is located at an approximate height of 2550 $m.a.s.l.$ and has an average temperature of $15,6°C$, which can range from $27,2°C$ to $-1,7°C$ (Plan Estratégico Cuenca 2020, 2004). For this investigation, mapping information for the GPAs established within the *Cinturón Verde de la ciudad de Cuenca* project was used as well as satellite images from April 20, 2018, with a resolution of $3,14m \times 3,14m$ per pixel and 19% cloud percentage.

2.2   Identification of forest species that are part of the GPA prunin

In order to evaluate the EP of forest waste, it is necessary to know what plant species of the study area are (Roberts et al., 2015). In this case, it was considered appropriate to identify them directly in the GPAs assisted by EMAC Public Company. This is because urban pruning consists of several small forest elements, a situation that makes it difficult to establish the identification of the species. According to the methodology suggested by Gutiérrez et al. (2015) monitoring was carried out during August 2018 for the identification of species. For this purpose, the sites of the GPA that met two criteria were chosen, those that had: (i) an area $\geq 0,05$ and
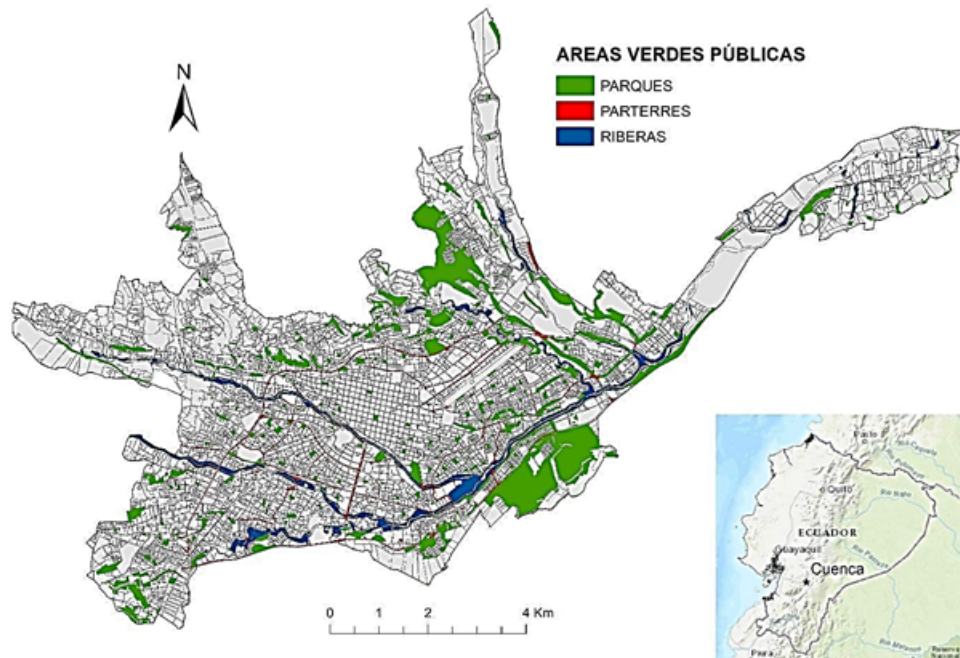
Figure 1. Study area.

$\leq$ 1,21 ha, and (ii) a Normalized Difference Vegetation Index (IVDN) $\geq$ 0.26.

The minimum and maximum surface limit was obtained through Equation 1 proposed by Olsson (2005), which corresponds to the reliability index, for which a 90 % confidence level was used. The value of 0.26 represents the average IVDN data, calculated for GPAs using the SIG ARCMap® program. Where, χ (ha) corresponds to the average area of GPA, σ (ha) is the standard deviation of the areas considered as GPA, *n* refers to the total number of GPA, Z (%) is the confidence level, and μ indicates the total number of GPAs found within the confidence interval (Olsson, 2005).

$$\chi - \frac{Z * \sigma}{\sqrt{n}} \leq \mu \leq \chi + \frac{Z * \sigma}{\sqrt{n}} \qquad (1)$$

This index suggested by Rabatel et al. (2011), analyzes the biophysical characteristics of plants and the vegetative distribution of the study area (Parthiban et al., 2015) by using Equation 2. Where, IRC (*μm*) refers to the Near Red Infra band that possess the satellite images and R (*μm*) corresponds to the Red band (Rabatel et al., 2011).

$$IVDN = \frac{IRC - R}{IRC + R} \qquad (2)$$

The monitoring of plant species distributed in GPA (selected under the criteria described above) was carried out on plots of 0.4 ha. With the ODK technology tool, which uses an online server to collect, manage, and store information in a given area, data was collected regarding: location coordinates, photo, common name, and scientific name of the individuals found.

2.3 The obtaining of the calorific power of forest biomass

In order to assess forest biomass energy, it is considered appropriate to pre-analyze its NCV. This parameter allows to estimate the amount of usable energy per unit of mass when the resource is in fully combustion (Arroyo and Reina, 2017). The calculation of the NCVis given by Equation 3 stated by Francis and Lloyd (Budí, 2016). Where, HHV (kcal/kg) corresponds to the Higher Heatig Value, 597 (kcal/kg) is an indicator that refers to the heat from the condensation of the water vapor formed in the combustion test. Number 9 indicates the kg of water generated by oxidizing 1 kg of hydrogen, H (%) is the percentage of hydrogen quantification and *w* (%) refers to the percentage of moisture that

the biomass has (Budí, 2016).

$$NCV = HHV - 597 * 9H + w \qquad (3)$$

Nine forest species were identified as the most abundant in urban pruning, corresponding to 59.49% of individuals found during field monitoring. They were listed in the study as representative species and their HHV and moisture percentage were determined by laboratory analysis. The quantification of the HHV was carried out in a calorimetric pump (IKA C200); samples consisting of branches and leaves of an individual, whichwere taken for each of the 9 species (Ortiz T., 2013), following the criteria of the STANDARD $UNE - EN - ISO 18135 : 2018$ (Solid biofuels Sampling). These individuals were selected according to the morphometric characteristics of an adult-considered specimen (Barahona, 2005; Minga and Verdugo, 2016; CONAFOR, 2013)

The samples were conditioned according to the parameters established by UNE-CEN/TS 14918: 2011 (Solid biofuels. Determination of the calorific power), subjecting them to a drying process at a temperature of $105°C \pm 1$, for 24 hours. Subsequently, the analysis of the HHV was carried out in the calorimetric pump, obtaining a digital result in units of energy by mass. As Vassilev et al. (2010) indicate, the forest biomass is usually composed of 6% hydrogen, and this was the value used. The percentage of moisture for representative species was calculated using the criteria described in UNE-CEN/TS 14774: 2010 (Solid biofuels. Determination of moisture content. Method of drying in stove), where Equation 4 is established for its calculation. Where, $m1$ (g) is the weight of a crucible with the sample before drying and $m2$ (g) is the weight of the same crucible with the dry sample (UNE-CEN/TS 14774: 2010).

$$w = \frac{m1 - m2}{m2} * 100 \qquad (4)$$

2.4 Estimation of the energetic potential of forest wastes

Özdemir and Gencer (2016) allows relating the NCV (tep/ton) to the mass of forest waste generated annually from the maintenance operations of the GPAs. The latter is represented in Equation 5 as m (ton/year). The NCV corresponds to the average lower heating value of representative species, whose units were transformed from kcal/kg to tep/ton. This value is considered conservative since the biomass evaluated was only of forest species (woody), whose organic composition is similar (cellulose, hemicellulose and lignin) (Déjardin et al., 2010). The total mass of the pruning was obtained through statistical data presented in Table 1 by the Green Areas Department of the EMAC Public Company, during 2018.

$$EP = NCV * m \qquad (5)$$

Table 1. Register of urban prunning, 2018. Taken from Emac (2018).

Month	Mass (ton)
January	50.71
February	50.72
March	50.72
April	43.93
May	66.08
June	58.35
July	47.52
August	44.37
Septembre	64.42
Octuber	41.01
November	64.95
December	25.81
TOTAL	**608.63**

2.5 Estimation of the energetic efficiency of forest wastes

Because urban forest waste can be exploited by converting it into electricity through thermal processes (Barragán, 2018), as a first approach to the energy valuation of this resource in Cuenca city, the energy efficiency has been estimated with Equation 6 (Panepinto et al., 2014). Considering 18 % as the percentage of forest biomass yield for conversion to electric energy.

This percentage allows the establishment of usable energy and refers to the efficiency of converting chemical energy of plant species to electricity; this factor taken from a study developed in the Basilicata–Italy region, where forest pruning has been evaluated as an RE source through an energy balance, allows to estimate electrical production by thermal processes. In the research of PPanepinto et al. (2014), a similar methodology is used, establishing as a hypothesis that it is possible to assess the efficiency for obtaining electricity by 18 %, based on a scenario that has data on the available energy power (calculated with the ratio of biomass amount and NCV).

On the other hand, there are methodologies that differ and that use efficiencies for the production of electricity of 10 % (Shi et al., 2013) and 4.37 % (Roberts et al., 2015). However, as this is a first analysis of the energy potential of urban pruning in the area, it has been relevant to use 18 % as a reference data. For specific cases, a more in-depth study is required that considers the efficiency of different power conversion devices, among other variables.

$$EE = EP * E \qquad (6)$$

Where, EE (tep/year) refers to the energy produced in one year, EP (tep/year) is the Energy Potential of forest biomass and E (%) corresponds to the efficiency percentage for the generation of electricity from the resource (Panepinto et al., 2014).

3 Results and Discussion

3.1 Forest species that are part of pruning in GPAs

According to the sampling developed in GPAs of Cuenca, urban pruning is formed by 72 forest species in total. Table 2 shows the species found, which are sorted in descending order with respect to abundance. For the purposes of the study, it was established that 59.49 % of the individuals correspond to 9 species listed as representative (*Eucalyptus globulus, Salix humboldtiana, Prunus serótina, Tecoma stans, Baccharis latifolia, Fraxinus excelsior, Callistemon salignus, Pinus radiata, Acacia dealbata*), since these are abundant.

3.2 Calorific power of forest biomass

From laboratory evaluations, the HHV of biomass from the representative species was determined (Table 3). By incorporating these values into the NCV calculation, it was possible to define that Pinus radiata specie is the one that has the greatest capacity to shed heat during the complete combustion processes, being the most efficient resource for obtaining energy. This is followed by Callistemon salignus and Prunus serotina. The latter is considered as one of the native species of Cuenca city, which is recommended to be incorporated into the reforestation plans managed by the EMAC Public Company, as it is an appropriate alternative for the use of GPAs as a source of energy resources.

The study states that for the use of biomass focused on energy generation in a sustainable scenario, it is better to use the waste of pruning of existing GPAs. In other words, the idea is not to sow plant species for energy purposes, but to use the existing ones with environmental, ornamental and landscape criteria.

The data presented in Table 3 allows to define the NCV average for forest species distributed in GPAs, which is about 0.38 tep/ton. It should be mentioned that to obtain this value it was considered appropriate to evaluate the NCV only of the 9 most abundant species (59.49 %), due to the restriction of the number of samples to be analyzed for the study. Because of the difference in the moisture content (Table 3), each requires a separate analysis and a minimum number of three tests. In addition, having worked only with forest species, whose organic composition is similar (Déjardin et al., 2010), it is possible to establish an average value. The result obtained (0.38 tep/ton) is close to which was determined by Panepinto et al. (2014), who show in their research that forest waste have a NCV of 0.34 tep/ton.

Scientific paper / Artículo científico
CARBON FRONTIERS

Yánez-Iñiguez, L., Urgilés-Urgilés, E., Zalamea-León, E. and Barragán-Escandón, A.

Table 2. Forest species identified in public Green areas.

Scientific name	Abundance	Scientific name	Abundance
Eucalyptus globulus	459	*Tipauna tipu*	7
Salix humboldtiana	80	*Acacia baileyana*	6
Prunus serótina	47	*Ferreyranthus verbascifolius*	6
Tecoma stans	47	*Rubus glaucus*	6
Baccharis latifolia	45	*Morella sp.*	6
Fraxinus excelsior	43	*Yucca guatemalensis*	6
Callistemon salignus	41	*Ficus Robusta*	4
Pinus radiata	37	*Eucalyptus citriodora*	4
Acacia dealbata	35	*Cotoneaster acuminatus*	4
Jacaranda mimosifolia	32	*Liabum floribundum*	4
Schinus molle	30	*Buddleja davidii*	3
Chionanthus pubescens	29	*Laurus nobilis*	3
Sambucus mexicana	27	*Monnina ligustrina*	3
Hibiscus rosa-sinensis	26	*Citrus x sinensis*	3
Juglans neotropica	26	*Arecaceae*	3
Alnus acuminata	25	*Myrcianthes hallii*	2
Cupressus lusitánica	24	*Buxus sínica*	2
Podocarpus sprucei	22	*Bougainvillea spectabilis*	2
Populus alba	21	*Annona cherimola*	2
Morella pubescens	21	*Cestrum nocturnum*	2
Syzygium paniculatum	17	*Brugmansia sanguínea*	2
Inga insignis	17	*Psidium guajava*	2
Acacia retinodes	16	*Lantana cámara*	2
Ambrosia arborescens	16	*Fuchsia boliviana*	2
Ficus benjamina	14	*Robinia Pseudoacacia*	1
Eriobotrya japónica	14	*Acalypha australis*	1
Ligustrum Japonicum	13	*Populus balsamífera*	1
Acacia melanoxylon	10	*Prunus persica*	1
Myrsine guianensis	10	*Mimosa andina*	1
Jasminum polyanthum	10	*Ligustrum sinense*	1
Callistemon citrinus	9	*Crataegus pubescens*	1
Duhaldea cappa	9	*Oreopanax ecuadorensis*	1
Erythrina edulis	8	*Buddleja americana*	1
Nerium oleander	8	*Rosmarinus officinalis*	1
Grevillea robusta	8	*Rosa gallica*	1
Delostoma integrifolium	7	*Citharexylum ilicifolium*	1
Delostoma integrifolium	7		

3.3 Energetic potential of forest wastes

Equation 5, which establishes the ratio of the amount of biomass available over a year to its usable energy corresponding to the NCV, determined that the EP for forest waste is approximately 233.13 tep/year. This energy comes from the pruning currently carried out by the EMAC Public Company in public areas that have forest biomass, which occupy 618.76 ha of the total area of Cuenca city.

Biomass from maintenance operations of the GPAs can become an alternative renewable resource to meet the city's energy needs, as proposed by Kook and Lee (2015), who in a study in South Korea's urban centers have determined that forest waste has a minimum potential of 76,760 tep/year. This difference of the Asian cities and the urban area of Cuenca is largely due to two main factors: first the size of the cities, wich is related to the available area to extract the resource and second, the final use that pruning currently has in each place. The cities in South Korea are classified as major metropolises, with green spaces producing abundant biomass (Kook and Lee, 2015), meanwhile Cuen-

ca has 7,200 ha of a total area. On the other hand, the town lacks a comprehensive forest waste management plan, a situation that differs from Korean cities, where the real importance of urban pruning has been understood as a resource for RE generation.

The research developed by Kook and Lee (2015) shows some limitations to be taken into account in integrating forest biomass as an energy source in cities; for example, the accelerated and continuous cities increase, whose area for buildings tends to incorporate more space compared to the surfaces of green areas (Franco, 2012), as well as the number increase of inhabitants and thus in energy needs

(Lahoz, 2010). These factors need to be analyzed in advance, in order to avoid overexploitation and unsustainable management of biomass due to pruning.

From a diversified source use perspective, forest waste is an available endogenous resource that can be supplemented by intermittent renewable energies such as solar and wind (Brown et al., 2018). For Cuenca, an appropriate alternative is the conversion of biomass to electricity, considering the minimum thermal demand available due to climate, unlike other latitudes where the need for spatial environment is predominant.

Table 3. Calorific power of representative species.

Scientific name	HCP (tep/ton)	Moisture content (%)	NCV (tep/ton)
Eucalyptus globulus	0.41	16.9	0.37
Salix humboldtiana	0.43	61.1	0.36
Prunus seótina	0.46	51.65	0.4
Tecoma stans	0.43	46.2	0.37
Baccharis latifolia	0.43	61.25	0.36
Fraxinus excelsior	0.42	45.02	0.42
Callistemon salignus	0.48	46.53	0.43
Pinus radiata	0.5	49.46	0.39
Acacia dealbata	0.45	41.22	0.3
Average			**0.38**

3.4 Estimated energetic efficiency for forest wastes

The city of Cuenca has a total electricity demand of 423 800 MWh/year (Barragán, 2018), of which 38% corresponds to the residential sector. In this context, when assessing forest waste as a resource that has 18% energy efficiency, it was obtained that the electricity generation from it will be approximately 476.83 MWh/year (41 tep/year). This production allows to supply about 0.30% of the demand in the residential sector, representing the coverage for 110 typical families with four members (average of the city families), considering that each of these households has a total annual consumption of 4.33 MWh/inhabitant (Barragán, 2018).

Today Cuenca has a RE model that uses domestic solid waste that reaches the landfill for the ope-

ration of a biogas generating plant, through which 502.60 tep/year of electricity are produced (Barragán et al., 2016). These levels of energy generation are higher than those obtained from forest waste due to management implemented for the secondary recovery of the household waste mentioned.

Energy from renewable sources could increase as technologies for the use of forest waste, such as an energy resource, are developed and incorporated as has been done in countries such as South Korea. The latter is an encouraging scenario, considering that forest biomass allows to strengthen a model of diversification of the energy matrix, in which endogenous resources can have an added value (Barragán, 2018). The use of residual biomass in bioenergy systems will require prior cost analysis for the transportation of urban pruning to power generation centers, which can be diminished by an as-

sessment of the existing spatial energy density in each location (Kook and Lee, 2015). The value of industrial process of conversion to energy and the cost of systems for the distribution of electricity to users (Yemshanov et al., 2014) should also be taken into account, then the real capacity of the resource can be analyzed.

4 Conclusions

A methodology is presented to determine the energy potential of urban forest waste applicable to any city. The evaluation of forest biomass for the purpose of electrical production represents an alternative for the pruning management from the GPAs belonging to the urban area of the city of Cuenca, Ecuador.

The information on the amount of energy per unit of mass (NCV) of the species studied allows to establish which work better to reforest the city. Prunus serotina is recommended for this activity, because it has been cataloged as a native species, which will allow the conservation of ornate. In this context, the proposal for reforestation of existing GPAs with species of heating also generates the possibility of meeting the minimum parameters of green area per inhabitant, established by the World Health Organization (WHO), as well as it helps increasing the share of renewable energy in the local energy matrix.

Annually in Cuenca city there are 608.63 ton of forest waste from the maintenance operations of GPAs, which is responsible for EMAC Public Company. In this sense, secondary recovery (energy production) will also represent a circular management model for urban pruning, giving them added value.

This study concludes that the energy potential of forest waste in the city of Cuenca is valued at 233.13 tep/year. This represents approximately 41 tep/year (476.83 MWh/year) of power generation. This production is marginal in relation to local electricity consumption, covering the needs of 110 average families. However, local pruning levels are low compared to other urban areas where a landscape work is done, because there is only a schedule of activities for the maintenance of GPAs where it is strictly necessary or in cases where forest species

are interfering with public lighting cables. Therefore, if planning is established for the continuous management of GPAs, that contemplates the increase of pruning, it will favor the obtaining of the resource for energy purposes, while it will be possible to optimize their collection. In addition, the amount of the resource could be increased if private, non-sized waste management is incorporated into the analysis.

The technical and economic evaluation is proposed as a future need to identify efficient and cost-effective technologies that are coupled with the characteristics of the natural resource assessed, as well as electricity supply requirements that exist in the area. These analyses should have a sustainable management approach, in order to avoid risks of overexploitation of forest biomass. In addition, they are a complement with intermittent renewable technologies, being able to introduce to the grid the energy generated during peak hours.

Forest waste from the city's pruning is part of the alternatives for diversification of resources that constitute the energy matrix at local and national level. Therefore, its assessment, within the framework of renewable energies, allows to strengthen a model of energy self-sufficiency consistent with the need to reduce dependence on fossil fuels.

Acknowledgment

References

Arrese, M. and Blanco, G. (2016). Territorio y energías renovables no convencionales: aprendizajes para la construcción de política pública a partir del caso de rukatayo alto, región de los ríos, chile. *Gestión y política pública*, 25(1):165–202. Online:https://bit.ly/2PrhbdS.

Arroyo, J. and Reina, W. (2017). Aprovechamiento del recurso biomasa a partir de los desechos de madera para una caldera de vapor. *Ingenius,*, page 20. Online:https://bit.ly/2DEvdGk.

Barahona, L. (2005). Variación de la composición química en albura duramen y altura de madera pulpable de eucalyptus globulus proveniente de monte alto y monte bajo. Master's thesis, Universidad de Chile.

Barragán, A. (2018). El autoabastecimiento energético en los países en vías de desarrollo en el marco del metabolismo urbano: caso cuenca, ecuador. Master's thesis, Universidad de Jaén.

Barragán, E., Arias, P., and Terrados, J. (2016). Fomento del metabolismo energético circular mediante generación eléctrica proveniente de rellenos sanitarios: estudio de caso, cuenca, ecuador. *Ingenius*, (16):36–42. Online:.

Barragán, E., Zalamea, E., Terrados, T., and Parra, A. (2019). Las energías renovables a escala urbana. aspectos determinantes y selección tecnológica. *Bitácora Urbano Territorial*, 29(2):39–48. Online:https://bit.ly/2DbkvHP.

Bristow, D. and Kennedy, C. (2013). Urban metabolism and the energy stored in cities: Implications for resilience. *Journal of Industrial Ecology*, 17(5):656–667. Online:https://bit.ly/3fslssb.

Brown, T., Bischof, T., Blok, K., Breyer, C., Lund, H., and Mathiesen, B. (2018). Response to 'burden of proof: A comprehensive review of the feasibility of 100% renewable-electricity systems'. *Renewable and Sustainable Energy Reviews*, 92:834–847. Online:https://bit.ly/33sOJk4.

Budí, A. (2016). Estimación del potencial energético de la biomasa residual agrícola y análisis de aprovechamiento en los municipios de la comarca del alto palancia. Master's thesis, Universitat Jaume I.

CONAFOR (2013). Fichas técnicas sobre características tecnológicas y usos de maderas comercializadas en méxico. online:https://bit.ly/2EOJH7f.

Déjardin, A., Laurans, F., Arnaud, D., Breton, C., Pilate, G., and Leplé, J. (2010). Wood formation in angiosperms. *Comptes rendus biologies*, 333(4):325–334. Online:https://bit.ly/39VAA04.

Emac (2018). Empresa municipal de aseo de cuenca.

Franco, M. (2012). Análisis de los cambios en la cobertura y funcionalidad de áreas verdes en la zona metropolitana de la ciudad de mérida (zmm). Technical report.

Gutiérrez, A., García, F., Rojas, S., and Castro, F. (2015). Parcela permanente de monitoreo de bosque de galería, en puerto gaitán, meta. *Corpoica. Ciencia y Tecnología Agropecuaria*, 16(1):113–129. Online:https://bit.ly/2DAB4g9.

INEC (2016). Proyecciones poblacionales, proyección de la población ecuatoriana, por años calenario, según cantones 2010-2020. Technical report, Instituto Nacional de Estadísticas y Censos.

Kook, J. W. and Lee, S. H. (2015). Analysis of biomass energy potential around major cities in south korea. *Applied Chemistry for Engineering*, 26(2):178–183. Online:https://bit.ly/2Xvqwpx.

Lahoz, E. (2010). Reflexiones medioambientales de la expansión urbana. *Cuadernos geográficos*, 46(46):293–313. Online:https://bit.ly/3fs0WYQ.

Manzano, F., Sanchez, M., Barroso, F., Martínez, A., Rojo, S., and Pérez, C. (2012). Insects for biodiesel production. *Renewable and Sustainable Energy Reviews*, 16(6):3744–3753. Online:https://bit.ly/3icZ08n.

Minga, D. and Verdugo, A. (2016). *Árboles y arbustos de los ríos de Cuenca*, volume Online: https://bit.ly/2DoEt1M. Universidad del Azuay, Cuenca.

Olsson, U. (2005). Confidence intervals for the mean of a log-normal distribution. *Journal of Statistics Education*, 13(1. Online:https://bit.ly/3ftC570).

Ortiz, P. (2018). Plan de acción territorial para la implantación de infraestructura verde en la ciudad de cuenca. Master's thesis, Universidad de Cuenca.

Ortiz T., L. (2013). Estudio de caracterización de las biomasas forestales de interés energético existentes en el sur de galicia y norte de portugal. mathesis, Universidad de Vigo, Online: https://bit.ly/33xlLiX.

Özdemir, Z. and Gencer, A. (2016). Determination of the biomass potential in kirklareli province based on agricultural residues. In Dincer, I., Colpan,

C., and Kadioglu, F., editors, *8TH EGE ENERGY SYMPOSIUM AND EXHIBITION, At Afyonkarahisar, TURKEY*, New York. doi: 10.1007/978-1-4614-7588-0. Springer.

Panepinto, D., Viggiano, F., and Genon, G. (2014). The potential of biomass supply for energetic utilization in a small italian region: Basilicata. *Clean Technologies and Environmental Policy*, 16(5):833–845. Online:https://bit.ly/2ELuAvi.

Parthiban, S., Thummalu, N., and Christy, A. (2015). Ndvi: Vegetation change detection using remote sensing and gis - a case study of vellore district. *Procedia Computer Science*, 57:1199–1210. Online:https://bit.ly/2XsERmJ.

Pérez, J., Borge, D., and Agudelo, J. (2010). Proceso de gasificación de biomasa: una revisión de estudios teórico-experimentales. *Revista facultad de ingeniería Universidad de Antioquia*, (52):95–107. Online:https://bit.ly/2BZQ46F.

Plan Estratégico Cuenca 2020 (2004).

Rabatel, G., Gorretta, N., and Labbé, S. (2011). Getting ndvi spectral bands from a single standard rgb digital camera: a methodological approach. In *Conference of the Spanish Association for Artificial Intelligence*, pages 333–342. Online:https://bit.ly/2Pph9mP.

Roberts, J., Cassula, A., Prado, P., Dias, R., and Balestieri, J. A. P. (2015). Assessment of dry residual biomass potential for use as alternative energy source in the party of general pueyrredón, argentina. *Renewable and Sustainable Energy Reviews*, 41:568–583. Online:https://bit.ly/30rHxCQ.

Shi, Y., Ge, Y., Chang, J., Shao, H., and Tang, Y. (2013). Garden waste biomass for renewable and sustainable energy production in china: Potential, challenges and development. *Renewable and Sustainable Energy Reviews*, 22:432–437. Online:https://bit.ly/3fvV3cS.

Vassilev, S., Baxter, D., Andersen, L., and Vassileva, C. (2010). An overview of the chemical composition of biomass. *Fuel*, 89(5):913–933. Online:https://bit.ly/30ttf4L.

Yaman, S. (2004). Pyrolysis of biomass to produce fuels and chemical feedstocks. *Energy conversion and management*, 45(5):651–671. Online:https://bit.ly/2EIDSYX.

Yemshanov, D., McKenney, D., Fraleigh, S., McConkey, B., Huffman, T., and Smith, S. (2014). Cost estimates of post harvest forest biomass supply for canada. *Biomass and Bioenergy*, 69:80–94. Online:https://bit.ly/3fz0iZj.

Rainwater storage in urban environments using green roofs

Almacenamiento de agua de lluvia en medios urbanos utilizado techos verdes

Nelson Andrés López Machado[1] , Christian Gonzalo Domínguez Gonzalez[2], Wilmer Barreto[3], Néstor Méndez[4], Leonardo José López Machado[1] , María Gabriela Soria Pugo[2], Ronnie Xavier Lizano Acevedo[5] and Vanessa Viviana Montesinos Machado[4]

[1] *Pontificia Universidad Católica de Chile. Av Libertador Bernardo O'Higgins 340, Santiago, Región Metropolitana, Chile.*

[2] *Department of Civil Engineering, Universidad Politécnica Salesiana. Av. Morán Valverde s/n y Rumichaca. Campus Sur. Quito, Ecuador.*

[3] *Department of Environmental Engineering, Universidad Católica de Temuco. Av Manuel Montt 56, Temuco, Araucanía, Santiago, Chile.*

[4] *Department of Civil Engineering, Universidad Centroccidental Lisandro Alvarado. Av. Carrera 19 entre calles 8 y 9, Barquisimeto 3001, Lara, Venezuela.*

[5] *Environmental Engineering Career, Research Group in Environmental Sciences GRICAM, Universidad Politécnica Salesiana. Av. Morán Valverde and Rumichaca, Quito, Ecuador.*

*Corresponding author: nalopez4@uc.cl

Abstract

This article discusses the use of green roofs as rainfall water storage in its soil matrix. The methodology is analytical based on mathematical models, where runoff produced in an urban area is compared with current conditions of ordinary roofs with ceramic or bituminous materials as the original scenario, against another where green roofs are used. The study area is located in the Palavecino municipality of Lara state in Venezuela, in the flood zone of Quebrada Tabure. In this research, a quantitative comparison of the direct runoff hydrographs of the proposed scenarios was used, obtaining as a main result the reduction of runoff between 60% and 80% according to the period of return. An interesting point of this research was the incorporation of the routing of hydrographs on the roofs, reducing even more the peak flow over 90%, and delaying the peak time of the generated hydrographs between 10 and 12 minutes while the total duration of the hydrographs increase more than three times.

Keywords: Green roofs, runoff, hydrographs, peak flow, rainwater storage, routing hydrographs.

López, N., Domínguez, C., Barreto, W., Méndez, N., López, L., Soria, M., Lizano, R. and Montesinos, V.

Resumen

El siguiente artículo de investigación trata sobre el uso de techos verdes como almacenadores de agua de lluvia en su matriz de suelo. La metodología es analítica basada en modelos matemáticos, en donde se compara la escorrentía producida en un urbanismo con condiciones actuales de techos ordinarios con materiales cerámicos o bituminosos como escenario original, contra otro donde se usan techos verdes. La zona de estudio se ubica en el municipio Palavecino del estado Lara en Venezuela, en la zona de inundación de la Quebrada Tabure. En esta investigación se empleó la comparación cuantitativa de los hidrogramas de escorrentía directa de los escenarios planteados, obteniendo como resultado principal, la reducción de la escorrentía. Un punto interesante de esta investigación fue la incorporación del tránsito de hidrogramas en los techos, reduciendo aún más el caudal pico y el tiempo al pico de los hidrogramas generados.

Palabras clave: Techos verdes, escorrentía, hidrogramas, caudal pico, almacenamiento de agua de lluvia, tránsito de hidrogramas.

Orcid IDs:

Nelson López: http://orcid.org/0000-0002-3111-7952

Christian Domínguez: http://orcid.org/0000-0003-2971-7163

Wilmer Barreto: http://orcid.org/0000-0002-1861-0742

Néstor Méndez: http://orcid.org/0000-0003-1300-5049

Leonardo López: http://orcid.org/0000-0002-1562-0662

María Gabriela Soria: http://orcid.org/0000-0001-9045-0870

Ronnie Lizano: http://orcid.org/0000-0002-9490-8882

Vanessa Montesinos: http://orcid.org/0000-0002-5355-5099

1   Introduction

Land use change due to urbanization has a significant impact on the local hydrology accompanied by other negative effects. Continuous growing of cities has increased the proportion of impervious areas in them. The progressive and uncontrolled waterproofing of surfaces alters the hydrological cycle (Figure 1), decreasing the response of a basins to a rain event, increasing the volume of drained water and, therefore, decreasing in the recharge of aquifers.
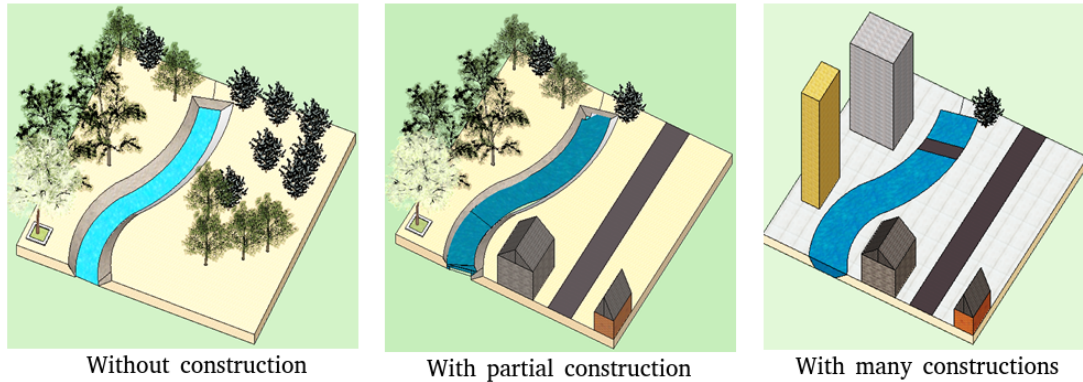

Figure 1. Effect of construction in hydrological cycle.

In addition, the growth of cities without planning can cause the alteration of natural courses, generating the need to build artificial channels that eventually will lead to worse problems in terms of urban drainage such as floods, collapse of longitudinal and transversal road drainages and delays during working hours of the inhabitants, in addition with the social tension caused by the aforementioned reasons. Water has a cycle that maintains a balance among evaporation, runoff, precipitation, infiltration, evapotranspiration, among others, which can be translated according to Chow et al. (1994) as shown in Equation 1. Where P is the total precipitation thickness, P_e is the effective precipitation thickness which generates runoff, I_a is the initial abstraction, F_a is the quantity of water retained in the basin, E is the evaporation related with vegetation or the properties of the basin.

$$P = P_e + I_a + F_a + E \qquad (1)$$

In these processes, natural channels take dimensions to be able to transit the generated runoff, a process that is naturally slow, depending of the characteristics of the basin, soil, vegetation, among others. In the case of urban areas, the infiltration process is reduced, thus runoff generated is much higher and natural channels are not able to circulate the new maximum flow. Another problem generated by the construction without repositioning of green areas is the heat island effect, which is generated in areas that are significantly warmer than nearby rural areas, since the production of oxygen decreases and that of carbon dioxide increases (Arabi et al., 2015). Besides it is necessary to consider rainfall intense events increased by Climate Change (Olivares, 2018; Serrano et al., 2012, 2017; Ilbay-Yupa et al., 2019). Moreover, ceramics and bituminous materials retain much more heat than soil with vegetation, contributing to this effect as well. According to EPA (2018), green roofs can be defined as a roof with vegetation. Components of green roofs can vary, but basically they consist of vegetation, growth substrate, filter layer, drainage layer, waterproofing layer and root barrier (Minke, 2017; Vijayaraghavan, 2016).

According to Berardi et al. (2014); Minke (2017), green roofs can be classified into two types, based on growth substrate thickness; (i) extensive green roofs, generally have a thickness of growth substrate below 20 cm, a maximum weight of 150 kg/m^2 and they do not need irrigation because their vegetation is common, such as moss, herb, grass; and (ii) intensive green roofs, that have a thickness of

growth substrate over 20 cm, generating a total weight above 300 kg/m^2 and they need drainage and irrigation because of the vegetation used in them correspond to small trees. Green roofs have multiple applications, and one of those is to retain and storage rainwater, decreasing runoff, and thus the impact of the heat island effect (EPA, 2018) and deforestation in urban environments, decreasing the negative impact on the local fauna.

Another benefit is that green roofs could be a valuable solution as an alternative to recover green spaces in urbanized areas (Berardi et al., 2014). Green roofs have a lot of benefits, according to BCIT (2018); Minke (2017); Berardi et al. (2014); Technology (2018) as expand roof life until 60 years; recover dead spaces and transform them into garden spaces; reduce stormwater runoff and the "heat island" effect (EPA, 2018); decrease smog, noise, energy demand and carbon monoxide impact and improve air quality; prevent combined sewer overflow; remove nitrogen pollution from rain; neutralize acid rain effect; restore habitat for wildlife; enhance urban air quality, among others.

Green roofs are an important part in Sustainable Urban Drainage Systems (SUDS), that try to recover the natural cycle of water in the city. SUDS are within the strategies used to improve the functioning and sustainability of the urban development of cities. Green roofs take a good role in SUDS applications because of their capacity to decrease storm water runoff generation in terms of runoff reduction, peak time and concentration time delay (Fioretti et al., 2010). The behavior of the hydrograph is modified significantly when the peak flow is reduced only by the change in roof use (conventional to green roof), and it is even more noticeable when making a transit for each roof using weir-like structures additional to green roofs.

The access to green spaces in Latin America is very limited specially in peripheric areas, due to the planning perspective is in service of neighborhoods with socio-economic power (Escobedo et al., 2006; Reyes and Figueroa, 2010; Romero and Vásquez, 2005; Vásquez and Romero, 2008), in this context the objective is to fight for environmental and spatial justice that allows all citizens to claim for green urban access, currently the recommendation from OMS is to have 9 $m^2/person$ of green space in a city;

nevertheless, there are many neighborhoods with less than 1 $m^2/person$. This analysis allows to think that the space construction it has been shaped excluding to many cities' areas, and the environmental and spatial justice strategies can help to recover the city spaces for urban and peri-urban forestry that can be complemented with green roofs. All these efforts can enhance the urban ecosystems and allows to improve the life quality of people.

Green roofs are one of the best tools for stormwater management in urban areas by decreasing the possibilities for flash flooding; furthermore, vegetation on the top of the roofs increases the evapotranspiration. The growing plants absorbs an amount of rain- water, decreasing the peak flow, peak time and runoff. Green roof has ability to capture the dangerous fine dust particles from the air that could help to improve the comfort of population in highly crowded urban areas (Shafique and Rafiq, 2018). Green roofs help to reduce air pollution by two different ways. Firstly, the greens capture the fine dust particles or called air pollutants through stomata. Secondly, the green roofs diminish the surface temperature which helps in fossils burning to meet energy requirements (Yang et al., 2008).

According to Huang (1994), 1000 m^2 of green roofs are capable to remove since 160 kg to 220 kg per year of dust, which results in the environment improvement. A grand total of 1675 kg of air pollutants was removed in only one year by 19.8 hectares of green roofs, with a O_3 accounting for 52 % of the total, 27 % of NO_2, 14 % of PM_{10} and 7 % of SO_2. The highest level of air pollution reduction occurred in May and the lowest amount in February. The annual reduction per hectare of green roof was about 85 kg/ha/year according to (Yang et al., 2008). The author mentioned that green roofs could be complementary strategies in the urban planning, the primary strategy is forestry and the possibility to introduce public places as parks. In addition, Connelly and Hodgson (2013) proved that green roofs are able to reduce noise frequency by 10 and 20 dB, also, they have the ability to absorb the sound waves and reduce the sound level in comparison to non-vegetated roofs.

Green roofs and green walls are not the only techniques for urban ecology reconciliation, private gardens, public parks, and planting of urban trees

are as well (Francis and Lorimer, 2011). According to MacIvor and Lundholm (2011),a variety of species of insects, common and uncommon, were collected from some green roofs, supporting the idea that these habitats help to sustain and restore biodiversity in cities.

2 Theoretical bases

The main objective is to determine rainwater storage in green roofs by using hydrographs and routing them; therefore, a correct method to calculate runoff and hydrographs is necessary in order to fulfil the objective. There are multiple methods to determine peak flows, depending of the basin area and available data, such as the rational method or the dimensionless unitary hydrograph method (Chow et al., 1994). The rational method is recommended for basins whose areas are lower than 200 hectares. The results of this method are limited to the peak flow value, therefore, the variation of runoff through the time is not possible to obtain.

Dimensionless unitary hydrograph method allows to determine the behavior of the discharge through the time with a hydrograph. Even though, the rational method could be applicable in this research (roof surface is lower than 200 hectares), the dimensionless unitary hydrograph was used to estimate the real volume of rainwater. In this method, basin hydrographs are calculated based on a unitary dimensionless hydrograph, which is obtained from the observation of real hydrographs. Estimation of precipitation and infiltration are necessary to determine the hydrograph of a basin. Maximum precipitation events (the ones that causes flooding) can be estimated using an Intensity-Duration-Frequency (IDF) curves, used in this research. Whereas, several methods can be used to estimate infiltration such as Horton, Green-Ampt, and the curve number proposed by the Soil Conservation Service of United States of America (SCS) (Viola et al., 2017).

2.1 Total precipitation thickness

Generally, precipitation do not have a linear behavior or intensity along the time but it changes. Precipitation can be expressed along the time with a precipitation hyetograph, which distributes the total thickness of rainwater in several time intervals, with a constant or variable distribution. The Soil Conservation Service (SCS) proposes a method to determine the precipitation hyetograph, using the dimensionless hyetograph (Chow et al., 1994). The precipitation hyetograph needs to estimate the total thickness of rainfall that produces runoff; thus, it is necessary to build the Intensity-Duration-Frequency (IDF) curves. According to the concentration time of the basin (time in which a drop of water lasts to travel the distance from the most distant point of a basin to its output) and the rainfall intensity given a certain return period, the total thickness of rainwater could be determine using Equation 2.

$$P = I * T \qquad (2)$$

Where I is the rainfall intensity (mm/h), P is the rainfall thickness (mm), T is the rainfall duration (hour). Intensity is estimated with IDF curves, which are generally known according to the region of study. The concentration time can be calculated by using the Kirpich's equation (Equation 3). With T_c is the basin concentration time (minutes), L is the channel length (ft, m) and S is the channel average slope (ft/ft, m/m).

$$T_c = 0,0078 * \frac{L^{0,77}}{S^{0,385}} \qquad (3)$$

2.2 Distribution of total precipitation thickness

To distribute the total thickness of rainfall, the alternating block method was used (Chow et al., 1994). In this method the concentration time is divided in subintervals (ΔT) and the cumulative intensity of rainfall is calculated using an IDF curve for a selected return period. For each subinterval of time, the partial intensity of rainfall is calculated and the thickness of rainfall (P) is determined using equation 1. A reorganization of P is necessary, in order to plot in a graphic (P in the vertical axis vs ΔT in the horizontal axis), the highest value of P in the center of horizontal axis, and then the second highest value of P just in the right side of highest value of P, and the third highest value of P in the left of the highest value of P, and so on (Figure 2).

Scientific paper / Artículo científico

CARBON FRONTIERS   *López, N., Domínguez, C., Barreto, W., Méndez, N., López, L., Soria, M., Lizano, R. and Montesinos, V.*
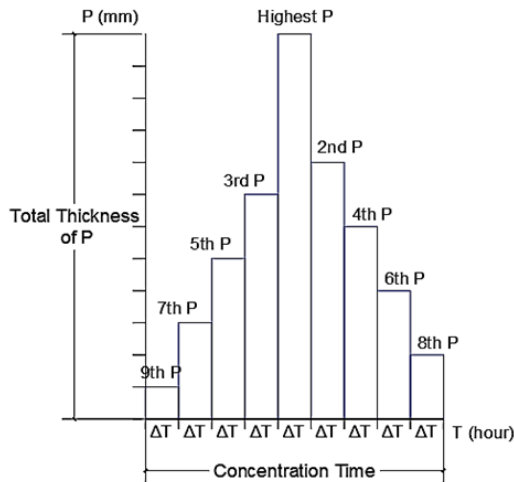
Figure 2. Precipitation hyetograph.

2.3   Infiltration

Infiltration was calculated using the curve number method (Chow et al., 1994), whose infiltration depends on the soil type, initial abstractions and antecedent humidity. Infiltration can be calculated using Equation 4 (Chow et al., 1994). Where *CN* is the curve number obtained from NRCS (1973). In this research, CN II was used due to the zone of study, which presents regular rainfall along the year. *S* is the total water retention capacity of the soil (mm). Infiltration in green roofs is restricted by the thickness of the soil matrix (Sims et al., 2016; Liu et al., 2019).

$$S = \frac{2540}{CN} - 25,4 \qquad (4)$$

2.4   Runoff hydrograph estimate

Partial runoff thickness is calculated using Equation 5, which represents the portion of rainfall water that soil cannot absorb. *S* is the soil total water retention capacity (mm), *P* is the rainwater runoff (mm) and *Q* is the portion of rainfall water that soil cannot absorb (mm). If the expression $P - 0,2 * S$ is lower than zero, there is no runoff because infiltration is higher than rainwater in mm. The dimensionless constant 0.2 is known as the initial abstraction, and it represents the estimated portion of the soil that effectively retains water. Once the value of *Q* is calculated for each value of *P*, hydrograph for the basin of

study can be obtained by applying the unitary hydrograph, in which vertical axis represents dimensionless runoff, and horizontal axis represents dimensionless time for runoff.

$$Q = \frac{(P - 0,2 * S)^2}{(P + 0,8 * S)} \qquad (5)$$

In order to build the hydrograph, the unitary hydrograph must be affected by the concentration time and the total runoff thickness. To transform the unitary hydrograph into the real hydrograph, peak flow for each runoff thickness must be calculated using Equation 6. Where *qp* is the peak flow (m^3/s), *A* is the basin area (km^2), *Q* is the rainfall thickness (mm), T_p is the peak time, estimated as 60% of the concentration time.

$$qp = 0,208 * \frac{(A * Q)}{T_p} \qquad (6)$$

Concentration time is the time in which rainfall reaches the point of study (Chow et al., 1994). For urban drainage and small basins, the use of equation 3 usually delivers short concentration times. However, it is known that runoff starts after the surface is saturated which could take several minutes and take longer than the calculated concentration time. In addition, the relation between rainfall intensity and duration is assessed considering the concentration time of the drainage surface. Such relation show that rainfall intensity tends towards infinity with short rainfall duration and thus the design with these intensities might be unrealistic. In order to avoid these issues, a 10-minutes concentration time has been considered if the value obtained by equation 3 is too short. This time is commonly used in drainage manuals (Ramke, 2018; TxDOT, 2019) for small catchments and urban areas.

2.5   Runoff hydrograph routing

Routing hydrographs is used to properly simulate the green roof water storage capacity and its effect to runoff generation. In order to decrease the magnitude of peak flow and extend the duration of hydrographs, a routing of them must be applied. Transit of hydrographs is a procedure that allows to calculate an attenuated output hydrograph given an input hydrograph. When a routing hydrograph is used, the peak flow time is delayed and its value is reduced. In some cases, if the input hydrograph is

being routed with a possibility of storage, the output hydrograph would have a minor volume than the input hydrograph.

The most common method to routing a hydrograph is the 3rd order Runge-Kutta method (Chow et al., 1994), based on the continuity equation shown in Equation 7 (Fenton, 2009). Where dS is the stored water volume, I_t is the input flow for an instant of time, Q_H is the output flow for an instant of time in a height of the reservoir (in this case of study, the weirs in the green roofs). The term dS could be expressed as the change of volume due the elevation in a reservoir, as shown in Equation 8.

$$\frac{dS}{dt} = I_t - Q_H \qquad (7)$$

$$dS = A(H)dH \qquad (8)$$

Where $A(H)$ is the area according to the elevation H, therefore, Equation 6 could be rewritten as shown in Equation 9. The solution for Equation 8 consists in the subdivision of the slope $\frac{dH}{dt}$ by three increments to transform the differential equation into $\frac{\Delta H}{\Delta t}$, where ΔH is calculated as shown in Equation 10. Where ΔH_1 and ΔH_3 are calculated as shown form equations 11 to 13.

$$\frac{dH}{dt} = \frac{I_t - Q_H}{A(H)} \qquad (9)$$

$$\Delta H = \frac{\Delta H_2}{4} + \frac{3\Delta H_3}{4} \qquad (10)$$

$$\Delta H_1 = \frac{I(t) - Q(H)}{A(H)}\Delta t \qquad (11)$$

$$\Delta H_2 = \frac{I\left(t + \frac{\Delta t}{3}\right) - Q\left(H + \frac{\Delta H_1}{3}\right)}{A\left(H + \frac{\Delta H_1}{3}\right)}\Delta t \qquad (12)$$

$$\Delta H_3 = \frac{I\left(t + \frac{2\Delta t}{3}\right) - Q\left(H + \frac{2\Delta H_2}{3}\right)}{A\left(H + \frac{2\Delta H_2}{3}\right)}\Delta t \qquad (13)$$

Values of $Q(H)$ are obtained by constructing the "height-surface-capacity" curve, in which the total height of the reservoir (the matrix of soil in this case) is subdivided in intervals, and the volume for each interval is calculated using Equation 14. The values of $Q(H)$ are obtained by an interpolation, once calculated the respective height for a value of the input flow (Chow et al., 1994).

$$V_H = \Delta_H * A \qquad (14)$$

3 Methodology

Methodology applied to calculate the estimate rainwater storage using green roofs was by a direct comparison between the runoff produced by a common roof and the runoff produced by a green roof. The necessary information to generate the hydrographs was obtained using a free license software, Quantum Gis (QGIS, 2014), in order to create a mosaic to cover the urbanization area near the "Quebrada Tabure" in the Palavecino municipality of Lara State, Venezuela, using photographs (.img extension files) and contour lines as shown in Figure 3. Roof distribution at each house was simplified into two sections with their respective slopes, thus two polygons were used to simulate each roof surface. IDF curves were calculated using maximum precipitation data from the nearest precipitation stations in the region of study, and applying a type I extreme distribution; the IDF curves are shown in Figure 4.

For each roof, hydrographs were calculated by applying the methodology explained in point 2, using a curve number value of 98 and 86, for a conventional roof with bituminous materials and green roofs (related to grass), respectively. Rainwater inputs were estimated using different return periods. Once the hydrograph is built, volumes of water generated by runoff can be estimated using equation 15. With V as the volume between an interval of time. Q_{i+1} and Q_i, are two consecutive flow values according to an interval of time and Δt is a user selected interval of time. Areas for each roof were calculated using Qgis.

$$V = \sum_i^n (Q_{i+1} - Q_i)\Delta t \qquad (15)$$

Figure 3. Region of study, based on López et al. (2014).
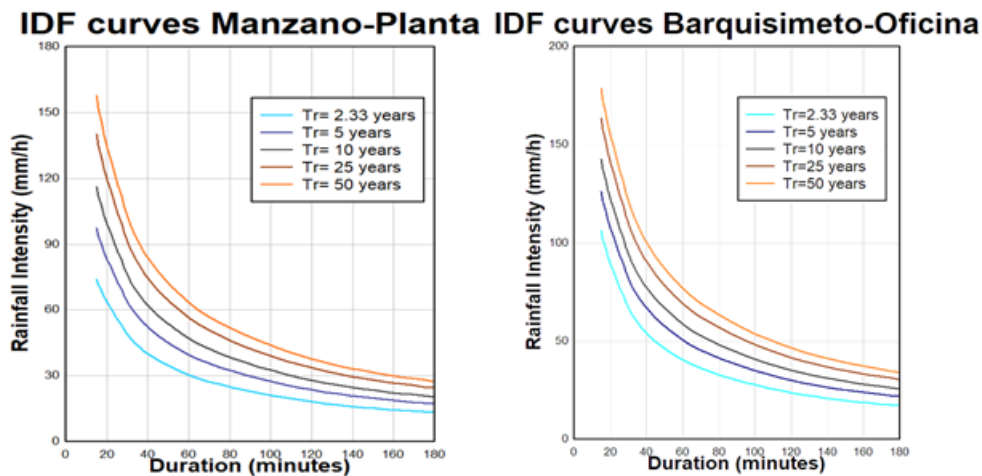
Figure 4. IDF curves for station "Manzano-Planta" and "Bqto-Oficina". Images based on López et al. (2014).

4 Results

In this paper, only results from the roof with $I_d = 1$ will be shown because of the magnitude of data. The complete data for the hydrology is shown from Table 1 to Table 5 (Bqto-oficina data). The hydrograph of roof 1 is shown in Figure 5. Note that there is a notable decrease of runoff using green roofs, and it can be translated in water storage. The wa-

ter storage is related to the matrix soil thickness, the vegetation species and soil porosity. The matrix soil thickness was estimated by adding the infiltration rate of the return 50-year return period, and assuming a total porosity of 20 %, and an effective porosity of 10 %, giving a thickness of 15 cm, but it was used as 20 cm. The hydrographs for roof 1 with and without green roof for each return period are shown from Figure 6 to Figure 8.

Table 1. Hydrology data for roof 1 (Tr=2.33 years).

Time (min)	Intensity (mm/h)	Cumulated water layer (mm)	Incremental water layer (mm)	Infiltration layer (mm)	runoff thickness (mm)
0	0	0	0	0	0
1.667	150	4.167	4.167	2.244	0
3.333	150	8.333	4.166	4.167	0
5	150	12.5	4.167	4.047	0.122
6.667	147.895	16.433	3.933	3.416	0.754
8.333	134.474	18.677	2.244	2.713	1.216
10	123.994	20.666	1.989	1.219	0.766

Table 2. Hydrology data for roof 1 (Tr=5 years).

Time (min)	Intensity (mm/h)	Cumulated water layer (mm)	Incremental water layer (mm)	Infiltration layer (mm)	runoff thickness (mm)
0	0	0	0	0	0
1.667	160	4.444	4.444	4.444	0
3.333	160	8.889	4.445	4.434	0.009
5	160	13.333	4.444	3.904	0.543
6.667	160	17.778	4.445	3.215	1.225
8.333	160	22.222	4.444	2.705	1.743
10	160	26.667	4.445	2.305	2.145

Table 3. Hydrology data for roof 1 (Tr=10 years).

Time (min)	Intensity (mm/h)	Cumulated water layer (mm)	Incremental water layer (mm)	Infiltration layer (mm)	runoff thickness (mm)
0	0	0	0	0	0
1.667	180	5	5	5	0
3.333	180	10	5	4.93	0.069
5	180	15	5	4.13	0.873
6.667	180	20	5	3.35	1.65
8.333	180	25	5	2.77	2.227
10	167.386	27.898	2.898	1.398	1.499

Table 4. Hydrology data for roof 1 (Tr=25 years).

Time (min)	Intensity (mm/h)	Cumulated water layer (mm)	Incremental water layer (mm)	Infiltration layer (mm)	runoff thickness (mm)
0	0	0	0	0	0
1.667	190	5.278	5.278	5.278	0
3.333	190	10.556	5.278	5.157	0.12
5	190	15.833	5.277	4.228	1.05
6.667	190	21.111	5.278	3.408	1.873
8.333	190	26.389	5.278	2.798	2.478
10	190	31.667	5.278	2.348	2.934

López, N., Domínguez, C., Barreto, W., Méndez, N., López, L., Soria, M., Lizano, R. and Montesinos, V.
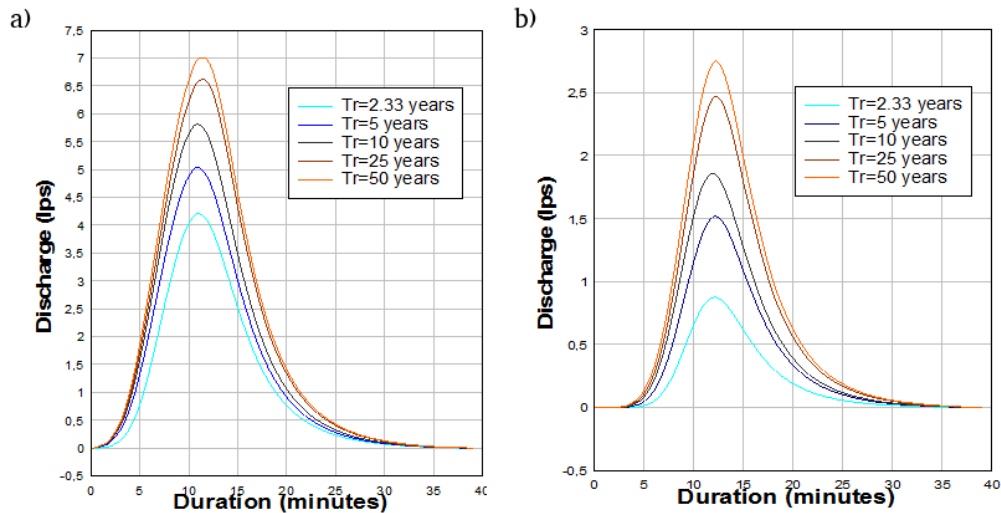
Table 5. Hydrology data for roof 1 (Tr=25 years).

Time (min)	Intensity (mm/h)	Cumulated water layer (mm)	Incremental water layer (mm)	Infiltration layer (mm)	runoff thickness (mm)
0	0	0	0	0	0
1.667	200	5.556	5.556	5.556	0
3.333	200	11.111	5.555	5.376	0.183
5	200	16.667	5.556	4.326	1.235
6.667	200	22.222	5.555	3.455	2.103
8.333	200	27.778	5.556	2.825	2.733
10	200	33.333	5.555	2.345	3.205

Figure 5. Hydrographs of roof 1 for different return periods with a) and without b) green roofs.

It is observed that there is a considerable peak flow reduction, also there is a retarding of peak time but not too significant, as shown in Table 6. The total volume of rainwater that theoretically could be stored in the green roofs is determined through the effective porosity of the soil matrix. Assuming that effective porosity is about 10%, the total volume storage for the roof 1 is shown in Table 7, and for all roofs is shown in Table 8.

According to Table 6, the potential retention of water for small rainfall events is higher than for higher events, and it is related with the volume of rainfall and the storage capacity of the roof. Table 7 and Table 8 show the maximum usable water volume, according to a 10 % of effective porosity, but the real

infiltrated volume of water was estimated by using the Equation 16.

$$P = Q_i + Q + E \qquad (16)$$

With P the total precipitation thickness (mm), Q_i is the total infiltration thickness (mm) and Q is the rainfall thickness (mm). E is the vegetation evapotranspiration (mm), for our purposes this is set $E = 0$. The real volume of rainwater storage for roof 1, is shown in Table 9. The volume shown in Table 9 must be affected by the effective porosity, in order to obtain the usable volume of water as shown in Table 10 and Table 11. According to (WRF, 2016), the quantity of water per household necessary is shown in Table 12.
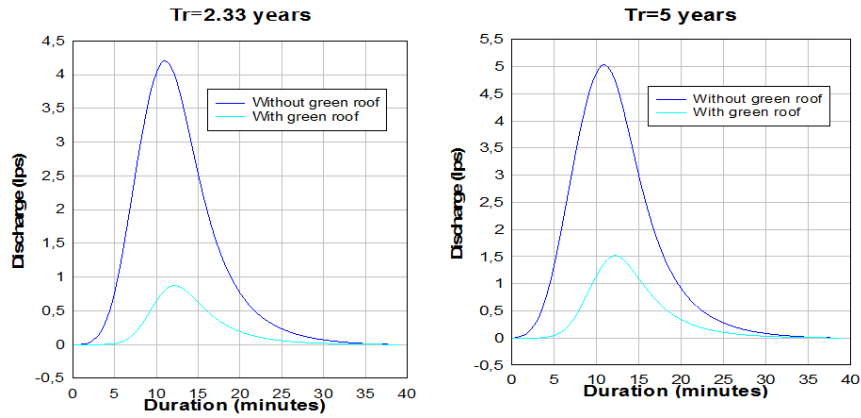
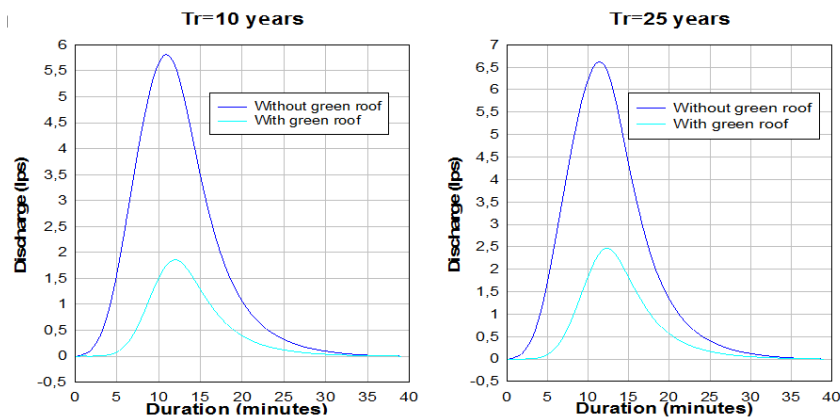**Figure 6.** Hydrographs of roof 1 for 2.33 years 5 years of Tr.

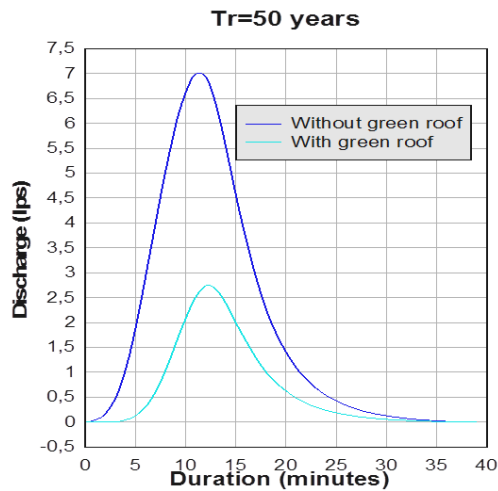**Figure 7.** Hydrographs of roof 1 for 10 years and 25 years of Tr.

Figure 8. Hydrographs of roof 1 for 50 years of Tr.

Table 6. Peak flow reduction and increase of peak time for roof 1.

Tr	Without green roofs		With green roofs		Peak flow reduction (%)	Delay of peak time (times)
	Peak flow (lps)	Peak time (min)	Peak flow (lps)	Peak time (min)		
2.33	4.16	10.5	0.87	12	0.79	1.14
5	5.00	10.5	1.51	12	0.69	1.14
10	5.77	10.5	1.86	12	0.67	1.14
25	6.54	12	2.45	12	0.62	0.00
50	6.93	12	2.73	12	0.60	0.00

Table 7. Maximum usable volume of water in green roof number 1.

ID	Roof surface (m^2)	Soil thickness (cm)	Effective porosity %	Maximum usable water volume (m^3)
1	163.03	20	0.10	3.26

Table 8. Maximum usable volume of water for all roofs.

ID	Roof surface (m^2)	Soil thickness (cm)	Effective porosity %	Maximum usable water volume (m^3)
1-68	14 554.20	20	0.10	291.08

Table 9. Real infiltrate volume for roof 1.

ID	Roof surface (m^2)	Soil thickness (cm)	Effective porosity %	Maximum usable water volume (m^3)	Real infiltrate volume (m^3).				
					2, 33	5	10	25	50
1	163.03	20	0.1	3.26	1.98	2.28	2.40	2.59	2.66

Rainwater stored in green roofs could be recycled for domestic water use. Indeed, rainwater cannot be used for drinking purposes without a correct treatment, but it can be used to supply other purposes such as toilet water and irrigation. According to (WRF, 2016), 125 liters per household/day (33.1 gphd), are needed for toilets usage. Considering that, in average, a toilet is used 5 times per person per day; if a part of the rainwater could be stored to be used by toilets, the own urbanism (68 houses) could supply, theoretically, the water demand as shown in Table 13, which is not negligible.

In addition, a considerable peak flow reduction could be obtained if structures such as rectangular weirs are used in ceilings, as shown in Figure 9. Applying the routing of hydrographs using 2 weirs of 10 cm in length and 10 cm in height, the output hydrograph of roof 1 for each return period is shown from Figure 10 to Figure 12. Green roofs are a good peak flow reducer, but when combining them with weirs the reduction of peak flow is even better, although the volume produced is the same, i.e., without additional storage of water for the use of weirs. Finally, the total peak flow for each period of return is shown in Table 14 and Table 15.
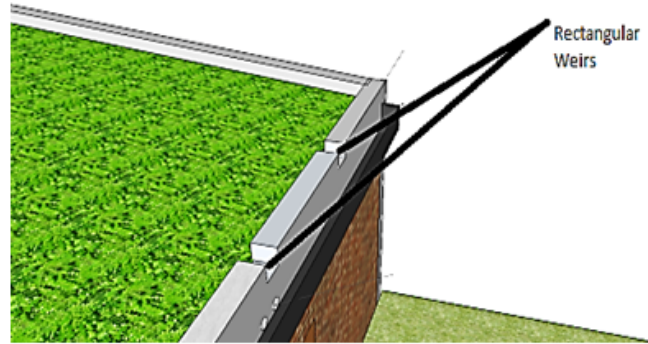
Figure 9. Rectangular weirs in green roofs.

Table 10. Real usable volume for roof 1.

ID	Roof surface (m^2)	Soil thickness (cm)	Effective porosity $\%$	Maximum usable water volume (m^3)	Real usable volume (m^3).				
					$2,33$	5	10	25	50
1	163.03	20	0.1	3.26	0.20	0.23	0.24	0.26	0.27

Table 11. Real usable volume for all roofs.

ID	Roof surface (m^2)	Soil thickness (cm)	Effective porosity $\%$	Maximum usable water volume (m^3)	Real usable volume (m^3).				
					$2,33$	5	10	25	50
1-68	14 554.2	20	0.1	291.08	17.65	20.31	21.44	23.09	23.76

Table 12. Quantity of water needed in liters per household per day. Source WRF (2016).

Water use	Quantity (lphd)
Toilet	125.3 (24 %)
Shower	106.4 (20 %)
Faucet	99.6 (19 %)
Clothes washer	85.9 (16 %)
Leak	64.4 (12 %)
Other	20.1 (4 %)
Bath	13.6 (3 %)
Dishwasher	6.1 (1 %)
Total	521.3 (100 %)

According to Table 14, peak flow reduction is over 96 %, assuming CN II and a first rainfall, but these results could be affected for continuous rainfall events. Another benefit of using green roofs and their routing is the design of urban drainage, and according to Table 16, a considerable decrease in volume (conventional roof vs green roof) and duration of the hydrograph (green roof vs green roof and

weirs), which means a positive impact on the drainage system. The decrease in peak flow will require pipes with smaller diameters and lower slopes that make up the drainage system. Using the manning equation, the diameter of the pipes through which the total flow of urbanism will flow (Equation 17).

With Q the discharge, S is the pipe slope, A is the flow area, R is the hydraulic ratio and n is the pipe rugosity.

$$Q = \frac{\sqrt{S} * A * R^{\frac{2}{3}}}{n} \qquad (17)$$

Table 13. Supply days for toilets (68 houses).

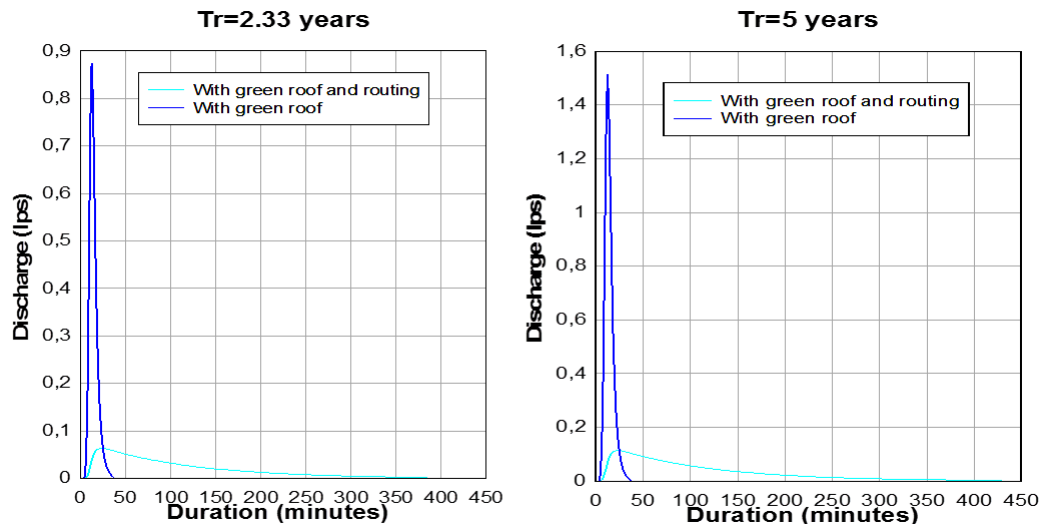| Tr	Water storage (liters)	Supply days
2.33	17 652.68	2.08
5	20 308.50	2.39
10	21 441.40	2.52
25	23 086.58	2.72
50	23 755.79	2.79

Figure 10. Hydrographs of roof 1 for 2.33 years and 5 years of Tr.

Table 14. Peak flow for each scenario (roof 1).

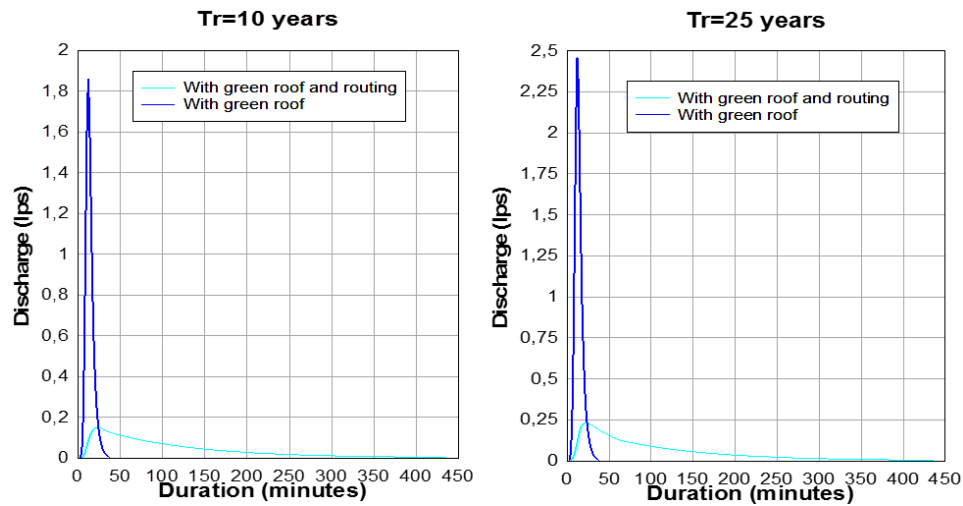| Tr	Peak flow (lps)			Peak flow reduction (%)		Hydrograph duration (min)	
	Conventional roof	Green roof	Green roof and routing (weirs)	Green roof	Green roof and routing (weirs)	Green roof	Green roof and routing (weirs)
2.33	4.161	0.874	0.064	78.995	98.462	40.0	>200
5	5.004	1.514	0.114	69.744	97.722	40.0	>200
10	5.778	1.86	0.15	67.809	97.404	40.0	>200
25	6.547	2.458	0.232	62.456	96.456	40.0	>200
50	6.936	2.738	0.27	60.525	96.107	40.0	>200

Figure 11. Hydrographs of roof 1 for 10 years and 25 years of Tr.

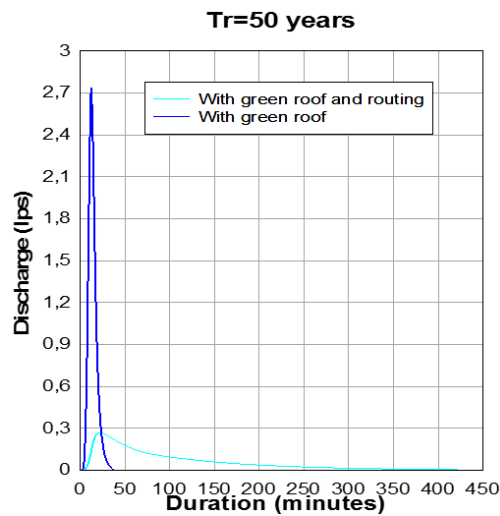**Figure 12.** Hydrographs of roof 1 for 50 years of Tr.

Table 15. Peak flow for each scenario (all roofs).

Tr	Peak flow (lps)		
	Conventional roof	**Green roof**	**Green roof and routing (weirs)**
2.33	371.491	77.978	4.395
5	446.689	135.007	7.941
10	515.813	165.995	10.505
25	584.451	219.436	16.175
50	619.191	244.369	18.82

Note that there is a considerable reduction on diameters for urban drainage (Locatelli et al., 2014; Pradhan et al., 2019), almost 100% of reduction. It should be noted that these results are valid in cases of first wash or first rainfall, due to green roofs saturate faster their matrix of soil and for continuous rainfall the results for drainage can be affected.

López, N., Domínguez, C., Barreto, W., Méndez, N., López, L., Soria, M., Lizano, R. and Montesinos, V.

Table 16. Required diameter for each scenario.

Tr	Conventional roof	Required diameter (mm)	Minimum slope (m/m)	Green roof	Required diameter (mm)	Minimum slope (m/m)	Green roof and routing	Required diameter (mm)	Minimum slope (m/m)
2,33	371,491	500	0,01	77,978	280	0,005	4,395	200	0,005
5	446,689	500	0,01	135,007	315	0,01	7,941	200	0,005
10	515,813	500	0,01	165,995	355	0,01	10,505	200	0,005
25	584,451	500	0,02	219,436	355	0,02	16,175	200	0,005
50	619,191	500	0,02	244,369	355	0,02	18,82	200	0,05

5 Conclusions

Green roofs, in addition to offering a good ecological alternative to replenish green areas in urban areas, also offer a viable alternative for the collection and storage of rainwater, which according to this study, can reach between 2 and 3 days of use for toilets in urbanisms (according to the intensity of the rainfall), which could represent savings for the inhabitants' economy and at a macro level for the state economy.

In addition to the paragraph above, the placement of flow-regulating structures as weirs offers a delay advantage in the production of the peak flow of the hydrographs of the roofs and therefore of the urbanization. According to the results for the urbanism, for first rains, the combined use of green roof and weirs offers a considerable delay on the total duration of the hydrographs, almost over three times in comparison with conventional roof (under the conditions studied in this research) helping with the urban drainage by reducing commercial diameters of the pipes almost to half of the size.

The harvest of water for various uses during the useful life of the house helps to preserve the water level of reservoirs and ecological flows of the natural channels and their cross section; the harvest of water rainfall proposed in this research has a good theoretical performing, not only to focus on the drainage but based on the fact that it delays the peak flow time of the urbanism and the hydrograph total duration; creates a gap between the hydrograph peak flow of the urbanism and the hydrograph peak flow of the natural channels for discharge, and decreases the risk of floods.

It is recommended to carry out a study on retaining water not only from the roof, but also from the

hydrograph with storage structures to increase the capacity to harvest rainwater, as well as studies to determine the real CN for them.

References

Arabi, R., Shahidan, M., Kamal, M., Ja Afar, M., and Rakhshandehroo, M. (2015). Mitigating urban heat island through green roofs. *Current World Environment*, 10(1):918–927. Online:https://bit.ly/2ViMLOt.

BCIT (2018). Centre for architectural ecology. Último acceso: 21 August 2018.

Berardi, U., GhaffarianHoseini, A., and GhaffarianHoseini, A. (2014). State-of-the-art analysis of the environmental benefits of green roofs. *Applied Energy*, 115:411–428. Online:https://bit.ly/3fZIYxn.

Chow, V. T., Maidment, D., and Ways, L. (1994). *Hidrología Aplicada*. Bogotá.

Connelly, M. and Hodgson, M. (2013). Experimental investigation of the sound transmission of vegetated roofs. *Applied Acoustics*, 74(10):1136–1143. Online:https://bit.ly/2ZeDlEZ.

EPA, A. (2018). Reducing urban heat islands: Compendium of strategies. green roofs. Último acceso: 18 August 2018.

Escobedo, F., Nowak, D., Wagner, J., De la Maza, C., Rodríguez, M., Crane, D., and Hernández, J. (2006). The socioeconomics and management of santiago de chile's public urban forests. *Urban Forestry & Urban Greening*, 4(3-4):105–114. Online:https://bit.ly/3fWDgfG.

Fenton, J. (2009). Reservoir routing. *Hydrological Sciences Journal*, 37(3):233–246. Online:https://bit.ly/3i3FP1y.

Fioretti, R., Palla, A., Lanza, L., and Principi, P. (2010). Green roof energy and water related performance in the mediterranean climate. *Building and environment*, 45(8):1890–1904. Online:https://bit.ly/2VghyeI.

Francis, R. and Lorimer, J. (2011). Urban reconciliation ecology: the potential of living roofs and walls. *Journal of environmental management*, 92(6):1429–1437. Online:https://bit.ly/2Zhhj4u.

Huang, J. (1994). *Roof garden design and construction.* Beijing.

Ilbay-Yupa, M., Zubieta, B., and Lavado-Casimiro, W. (2019). Regionalizaci la precipitaciu agresividad y concentraci la cuenca del ruayas, ecuador. *La Granja: Revista de Ciencias de la Vida.*, 30(2):57–76. Online:https://bit.ly/2P9eCNE.

Liu, W., Feng, Q., Chen, W., Wei, W., and Deo, R. C. (2019). The influence of structural factors on stormwater runoff retention of extensive green roofs: new evidence from scale-based models and real experiments. *Journal of Hydrology*, 569:230–238. Online:https://bit.ly/2BL92gJ.

Locatelli, L., Mark, O., Steen Mikkelsen, P., Arnbjerg-Nielsen, K., Bergen Jensen, M., and Binning, P. (2014). Modelling of green roof hydrological performance for urban drainage applications. *Journal of Hydrology*.

López, N., Barreto, W., and Méndez, N. (2014). Techos verdes como solución al problema de inundaciones en medios urbanos. *Gaceta Técnica DIC*, (14):9–20.

MacIvor, J. and Lundholm, J. (2011). Insect species composition and diversity on intensive green roofs and adjacent level-ground habitats. *Urban ecosystems*, 14(2):225–241. Online:https://bit.ly/3g1iZ8J.

Minke, G. (2017). Inclined green roofs - ecological and economical advantages, passive heating and cooling effect. In Faculty of Civil Engineering, editor, *Conference Central Europe towards Sustainable Building: proceedings*. Czech Technical University,.

NRCS (1973). A method for estimating volume and rate of runoff in small watersheds. Último acceso: 18 August 2018.

Olivares, B. O. (2018). Condiciones tropicales de la lluvia estacional en la agricultura de secano de carabobo, venezuela. *La Granja: Revista de Ciencias de la Vida.*, 27(1):86–102. Online:https://bit.ly/3hRE7iI.

Pradhan, S., Al-Ghamdi, S., and Mackey, H. (2019). Greywater recycling in buildings using living walls and green roofs: A review of the applicability and challenges. *Science of The Total Environment*, 652:330–344. Online:https://bit.ly/2YDkBQ4.

QGIS, D. (2014). Qgis geographic information system. open source geospatial foundation project.

Ramke, H. (2018). *Solid Waste Landfilling*, chapter 8.2 Drainage Systems-Collection of Surface Runoff and Drainage of landfill Top Cover Systems, pages 373–416. Elsevier.

Reyes, S. and Figueroa, I. (2010). Distribución, superficie y accesibilidad de las áreas verdes en santiago de chile. *EURE (Santiago)*, 36(109):89–110. Online:https://bit.ly/3dBLFDU.

Romero, H. and Vásquez, A. (2005). La comodificación de los territorios urbanizables y la degradación ambiental en santiago de chile. *Revista Electrónica de Geografía y Ciencias Sociales*, 9(194):1–68. Online:https://bit.ly/383rE7U.

Serrano, S., Ruíz, J. C., and Bersosa, F. (2017). Heavy rainfall and temperature proyections in a climate change scenario over quito, ecuador. *La Granja: Revista de Ciencias de la Vida.*, 25(1):16–32. Online:https://bit.ly/313gsFn.

Serrano, S., Zuleta, D., Moscoso, V., Jácome, P., Palacios, E., and Villacís, M. (2012). Ansis estadico de datos meteorolos mensuales y diarios para la determinaci variabilidad climca y cambio climco en el distrito metropolitano de quito. *La Granja: Revista de Ciencias de la Vida.*, 16(2):23–47. Online:https://bit.ly/3flS7iV.

Shafique, M.and Kim, R. and Rafiq, M. (2018). Green roof benefits, opportunities and challenges–a review. *Renewable and Sustainable Energy Reviews*, 90:757–773. Online:https://bit.ly/2NwCF8a.

Sims, A., Robinson, C., Smart, C.and Voogt, J., Hay, G., Lundholm, J.and Powers, B., and O'Carroll,

D. (2016). Retention performance of green roofs in three different climate regions. *Journal of Hydrology*, 542:115–124. Online:https://bit.ly/2CENbbm.

Technology, G. (2018). Advantages of green roofs. Último acceso: 21 August 2018.

TxDOT, T. (2019). Hydraulic design manual. Último acceso: June 10, 2020.

Vásquez, A. and Romero, H. (2008). Vegetación urbana y desigualdades socioeconómicas en la comuna de peñañolen, santiago de chile. mathesis.

Vijayaraghavan, K. (2016). Green roofs: A critical review on the role of components, benefits, limitations and trends. *Renewable and sustainable energy reviews*, 57:740–752. Online:https://bit.ly/31n7nsO.

Viola, F., Hellies, M., and Deidda, R. (2017). Retention performance of green roofs in representative climates worldwide. *Journal of Hydrology*, 553:763–772. Online:https://bit.ly/2A6jIpR.

WRF (2016). W.R.F., residential end uses of water, version 2. excecutive report.. s.l.:s.n.

Yang, J., Yu, Q., and Gong, P. (2008). Quantifying air pollution removal by green roofs in chicago. *Atmospheric environment*, 42(31):7266–7273. Online:https://bit.ly/2Vlr1BF.

SUSTAINABILITY AND EVALUATION OF THE IMPACT CAUSED BY THE LANDFILL OF THE MUNICIPALITY OF CARMEN, CAMPECHE, MÉXICO

SUSTENTABILIDAD Y EVALUACIÓN DEL IMPACTO OCASIONADO POR EL RELLENO SANITARIO DEL MUNICIPIO DE CARMEN EN CAMPECHE, MÉXICO

Areli Machorro-Román[1] , Genoveva Rosano-Ortega[1] , María Elena Tavera-Cortés[2] , Juan Gabriel Flores-Trujillo[3] , María Rosa Maimone-Celorio[1] , Estefanía Martínez-Tavera[1] , Sonia Martínez-Gallegos[4,5] and Pedro Francisco Rodríguez-Espinosa[6]

[1] *Facultad de Ingeniería Ambiental, Universidad Popular Autónoma del Estado de Puebla. Av. 21 sur, 1103, Barrio de Santiago, 72410, Puebla, México.*

[2] *Instituto Politécnico Nacional. Av. Luis Enrique Erro S/N, Unidad Profesional Adolfo López Mateos, Zacatenco, Alcaldía Gustavo A. Madero, 07738, Ciudad de México, México.*

[3] *Facultad de Ingeniería, Universidad Autónoma del Carmen. Av. 56 No. 4 Esq. Avenida Concordia Col. Benito Juárez, 24180, Ciudad del Carmen, Campeche, México.*

[4] *Tecnológico Nacional de México. Avenida Universidad 1200, Colonia Xoco, Coyoacán, 03330, Ciudad de México, México.*

[5] *Instituto Tecnólogico de Toluca. Av. Tecnológico s/n. Colonia Agrícola Bellavista Metepec, 52149, Edo. De México, México.*

[6] *Centro Interdisciplinario de Investigaciones y Estudios sobre Medio Ambiente y Desarrollo (IPN-CIIEMAD), Instituto Politécnico Nacional. Calle 30 dejunio de 1520, Barrio de la Laguna Ticomán, Del. Gustavo A Madero, C.P. 07340, Ciudad de México, México.*

*Corresponding author: mtavera@ipn.mx

Abstract

The sustainability indicators allow the evaluation of the environmental impacts related to the sustainable development strategy. The research was conducted in ciudad del Carmen, Campeche, which is considered a barrier island located at the southeast of Mexico. The municipality channels the final disposal of solid urban waste (MSW) through a sanitary landfill which is located in a mangrove area, having a negative impact on the environment, negatively affects the sustainable development. This research identified a sequence of carbonated sands by means of subsoil sediment analysis, which allowed to define a porosity of 20.2 to 40.1% and a permeability of $\pm 10^{-2}$-10^{-4} ms^{-1}, i.e., the sediments have good porous and high permeability. On the other hand, and with respect to water quality, concentrations of BOD_5 and COD in the mangrove were 63.06 and 1338.13 mg L^{-1}, respectively, as well as the presence of trace

Scientific paper / Artículo científico

WASTE MANAGEMENT   *Machorro, A., Rosano, G., Tavera, M., Flores, J., Maimone, M., Martínez, E., Martínez, S. and Rodríguez, P.*

concentrations of some heavy metals. These values allowed to classify it as a strongly contaminated body of water.

Keywords: Mexico, sustainability, waste, leachate, pollution, water, sediments.

Resumen

Los indicadores de sustentabilidad permiten evaluar los impactos ambientales relacionados con la estrategia del desarrollo sustentable. Este estudio se realizó en Ciudad del Carmen, Campeche, que es considerada una isla de barrera que se localiza al sureste de México. El municipio canaliza la disposición final de los residuos sólidos urbanos (RSU) a través de un relleno sanitario el cual se encuentra ubicado en una zona de manglar, teniendo un impacto negativo en el medio ambiente lo que incide negativamente en el desarrollo sustentable. Mediante el análisis sedimentológico del subsuelo, se obtuvieron resultados que identificaron la dominancia de arenas carbonatadas, lo que permitió definir un rango de porosidad del 20,2 al 40,1 %, y permeabilidad de $\pm\ 10^{-2}$-$10^{-4}\ ms^{-1}$ darcys, es decir, los sedimentos presentan una buena porosidad y una permeabilidad alta. Por su parte, mediante un análisis de la calidad del agua se detectaron concentraciones de Demanda Bioquímica de Oxígeno (DBO_5) y Demanda Química de Oxígeno (DQO) de 63,06 y 1338,13 mg L^{-1}, respectivamente, así como la presencia de concentraciones de trazas de algunos metales pesados. Estos valores permitieron clasificarlo como un cuerpo de agua fuertemente contaminado.

Palabras clave: México, sustentabilidad, residuos, lixiviados, contaminación, agua, sedimentos.

Orcid IDs:

Areli Machorro Román: http://orcid.org/0000-0003-4666-4489

Genoveva Rosano-Ortega: http://orcid.org/0000-0002-7297-3456

María Elena Tavera-Cortés: http://orcid.org/0000-0002-2179-2735

Juan Gabriel Flores-Trujillo: http://orcid.org/0000-0002-6221-216X

María Rosa Maimone Celorio: http://orcid.org/0000-0002-9638-1578

Sonia Martínez-Gallegos: http://orcid.org/0000-0002-7297-3456

Pedro Francisco Rodríguez Espinosa: http://orcid.org/0000-0002-0443-5728

Estefanía Martínez Tavera: http://orcid.org/0000-0003-0449-037X

1 Introduction

Ciudad del Carmen, Campeche, is a barrier island of sedimentary origin of Quaternary age (2.58 Ma. approx.) (SGM, 2005; CONABIO, 2012; ICS, 2018) located in the southeastern Mexico (Figure 1). The island is part of Mexico's largest and most valuable estuarine lagoon system: Laguna de Términos (Escudero et al., 2014). This system has an ellipsoid shape with a length of 70 km and a width of 30 km, and covers an area of 2500 Km^2, with an average depth of 3-3.5 m. The main rivers that deposit sediments in this lagoon system are the Palizada River (240 m^3 s^{-1}), the Candelaria River (35 m^3 s^{-1}) and the Chumpán River (2 m^3 s^{-1}), which provides a significant discharge of fresh water of 400 m^3 s^{-1} (Magallanes-Ordóñez et al., 2015).
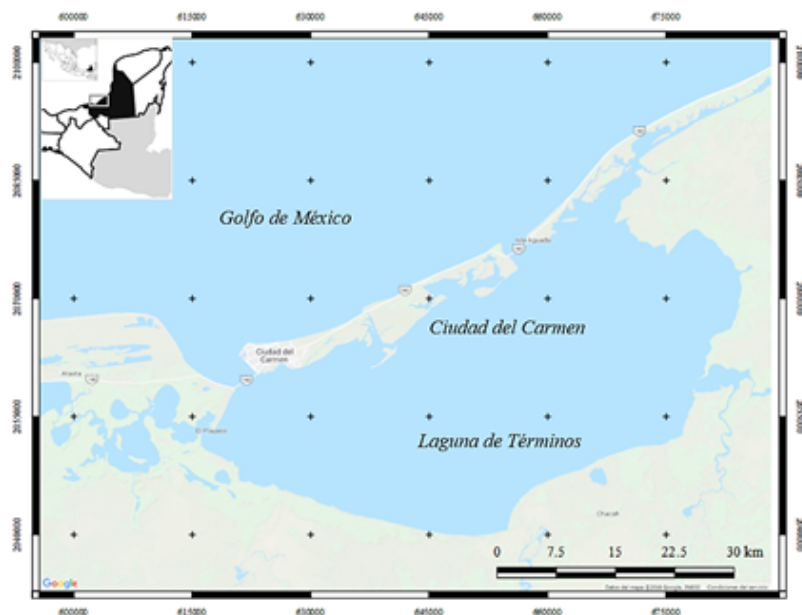
Figure 1. . Location of Ciudad del Carmen, Campeche (Modified by INEGI (2010)).

The island has great ecological importance because it is dominated by a mangrove-like ecosystem (mangrove "Isla del Carmen"; 43.92 Km^2) that extends over 43.92 Km^2 (4392 ha) (CONABIO, 2012) and is part of the RAMSAR area called "Area de Protection de Flora y Fauna Laguna de Términos", which has an area of 705 016 ha that includes the island, the Laguna de Protección and some portions surrounding them (CONANP, 2018).

Wetlands represent one of the most important types of ecosystems in the world, and are also one of the most threatened (Hu et al., 2017). Such ecosystems are ecologically important because they serve as habitat for various fish and wildlife communities, as well as various commercially valuable species, and are buffers of the coastline, provide fresh water, reduce sedimentation in navigable waters, and potentially aid in the storage of floodwaters. In addition to this, its soils contain some of the largest carbon reserves in the biosphere (Maynard et al., 2014; Ghosh et al., 2016; Nahlik and Fennessy, 2016; Rains et al., 2016).

1.1 Lithology

The study area is located 8 km (approx.) from Ciudad del Carmen, in the vicinity of the municipal landfill (Figure 1), former delta Cocoyotes-el Cayo (Palacio-Prieto et al., 1999). This landfill is surrounded by a series of channels that flow into Laguna de Términos (current direction N-S), all these channels were part of the old internal delta.

Isla del Carmen (of Quaternary age) is formed by a coastal plain to the north, made up of high and low beach cords on sandy sediments, and a low floodplain lagoon to the south dominated by a fluvial-marine over slimy clay sediments (Ramos-Reyes et al., 2016). Lithologically, the island consists of a sequence of coastal sediments to the north, and a sequence of palustre sediments to the south; in the Laguna de Términos are reported silts rich in organic matter, as well as sands rich in aluminosilicates and carbonates derived from the alluvial supply of the sea and isla del Carmen (Darnell, 2015; Jones, 2015; Magallanes-Ordóñez et al., 2015).

Palustres deposits are characterized by a low energy level. In these environments the dynamics of sediments and all processes are linked to tides and currents, which play an essential role in this type of environment, and the silts are predominant. Meanwhile, coastal deposits are characterized by a high level of energy, which allows the deposit of sands (Martínez et al., 2015).

The spatial distribution of sediments is as follows: 1) sands on the island's inland coast, 2) slimy sands at the entrance of the island (west) and at the mouths of the Palizada, Chumpán and Candelaria rivers, and 3) the sands are present on the island coast (Magallanes-Ordóñez et al., 2015).

1.2 Regulations

The general rules applicable for the final disposal of waste correspond to NOM-083-SEMARNAT-2003 (SEMARNAT, 2003), en el apartado de "Specifications for the Site Selection " and "Restrictions for the Site Location" in which is stated:

- Final disposition sites should not be located within protected natural areas. In any case, the order in the corresponding "Declaration of Creation and the subzonification and administrative rules contained in the Management Program" must be observed. According to CONANP (2018), the municipal landfill is located within the Area of Protection of Flora and Fauna Laguna de Términos.

- "It should not be located in areas of: marshes, mangroves, swamps, wetlands, estuaries, alluvial plains, river, aquifer recharge; nor on caverns, fractures or active geological faults". According to CONABIO (2012), the island is dominated by a mangrove-like ecosystem.

- On the other hand, according to the Guidelines of technical specifications for the construction of landfills for MSW and RME (SEMARNAT, 2009), a landfill must have the following technical specifications: (i) cells, (ii) waterproofing system, (iii) biogas extraction, uptake and control system, and (iv) leach extraction, capture and control system. The municipal landfill fails to comply with the engineering established by this guideline, so its operation is affects the environmental protection of the area.

The objective of this article is to evaluate the environmental impact generated by the landfill of the Carmen municipality, Camp, in the subsoil of the central northern region of "Área de Protección de Flora y Fauna Laguna de Términos (APFFLT)" through a sedimentological analysis, to determine the infiltration capacity of leachates in the sustainable development. In order to differentiate sediment samples from water samples, the VP key (vertical profile) for sediments and WS (water sample) were used for water, respectively.

2 Materials and methods

Sustainability indicators (SI) allow environmental and social information to be related to information on pollution, deterioration of productive development or well-being achieved by the population (Ibáñez-Forés et al., 2013). According to the information of the National Census of Municipal Governments of the National Institute of Statistics and Geography (INEGI, 2017), 792 190 kg of solid urban waste (RSU) is collected daily in Campeche, of which 289 140 kg per day are collected in Ciudad del Carmen, representing a total of 36.5 % of the total waste collected in Campeche; MSWs are not subjected to any treatment or selection and are transported to the landfill selected in this research.
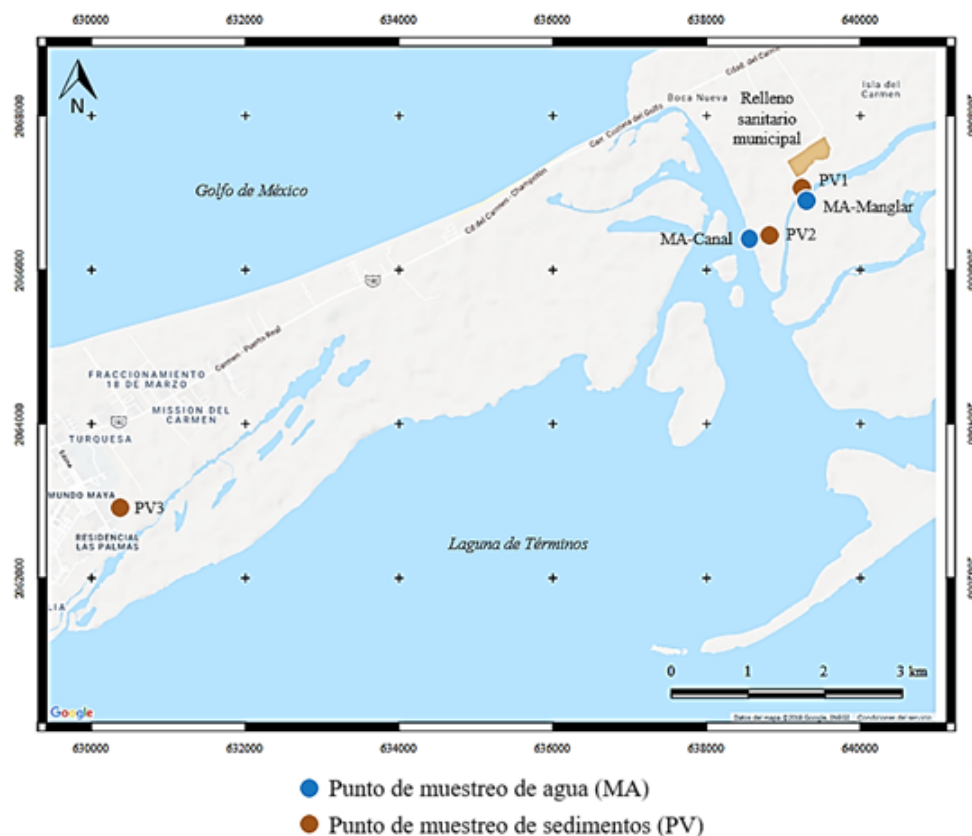
Figure 2. Location of sampling areas.

The ampling was carried out during the time of wattage, considering that during this period leachates are more mobile due to increased rainfall runoff, which is considered feasible for the sampling of water quality. Sediment samples were collected at 3 stations on the periphery of the municipal landfill and within the mangrove of the study area, as shown in Figure 2, following NOM-021-SEMARNAT-2000 which "establishes fertility, salinity and soil classification specifications, studies, sampling and analysis" (SEMARNAT, 2000). The collection points were selected according to the proximity to the landfill of the municipality of Carmen and randomly around it, considering the uniformity of the sedimentary facies throughout the island. Pv1 is located at $\pm$ 407.25 m from the landfill ($18°41'25.332''$ N, $91°40'46.307''$ W). Pv2 is located at $\pm$ 1184.21 m from the landfill ($18°41'5.46''$ N, $91°41'4.199''$ W). And finally the PV3 is located at $\pm$ 10104.23 m from the landfill ($18°39'12''$ N, $91°45'51''$ W). The sedimentological analysis was carried out according to the methodology proposed by Álvarez Arellano (2003) and Honarpour (2018). As a first step, the samples were subjected to the sieving method for granulometric analysis, using 14 sieves of openings -2 to 4 φ (4 a 0.063 mm), every 0.5 φ. This procedure was performed in the Geophysics Laboratory of Universidad Autónoma del Carmen (UNACAR). Subsequently, the samples were transferred to the Biotechn o-environmental Research Laboratory of Universidad Popular Autónoma del Puebla (UPAEP), where sedimentary components were determined and the determination of mass properties (porosity) was carried out. Particle size measurements and porosity determination were done in triplicate to obtain a valid data. The corresponding tables and graphs were created by applying descriptive statistics (Rendón-Macías et al., 2016). Within the analysis of the survey conditions of the study area, a trigonometry calculation (by differentiation of elevations) was implemented to obtain the inclination angle of the area to determine the runoff slope of the leachates to the main channels.
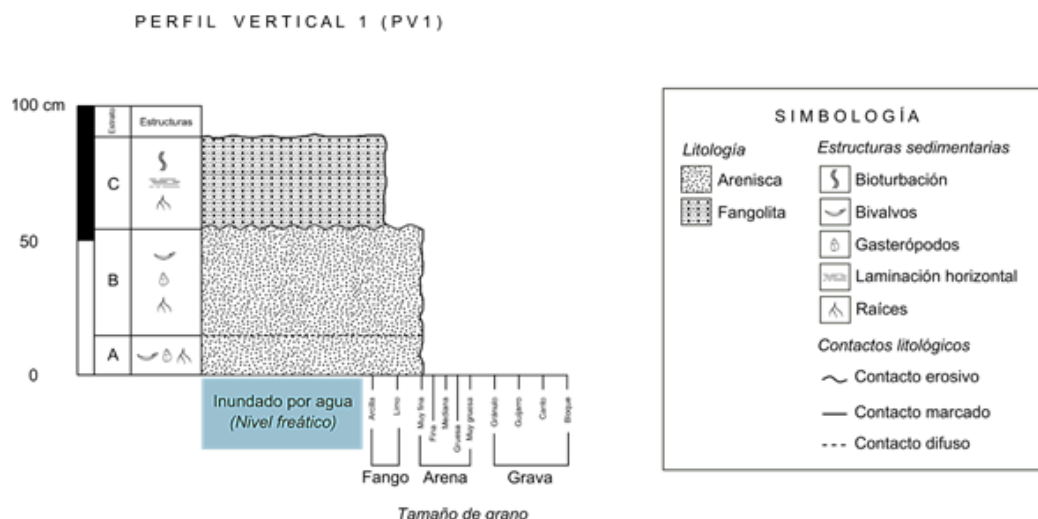
Figure 3. Lithological column of the VP1.

Water samples were collected at two stations (Figure 2), according to NMX-AA-003-1980 ("Wastewater – Sampling") (SCFI, 1980a) and NMX-AA-014-1980 ("Receiver Bodies – Sampling") (SCFI, 1980b), and were preserved according to NMX-AA-028-SCFI-2001 ("Water Analysis - Determination of Biochemical Oxygen Demand in Natural Water, Waste (DBO_5) and treated residuals - Test Method") (SCFI, 2001a) for DBO_5, NMX-AA-030/2-SCFI-2011 ("Water Analysis - Determination of Chemical Demand for Oxygen in Natural, Waste and Treated WasteWater - Test Method - Part 2 -Determination of the Chemical Oxygen Demand Index – Small-Scale Sealed Tube Method") (SCFI, 2011b) for COD, NMX-AA-029-SCFI-2001 ("Water Analysis - Determination of Total Phosphorus in Natural Water, Waste and Treated Waste - Test Method") (SCFI, 2001b) for Total Phosphorus Total Phosphorus , NMX-AA-026-SCFI-2010 ("Water Analysis - Total Kjeldahl Nitrogen Measurement in Natural Water, Waste and Treated Wastewater - Test Method") (SCFI, 2011a) for Total Kjeldahl Nitrogen, and NMX-AA-051-SCFI-2016 ("Water Analysis - Measurement of metals by atomic absorption in natural, drinking, waste and treated wastewater- Test method") (SCFI, 2016) for metals.

The collection points were selected, the first is close to the landfill of the municipality of Carmen ($\pm$481.65 m from landfill; coordinates 18°41′22.452″ N, 91°40′45.732″ W), and the second considering

the transport of the effluent through the main channel (at $\pm$1270.46 m from the landfill; coordinates 18°41′4.416″ N, 91°41′7.62″ W).

It should be noted that the relationship between the distance of the points with the municipal landfill and the topography of the area (pending in favor of the runoff towards the mangrove) allowed to evaluate the environmental impact. For the determination of DBO_5, DQO, Total Phosphorus and Total Kjeldahl Nitrogen, the samples were analyzed by Litoral Laboratorios Industriales (Cd. del Carmen, Camp.; with the accreditation EMA: AG-0135-015/11), under the compliance of NOM-001-SEMARNAT-1996 which "sets the maximum permissible limits of pollutants in discharges of wastewater in domestic water and goods. Ministry of Environment and Natural Resources" (SEMARNAT, 1996).

For the determination of heavy metals, the samples were transferred for analysis at the UPAEP Bioengineering Laboratory, where the quantitative analysis carried out from the atomic absorption spectrophotometry methodology was carried out, according to NMX-AA-051-SCFI-2001 (SCFI, 2016). Descriptive statistics were also applied for the analysis of the above data (Rendón-Macías et al., 2016).

3 Results

3.1 Sedimentological analysis

3.1.1 VP1 (Vertical Profile 1)

A lithological column with a thickness of 0.90 m.s.n.m. was identified, consisting of 3 strata. Granulometrically, sands of 0.125 to 0.062 mm composed of calcareous bigens and organic matter dominate the area. A porosity with a range of 20.2 to 30,2 % was determined (Figure 3).

Stratum A (VP1-A): Dominated by particles of very fine sand size (3.5 φ to 0.125 mm) (Figure 4). It belongs to the textural group Gravelly Sand, classified with the name of the sediment Fine Gravelly Fine Sand. Compositionally dominated by calcareous bigens and organic matter and with a porosity percentage of 20.2 %.

Stratum B (VP1-B): It is dominated by particles of fine-sized sands (2.5 φ to 0.25 mm) (Figure 5). It belongs to the Gravelly Sand textural group, classified as very Fine Gravelly Fine Sand sediment. Compositionally dominated by organic matter and quartz. It has a porosity percentage of 30.2 %.
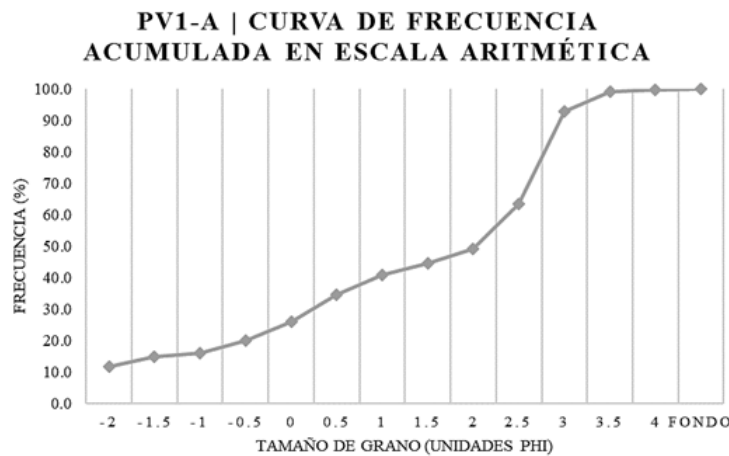

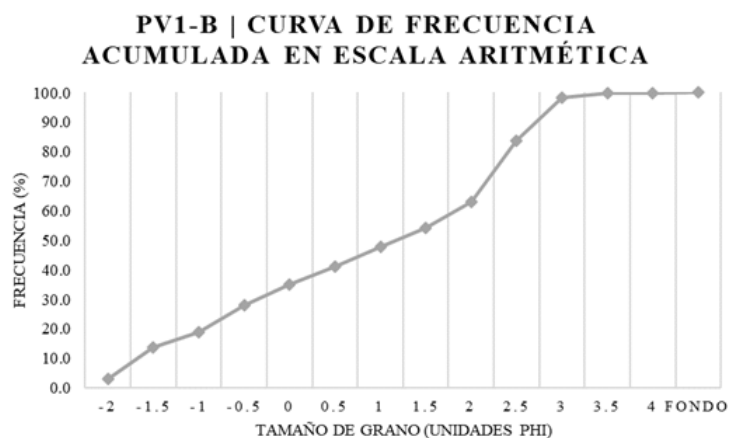**Figure 4.** Curve of accumulated frequency in artithmetic scale of VP1-A

Figure 5. Curve of accumulated frequency in arithmetic scale of VP1-B

Scientific paper / Artículo científico

WASTE MANAGEMENT *Machorro, A., Rosano, G., Tavera, M., Flores, J., Maimone, M., Martínez, E., Martínez, S. and Rodríguez, P.*
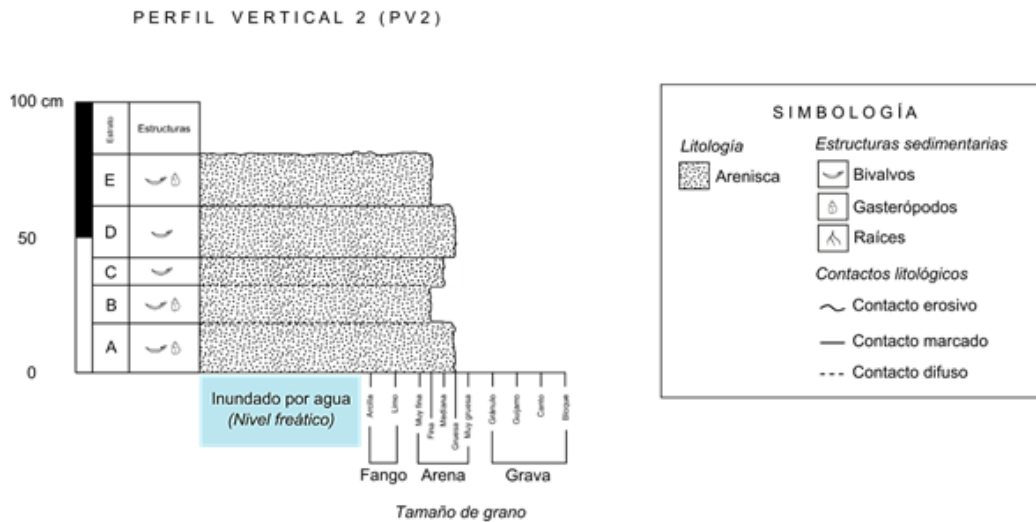

Figure 6. Lithological colum of VP2

3.1.2 VP2 (Vertical Profile 2)

It was identified as a lithological column with a thickness of 0.83 m.a.s.l, consisting of 5 strata. Granulometrically, sands of 1 to 0.125 mm composed of calcareous biogens and dethyritic material dominate the area. A porosity with a range of 20.3 to 36.5 % was determined (Figure 6).

Stratum A (VP2-A): It is dominated by particles thick-size sands (0.5 φ to 1 mm) (Figure 7). It belongs to the textural group Gravelly Sand, classified with the name of the sediment Fine Gravelly Coarse Sand. Compositionally, it is dominated by calcareous bigens and quartz. It has a porosity percentage of 20.3 %.

Stratum B (VP2-B): It is dominated by particles of very fine size to fine sands (3.5 φ to 0.25 mm) (Figure 8). It belongs to the textural group Gravelly Sand, classified with the name of the sediment Fine Gravelly Fine Sand. Compositionally, it is dominated by calcareous bigens and rock fragments. It has a porosity percentage of 36.5 %.

Stratum D (VP2-D): It is dominated by particles of very fine to very thick size sands (3.5 φ to 2 mm) (Figure 9). It belongs to the textural group Gravelly Sand, classified with the name of the sediment Fine Gravelly Fine Sand. Compositionally, it is dominated by calcareous bigens and rock fragments. It has

a porosity percentage of 36.5 %.

Stratum E (VP2-E): It is dominated by particles of very fine to fine size sands (3.5 φ to 0.25 mm) (Figure 10). It belongs to the textural group Gravelly Sand, classified with the name of the sediment Fine Gravelly Fine Sand. Compositionally, it is dominated by calcareous and calcite bigens. It has a porosity percentage of 29.7 %.

3.1.3 VP3 (Vertical Profile 3)

A lithological column with a thickness of 0.88 m.a.s.l was identified consisting of 5 strata. Granulometrically, gravel and sands from 4 mm to 0.25 mm dominate, composed of calcareous biogens and dethyritic material. A porosity with a range of 26.1 to 40.1 % was determined (Figure 11).

Stratum A (VP3-A): It is dominated by granule-sized particles (2.8 to 4 mm) (Figure 12). It belongs to the sandy gravel textural group, classified with the sediment name Sandy Fine Gravel. Compositionally, it is dominated by calcareous bigens and rock fragments. It has a porosity percentage of 36.8 %.

Stratum B (VP3-B): It is dominated by particles of fine to medium size sands (2.5 φ to 0.5 mm) (Figure 13). It belongs to the gravelly Sand textural group, classified with the name fine Gravelly Medium Sand. Compositionally, it is dominated by

Figure 7. Curve of accumulated frequency in arithmetic scale of VP2-A
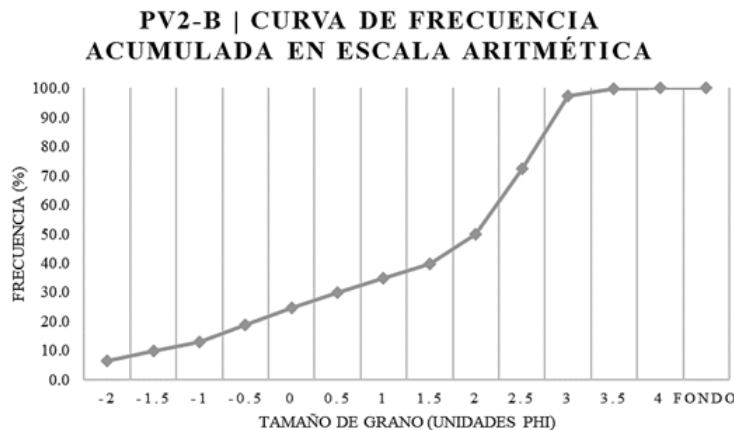
Figure 8. Curve of accumulated frequency in arithmetic scale of VP2-B

calcareous bigens and rock fragments. It has a porosity percentage of 26.1 %.

Stratum C (VP3-C): It is dominated by particles of very thick size sands to granules (1.4 to 4 mm) (Figure 14). It belongs to the sandy gravel textural group, classified with the sediment name Sandy Very Fine Gravel. Compositionally, it is dominated by calcareous bigens and rock fragments. It has a porosity percentage of 33.2 %.

Stratum D (VP3-D): It is dominated by particles of fine to thick size sands (2.5 phi to 1 mm) (Figure 15).

It belongs to the textural group Slightly Gravelly Sand, classified with the name of the very Slightly Fine Gravelly Medium Sand sediment. Compositionally, it is dominated by calcareous bigens and rock fragments. It has a porosity percentage of 36.6 %.

Stratum E (VP3-E): It is dominated by particles of medium to thick size sands (1.5 φ to 1 mm) (Figure 16). It belongs to the textural group Gravelly Sand, classified with the name of the very Fine Gravelly Coarse Sand sediment. Compositionally, it is dominated by calcareous bigens and organic matter. It has a porosity percentage of 40.1 %.
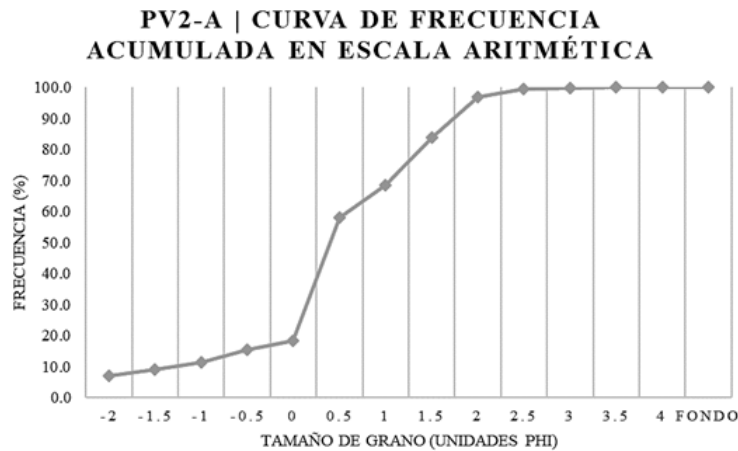
Figure 9. Curve of accumulated frequency in arithmetic scale of VP2-D
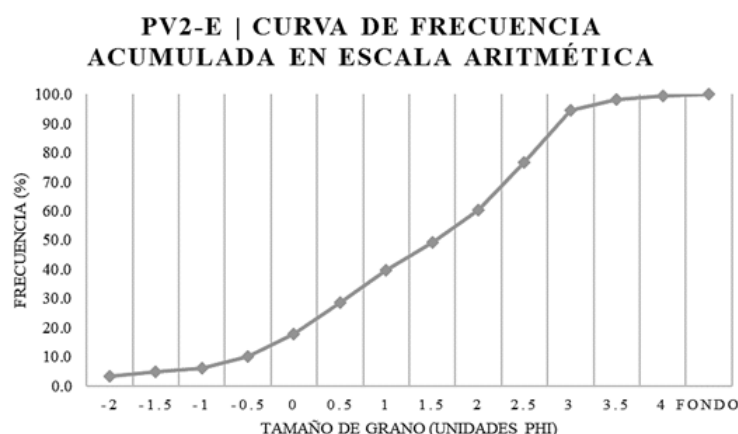
Figure 10. Curve of accumulated frequency in arithmetic scale of VP2-E

3.2 Water quality

The first sampling point is located at ±481.65 m from the landfill (18°41′22.452″ N, 91°40′45.732″ W), in one of the aqueous bodies of the mangrove area, which allowed this point to be classified as a dilution zone for leachate from the landfill. The water quality analysis for this sampling point is described in Table 1.

For its part, the second sampling point is located at ±1270.46 m from the landfill (18°41′4.416″ N, 91°41′7.62″ W), within the main channel (laminar flow with an N-S current direction) that crosses the study area. The concentrations of the different water quality parameters for this sampling point are

described in Table 1.

For heavy metals, and considering sampling points as a dilution zone (MA-Mangrove and MA-Channel), trace concentrations of the metals Cd, Cu, Ni and Zn (Table 2) were detected.

4 Discussion

4.1 Sedimentological analysis

A similarity was found between VP2 and VP3 from the granulometric analysis and sedimentary components of the three vertical profiles (VP), since both have the same size range (2.5 φ to 2 mm) and com-

ponents (calcareous biogens and rock fragments), thus a lateral continuity of the strata was determined. Meanwhile, the first stratum (VP2-A) of VP2 with the last stratum (VP1-B) of VP1, bears a similarity in granulometry (2.5 φ), sedimentary components (calcareous biogens, organic matter and quartz) and correspondence in topographical elevation, which allowed them to be stratigraphically correlated (Figure 17).

Therefore, points VP1 and VP2 make up the lithological column of the study area, with VP2 and VP3 being the stratigraphic continuation of VP1, and forming the same sandy and silty sedimentary facies (Darnell, 2015; Jones, 2015; Magallanes-Ordóñez et al., 2015; Ramos-Reyes et al., 2016).
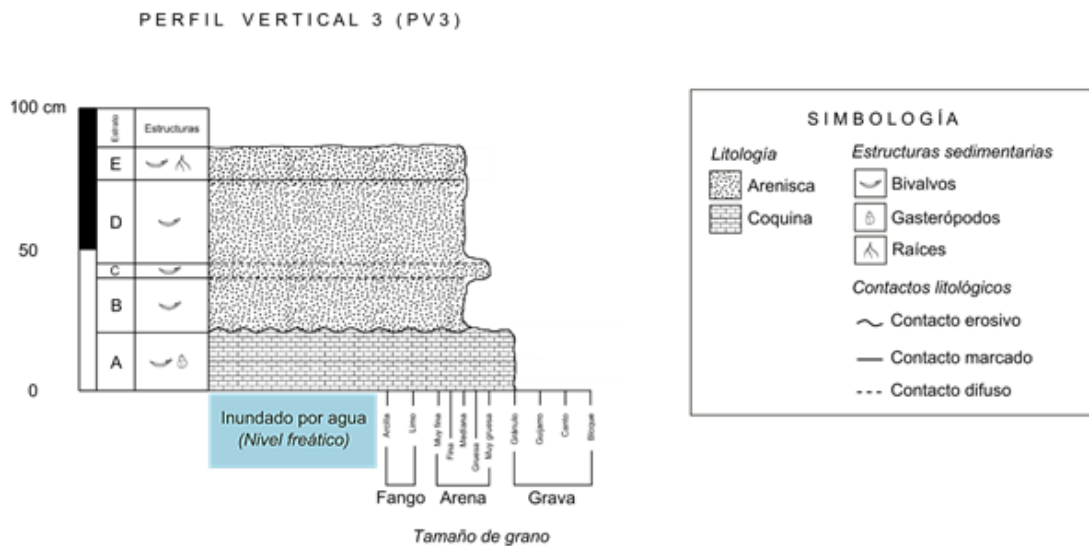
Figure 11. Lithological column of VP3
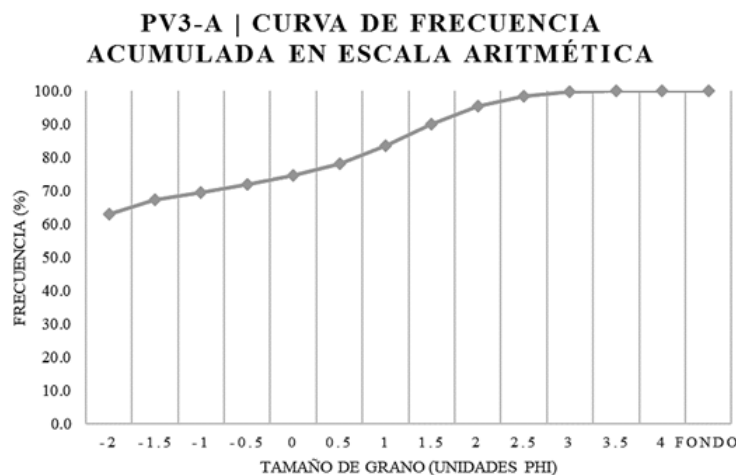
Figure 12. Curve of accumulated frequency in arithmetic scale of VP3-A

Scientific paper / Artículo científico

WASTE MANAGEMENT   *Machorro, A., Rosano, G., Tavera, M., Flores, J., Maimone, M., Martínez, E., Martínez, S. and Rodríguez, P.*
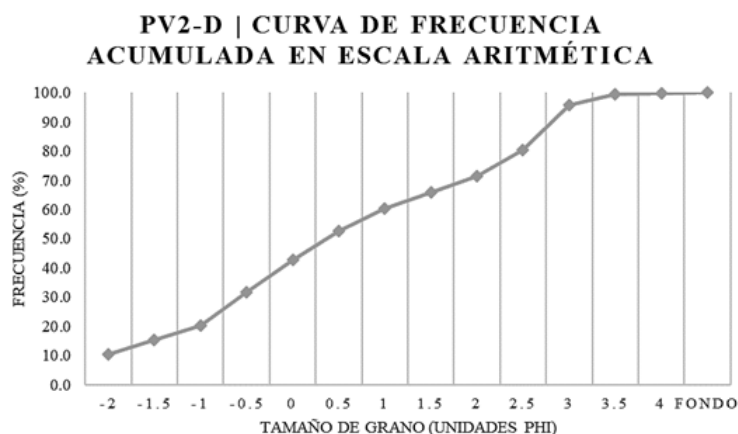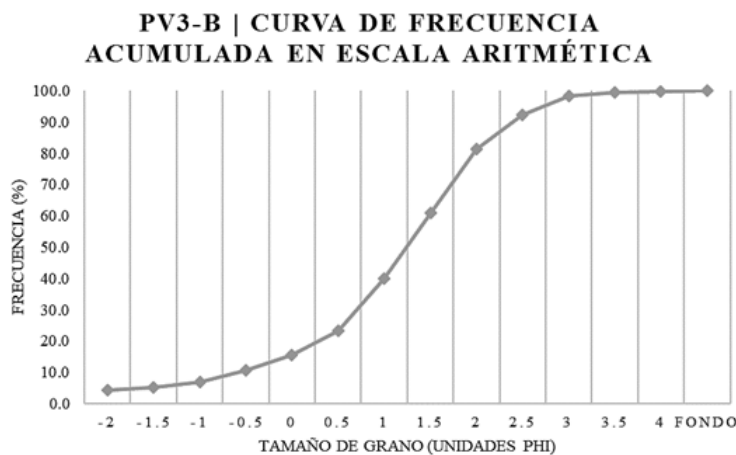
Figure 13. Curve of accumulated frequency in arithmetic scale of VP3-B
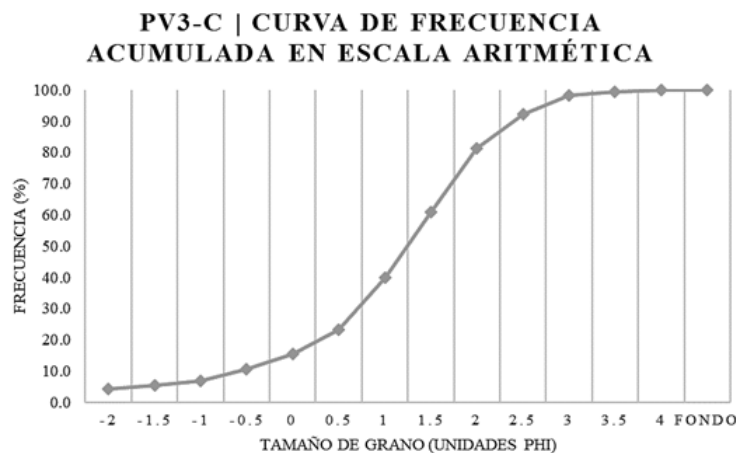
Figure 14. Curve of accumulated frequency in arithmetic scale of VP3-C

Thus, it was determined that the study area is formed by a lithological column consisting of six main strata, granulometrically dominated by sands of sizes 0.062 to 4 mm, composed of calcareous bigens and earthic material (Figure 18). According to Magallanes-Ordóñez et al. (2015), the sands could come from the sea; and the clays are from the adjacent continent.

The grains in a sand are usually in tangential contact, forming an open network, i.e. three-dimensional. As a result, the sands have a great po-

rosity (they have a pore system full of fluid) (Pettijohn et al., 2014). From the analysis of the mass properties, a porosity range of 20.2 – 40.1 % was determined, and depending on the particle size it was possible to determine a permeability range of ±10-2 -10-4 m/s. These values allowed to define that the sediments have a good porosity and a very fast permeability capacity indicative of good aquifers, i.e., the fluids are transported quickly through the porous medium (Álvarez Arellano, 2003; Anovitz et al., 2018).

**PV3-D | CURVA DE FRECUENCIA
ACUMULADA EN ESCALA ARITMÉTICA**
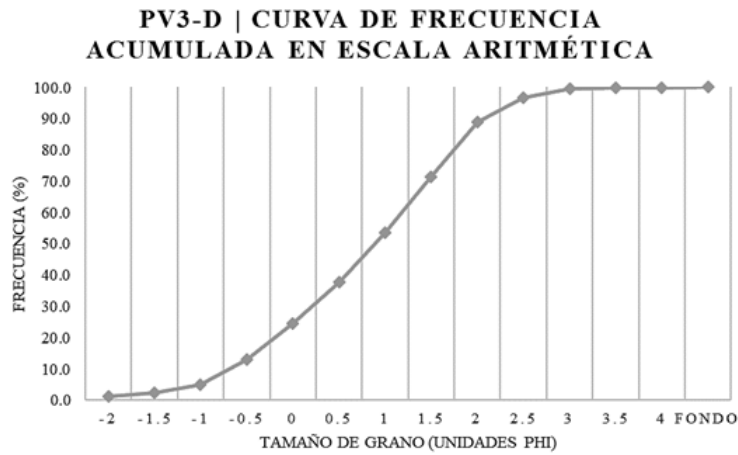
Figure 15. Curve of accumulated frequency in arithmetic scale of VP3-D

**PV3-E | CURVA DE FRECUENCIA
ACUMULADA EN ESCALA ARITMÉTICA**
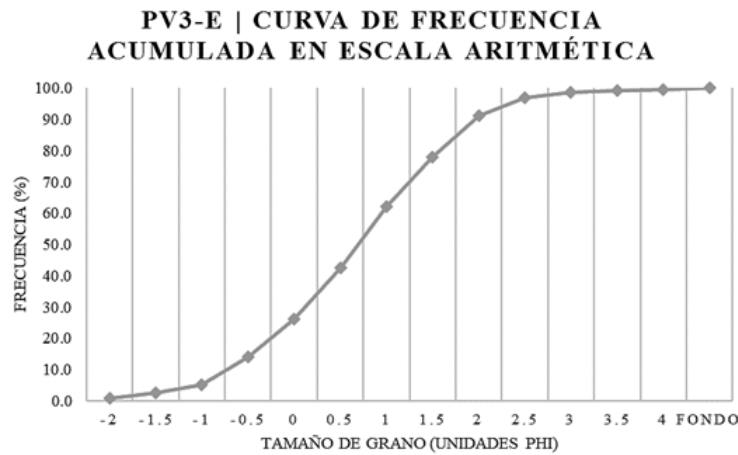
Figure 16. Curve of accumulated frequency in arithmetic scale of VP3-E

Table 1. Concentrations of determined parameters in the water quality in the MA-Mangrove and MA-Channel points

Sample	Parameter	Concentration (mg/L)	Maximum permissible limits (according to CONAGUA (2016))
MA-Mangrove	DBO_5	63.06	30
	DQO	1338.13	40
	Total phosphorous	1.17	N/A
	Total Kjeldahl nitrogen	5.49	N/A
MA-Channel	DBO_5	<20	30
	DQO	71.94	40
	Total phosphorous	1.17	N/A
	Total Kjeldahl nitrogen	5.49	N/A

The dominance of calcareous biogens, as well as the evidence of dissolution in some grains allowed to consider a secondary porosity in the sediments.

According to Braga et al. (2015), dissolution processes significantly increase porosity. These processes include 1) stormwater discharge, 2) quartz alkaline
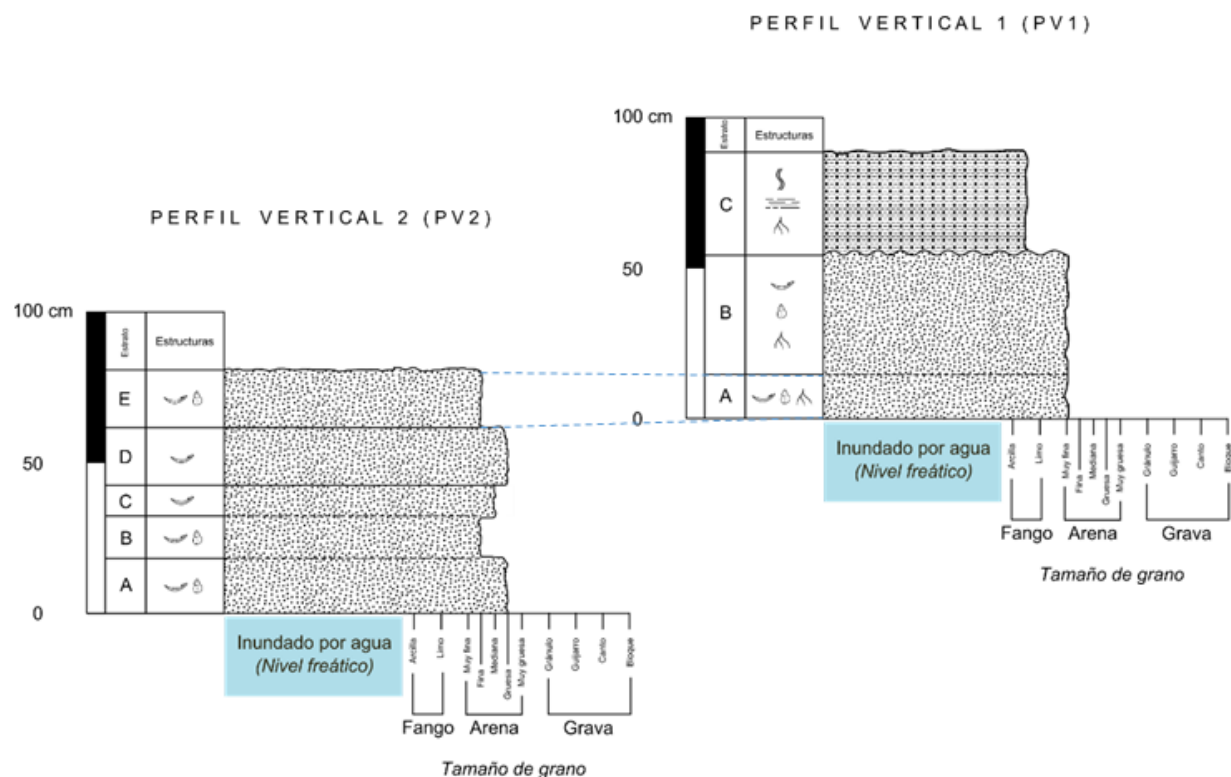
Figure 17. Stratigraphic correlation of VP1-a with VP2-E

solution, 3) leaching of unstable minerals (e.g. feldspars, carbonate cements and rock fragments) with respect to acidic fluids generated by the thermal maturation of organic matter or clay, when mineral reactions occur in adjacent lutites (Zheng et al., 2015).

Table 2. Heavy metal concentrations determined in the water quality of the MA-Mangrove and MA-Channel points.

Sample	Parameter	Concentration (mg/L)	Maximum permissible limits (according to NOM-001-SEMARNAT-1996)
MA-Mangrove	Cadmium	0.038	0.2
	Copper	0.168	6
	Nickel	0.41	4
	Zinc	3.037	20
MA-Channel	Cadmium	0.008	0.2
	Copper	0.013	6
	Nickel	0.16	4

Groundwater flows play an important role as means of transportation for leachates, both vertically and horizontally; for this reason, they are important to perceive the risks associated with this flow (Lobo-García de Cortázar et al., 2017; Niño-Carvajal et al., 2016). Therefore, the sedimentological characteristics of the subsoil of the municipal landfill allow the generated leachates (and accumulated in the hydrological environment over the years), to infiltrate and move, heading at a maxi-
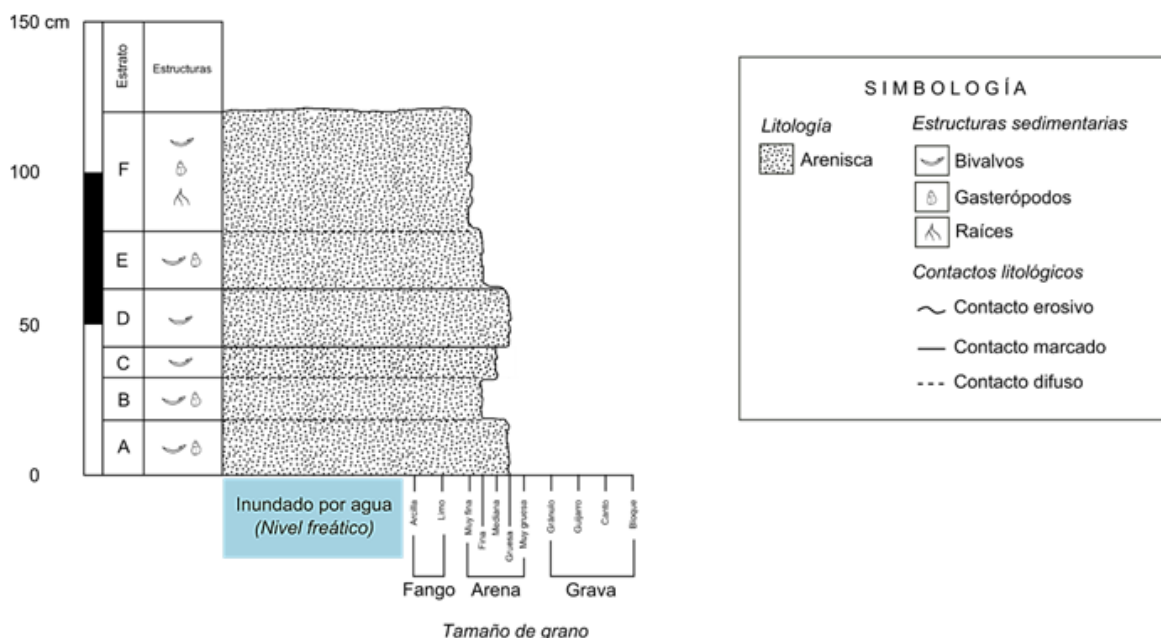
Figure 18. Lithological column of the study area

mum angle of ±1,7° (naturally and from the topographical elevation to the midpoint of the landfill) towards the areas of runoff, i.e., towards the aqueous bodies that make up the mangrove area.

It should be noted that one of the elements that influence this transport is the water table, which was found at ±0.87 m (i.e. classifying it as a flood zone). Thus, during the vertical and horizontal transportation of the leachates, they are mixed in the water table. A case study very similar to this is reported by Niño-Carvajal et al. (2016) at the final solid waste disposal site of El Carrasco, located in the municipality of Bucaramanga, Colombia, where the same problem was reported and subsoil areas were found completely saturated by leachates that were not properly managed at the disposal site.

4.2 Water quality

Considering the maximum permissible limits according to NOM-001-SEMARNAT-1996 (SEMARNAT, 1996), and the surface water classification of CONAGUA (2016), the concentrations found corresponding to the DBO_5 and DQO parameters indicate contaminated and heavily contaminated bodies, respectively.

Therefore, it was determined that the main source of contamination in the aqueous bodies comes from inorganic materials, with the first sampling point (MA-Mangrove) being the most representative due to the ratio of 4.7% organic, and 95.3% inorganic. For its part, the total phosphorus and total Kjeldahl nitrogen values at both sampling points are within the maximum permissible limits according to NOM-001-SEMARNAT-1996. The concentration of these parameters is associated with the biological activity of mangroves that dominate the study area, since both phosphorus and nitrogen are essential macronutrients in the photosynthesis process of the biota that makes up the mangrove (Bravo-Chaves et al., 2012).

In the case of heavy metals, trace concentrations of Cd, Cu, Ni and Zn were detected below the maximum permissible limits by NOM-001-SEMARNAT-1996 (SEMARNAT, 1996). However, it should be noted that when they enter the aquatic system directly via atmospheric or with runoff waters, they can cause serious impacts at high concentrations due to their high toxicity (Bravo-Chaves et al., 2012). The obvious decrease in the concentration of heavy metals from point 2 (MA-Channel) to point 1 (MA-

Mangrove) is due to the fact that point 1 is located in one the aqueous bodies of the mangrove, i.e., without any influence by internal marine currents. While point 2 is located in one of the main channels of the area, where internal marine currents significantly influence the dissolution of pollutants.
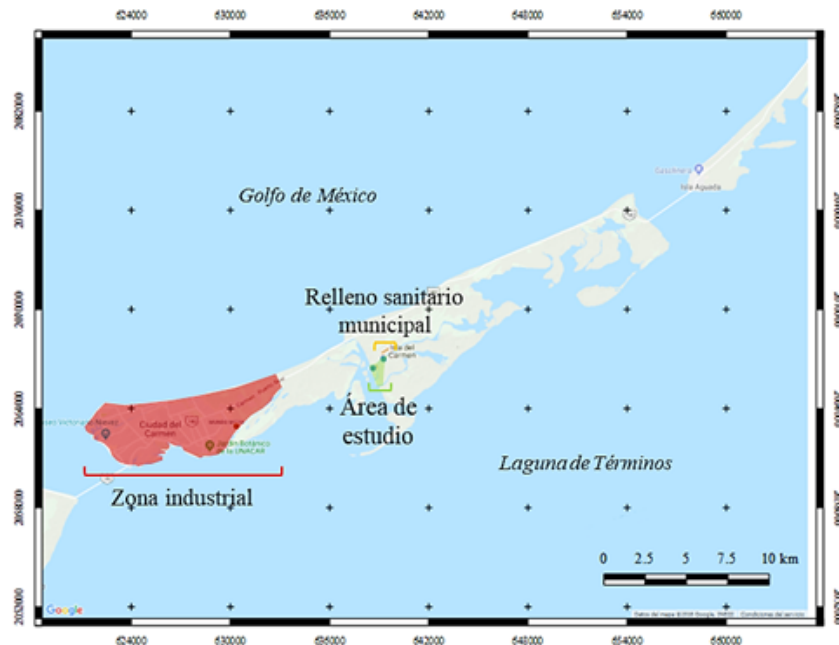
Figure 19. Geographical relationship between the industrial area, the municipal landfill and the study area. (Modified from INEGI (2017)).

The origin of this type of contamination can be natural (wear of igneous and metamorphic rocks, oceanic aerosols and decomposition of detritus) or anthropogenic (industrial and domestic water discharges) (Bravo-Chaves et al., 2012). In this case, the presence of landfill, and the absence of industries on the periphery of the study area ($\pm 127 \ Km^2$) (INEGI, 2017) (Figure 19), suggests that the origin of these concentrations may be associated with leachates from the landfill, which infiltrate the subsoil (highly porous and permeable) and are deposited in the aqueous bodies of the area. Heavy metals are one of the most important contaminants in aquatic ecosystems due to their potential toxicity, persistence and bioaccumulation. It is well known that heavy metals have a significant risk in the human health when the exposure dose exceeds safe consumption levels (Mussali-Galante et al., 2013; Zhong et al., 2018). Several authors have detected accumulation of toxic metals in fish tissues and molluscs for the human consumption (Covarrubias and Peña-Cabriales, 2017).

From the comparison of the values of DBO_5 and DQO identified in the point MA-Mangrove (aqueous body inside the mangrove) with the leachate effluents of two municipal landfills and a drinking water well (case study: Landfill "Tultitlán", Tultitlán, Mexico state and Landfill "El Milagro", Ixtapaluca, Mexico state, M. E. Tavera, personal communication , December 06, 2017) (Table 3), both BOD_5 and DQO of the MA-Mangrove were found to be below the values presented in the leachates of a typical municipal landfill. On the other hand, for the case of the drinking water well near a municipal landfill, the values of the MA-Mangrove are above it, which confirms the previous determination by classifying it as a contaminated body according to CONAGUA (2016).

It is important to consider that the proliferation of algae and macrophytes depending on the burden of nutrients (nitrogen (N) and phosphorus (P)) is one of the main manifestations of the eutrophication process in aqueous bodies. Wastewater discharges from anthropic activities are mainly responsible for this phenomenon (Ramos, 2018). Eutrophication has the adverse effect of an increase in algae biomass, oxygen loss and mortality of some aquatic species (Espósito et al., 2016).

Table 3. Comparison of leachate and drinking water well values of two typical landfills with the MA-Mangrove sample (Modified by Tavera Cortés M. E., personal communication, December 06, 2017).

Sampling area	Medium	DBO_5 (mg/L)	DQO (mg/L)
RS "Tultitlán" (Tultitlán, Mexico state)	Leachate 1	958.562	19166.667
	Leachate 2	3717.461	20833.333
RS "El Milagro" (Ixtapaluca, Mexico state)	Leachate	1337.134	45833.333
Drinking water well (near the RS "El Milagro")	Water	Lower than 4,757	2.882
Mangrove (MA-Mangrove) (Ciudad del Carmen, Camp.)	Water	63,06	1338.13

5 Conclusions

Litologically, the study area consists of a sandy and silty sedimentary facies, composed of a succession of six strata of sands with sizes from 0.062 to 4 mm, compositionally formed by calcareous bigens and terrigenous material. A porosity range of 20.2-40.1 %, and a permeability range of ±10-2-10-4 m/s were determined.

This relationship, along with the dissolution of carbonated particles (dominant in the sediments analyzed), made it possible to determine that the sedimentological characteristics of the subsoil of the municipal landfill allow the generated leachates to infiltrate and move through it, heading (naturally and from the topographical elevation of the area by a maximum angle of ±1.7°) towards the aqueous bodies that make up the mangrove area. It should be noted that one of the elements that influence this transport is the water table level, located at ±0.87 m. Thus, during the vertical transportation of the leachates, these mix in the water table, representing a negative impact on the environment.

Evidence of the above can be reflected in water quality, where from the analysis of the values of DBO_5 and DQO, it was possible to classify the aqueous bodies (according to CONAGUA (2016) and their comparison with the monitoring of the aqueous bodies of the country) in a range of "contaminated to heavily contaminated", which is attributed to the high concentration of inorganic constituents (DQO), within which are considered trace concentrations of heavy metals such as cadmium, copper, nickel and zinc, the origin of which is related to the presence of municipal landfill in the study area.

As a point above, there is a negative environmental impact on the study area and a comprehensive management plan that mitigates and restores the ecosystem is required. Considering the works of Bravo-Chaves et al. (2012) it is proposed that the most viable option would be the closure of the municipal landfill, and the opening of a new one that complies with the guidelines established in the corresponding regulations. However, Ciudad del Carmen does not have an area that meets the requirements for its selection as a landfill, due to the granulometric characteristics of the sub-soil and the slight presence of the water table level (±0.87 m).

6 Recommendations

1. Characterize the waste associated with a control of the types available in the landfill, limiting them only to urban solid waste.

2. Close the landfill in stages, proposing a re-

engineering in it to implement new areas that have the corresponding systems of waterproofing and the capture and extraction of leachates, considering the work of Lobo-García de Cortázar et al. (2017) and Niño-Carvajal et al. (2016).

3. Carry out (in parallel to the previous point) the treatment and/ or recovery of the residues present in it. It is important to note that the comprehensive management of MSW, in accordance with environmental standards, will reduce negative impacts on the environment and, therefore, on the sustainable development.

References

Álvarez Arellano, A. (2003). *Manual de Prácticas del Laboratorio de Sedimentología*.

Anovitz, L. M., Freiburg, J. T., Wasbrough, M., Mildner, D. F. R., Littrell, K. C., Pipich, V., and Ilavsky, J. (2018). The effects of burial diagenesis on multiscale porosity in the st. peter sandstone: An imaging, small-angle, and ultra-small-angle neutron scattering analysis. *Marine and Petroleum Geology*, 92:352–371. Online: https://bit.ly/2yvgjjN.

Braga, J. C., Martín, J. M., and Puga-Bernabéu, A. (2015). Origen de la porosidad y la permeabilidad en sedimentos y rocas carbonatadas. 07/08/2018.

Bravo-Chaves, F. M. B., Piedra-Marín, G. P., and Piedra-Castro, L. P. (2012). Evaluación físico-química de los sedimentos en el estero tamarindo y sus tributarios, guanacaste, costa rica. *Uniciencia*, 26(1):41–50. Online: https://bit.ly/3gzjwQs.

CONABIO (2012). Sitios de manglar con relevancia biológica y con necesidades de rehabilitación ecológica: Isla del carmen. 06/06/2018.

CONAGUA (2016). Monitoreo de calidad del agua. 30/03/2018.

CONANP (2018). Región planicie costera y golfo de méxico: Área de protección de flora y fauna laguna de términos. 14/07/2018.

Covarrubias, S. and Peña-Cabriales, J. (2017). Contaminación ambiental por metales pesados en méxico: Problemática y estrategias de fitorremediación. *Revista Internacional de Contaminación Ambiental*, 33:7–21. Online: https://bit.ly/36s8SWS.

Darnell, R. (2015). *The American Sea: A Natural History of the Gulf of Mexico*. Texas A&M University Press.

Escudero, M., Silva, R., and Mendoza, E. (2014). Beach erosion driven by natural and human activity at isla del carmen barrier island, mexico. *Journal Of Coastal Research*, 71(sp1):62–74. Online: https://bit.ly/3eB5Vq9.

Espósito, M. E., Blanco, M. d. C., Sequeira, M. E., Paoloni, J. D., Fernández, S. N., Amiotti, N. M., and Díaz, S. L. (2016). Contaminación natural (as, f) y eutrofización (n, p) en la cuenca del arroyo el divisorio, argentina. *Phyton*, 85(1):51–62. Online: https://bit.ly/3d33tbi.

Ghosh, S., Mishra, D. R., and Gitelson, A. A. (2016). Long-term monitoring of biophysical characteristics of tidal wetlands in the northern gulf of mexico - a methodological approach using modis. *Remote Sensing of Environment*, 173:39–58. Online: https://bit.ly/3bW9G7P.

Honarpour, M. M. (2018). *Relative Permeability Of Petroleum Reservoirs*. CRC press.

Hu, S., Niu, Z., Chen, Y., Li, L., and Zhang, H. (2017). Global wetlands: Potential distribution, wetland loss, and status. *Science of The Total Environment*, 586:319–327. Online: https://bit.ly/2XqAWGb.

Ibáñez-Forés, V., Bovea, M. D., and Azapagic, A. (2013). Assessing the sustainability of best available techniques (bat): methodology and application in the ceramic tiles industry. *Journal of Cleaner Production*, 51:162–176. Online: https://bit.ly/3ggHX4V.

ICS (2018). International chronostratigraphic chart. 02/09/2018.

INEGI (2010). División municipal. instituto nacional de estadística y geografía. Catálogo de metadatos geográficos. Comisión Nacional para el Conocimiento y Uso de la Biodiversidad.

INEGI (2017). Espacio y datos de méxico. 20/06/2018.

Jones, S. J. (2015). *Introducing sedimentology*. Dunedin Academic Press Ltd.

Lobo-García de Cortázar, A., Szantó-Narea, M., and Llamas, S. (2017). Cierre, sellado y reinserción de antiguos vertederos. experiencias en iberoamérica. *Revista Internacional de Contaminación Ambiental*, 32:123–139. Online: https://bit.ly/2LVpUU3.

Magallanes-Ordóñez, V. R., Marmolejo-Rodríguez, A. J., Rodríguez-Figueroa, G. M., Sánchez-González, A., Aguíñiga García, S., Arreguín-Sánchez, F., Zetina-Rejón, M., Tripp-Valdez, A., and Romo-Ríos, J. A. (2015). Characterization of lithogenic and biogenic zones and natural enrichment of nickel in sediments of the terminos lagoon, campeche, mexico. *Estuarine, Coastal and Shelf Science*, 156:116–123. Online: https://bit.ly/2LW0DsS.

Martínez, A., Ángel, A., Rodríguez, J., Cabrera-Hernández, J., and Sánchez-Vicens, R. (2015). El enfoque de paisajes en la clasificación de humedales. caso de estudio provincia de matanzas, cuba. *Verbum*, 10(10):79–93. Online: https://bit.ly/36HO7Xr.

Maynard, J. J., Dahlgren, R. A., and O'Geen, A. T. (2014). Autochthonous and allochthonous carbon cycling in a eutrophic flow-through wetland. *Wetlands*, 34:285–296. Online: https://bit.ly/2XmIhqe.

Mussali-Galante, P., Tovar-Sánchez, E.and Valverde, M., and Rojas del Castillo, E. (2013). Biomarcadores de exposición para determinar la contaminación ambiental por metales pesados: de las moléculas a los ecosistemas. *Revista internacional de contaminación ambiental*, 29(1):117–140. Online: https://bit.ly/2XdyPXb.

Nahlik, A. and Fennessy, S. (2016). Carbon storage in us wetlands. *Nature Communications*, 7:1–9. Online: https://go.nature.com/2LRFArs.

Niño-Carvajal, L. X., Ramón-Valencia, J. A., and Ramón-Valencia, J. L. (2016). Contaminación fisicoquímica de acuíferos por los lixiviados generados del relleno sanitario el carrasco, de bucaramanga. *Producción + Limpia*, 11(1):66–74. Online: https://bit.ly/2M8nYHR.

Palacio-Prieto, J. L., Ortíz-Pérez, M. A., and Garrido-Pérez, A. (1999). Cambios morfológicos costeros en isla del carmen, campeche, por el paso del huracán roxanne. *Investigaciones Geográficas (Mx)*, (40):48–57. Online:https://bit.ly/2ZKrSyT.

Pettijohn, F. J., Potter, P. E., and Siever, R. (2014). *Sand and sandstone*. Springer Science & Business Media, New York.

Rains, M. C., Leibowitz, S. G., Cohen, M. J., Creed, I. F., Golden, H. E., Jawitz, J. W., Kalla, P., Lane, C. R., Lang, M. W., and McLaughlin, D. L. (2016). Geographically isolated wetlands are part of the hydrological landscape. *Hydrological Processes*, 30:153–160. Online: https://bit.ly/3cfFnsX.

Ramos, A. (2018). Evaluación del riesgo de eutrofización del embalse el quimbo, huila (colombia). *Revista Logos Ciencia y Tecnología*, 10(2):172–192. Online: https://bit.ly/3gK8oQW.

Ramos-Reyes, R., Zavala-Cruz, J., Gama-Campillo, L. M., Pech-Pool, D., and Ortiz-Pérez, M. A. (2016). Indicadores geomorfológicos para evaluar la vulnerabilidad por inundación ante el ascenso del nivel del mar debido al cambio climático en la costa de tabasco y campeche, méxico. *Boletín de la Sociedad Geológica Mexicana*, 68(3):581–598. Online: https://bit.ly/2Aq48Fh.

Rendón-Macías, M. E., Villasís-Keeve, M. A., and Miranda-Novales, M. G. (2016). Estadística descriptiva. *Revista Alergia México*, 63(4):397–407. Online:https://bit.ly/36OMTda.

SCFI (1980a). Norma mexicana nmx-aa-003-1980. aguas residuales. – muestreo. Technical report, Secretaría de Comercio y Fomento Industrial. Diario Oficial de la Federación. 25 de marzo de 1980.

SCFI (1980b). Norma mexicana nmx-aa-014-1980. cuerpos receptores. – muestreo. Technical report, Secretaría de Comercio y Fomento Industrial. Diario Oficial de la Federación. 5 de septiembre de 1980.

SCFI (2001a). Norma mexicana nmx-aa-028-scfi-2001. análisis de agua - determinación de la demanda bioquímica de oxígeno en aguas naturales, residuales (dbo5) y residuales tratadas - método de prueba (cancela a la nmx-aa-028-1981). Technical report, Secretaría de Comercio y Fomento Industrial. Diario Oficial de la Federación.

Scientific paper / Artículo científico

WASTE MANAGEMENT   *Machorro, A., Rosano, G., Tavera, M., Flores, J., Maimone, M., Martínez, E., Martínez, S. and Rodríguez, P.*

SCFI (2001b). Norma mexicana nmx-aa-029-scfi-2001. análisis de aguas - determinación de fósforo total en aguas naturales, residuales y residuales tratadas - método de prueba (cancela a la nmx-aa-029-1981). Technical report, Secretaría de Comercio y Fomento Industrial. Diario Oficial de la Federación.

SCFI (2011a). Norma mexicana nmx-aa-026-scfi-2010. análisis de agua - medición de nitrógeno total kjeldahl en aguas naturales, residuales y residuales tratadas - método de prueba - (cancela a la nmx-aa-026-scfi-2001). Technical report, Secretaría de Comercio y Fomento Industrial. Diario Oficial de la Federación. 3 de marzo de 2011.

SCFI (2011b). Norma mexicana nmx-aa-030/2-scfi-2011. análisis de agua - determinación de la demanda química de oxígeno en aguas naturales, residuales y residuales tratadas - método de prueba - parte 2 -determinación del índice de la demanda química de oxígeno – método de tubo sellado a pequeña escala. Technical report, Secretaría de Comercio y Fomento Industrial. Diario Oficial de la Federación. 27 de junio 2013.

SCFI (2016). Norma mexicana nmx-aa-051-scfi-2016. análisis de agua. - medición de metales por absorción atómica en aguas naturales, potables, residuales y residuales tratadas- método de prueba (cancela a la nmx-aa-051-scfi-2001). Technical report, Secretaría de Comercio y Fomento Industrial. Diario Oficial de la Federación. 7 de diciembre de 2016.

SEMARNAT (1996). Norma oficial mexicana nom-001-semarnat-1996. que establece los límites máximos permisibles de contaminantes en las descargas de aguas residuales en aguas y bienes nacionales. Technical report, Diario Oficial de la Federación. Secretaría de Medio Ambiente y Recursos Naturales. 6 de enero de 1997.

SEMARNAT (2000). Norma oficial mexicana nom-021-semarnat-2000. que establece las especificaciones de fertilidad, salinidad y clasificación de suelos. estudios, muestreo y análisis. Technical report, Secretaría de Medio Ambiente y Recursos Naturales. Diario Oficial de la Federación. 31 de diciembre de 2002.

SEMARNAT (2003). Norma oficial mexicana nom-083-semarnat-2003. especificaciones de protección ambiental para la selección del sitio, diseño, construcción, operación, monitoreo, clausura y obras complementarias de un sitio de disposición final de residuos sólidos urbanos y de manejo especial. Technical report, Secretaría de Medio Ambiente y Recursos Naturales. Diario Oficial de la Federación. 04 de agosto de 2015.

SEMARNAT (2009). Manual de especificaciones técnicas para la construcción de rellenos sanitarios para residuos sólidos urbanos (rsu) y residuos de manejo especial (rme). Technical report, Secretaría de Medio Ambiente y Recursos Naturales. 22/05/2018.

SGM (2005). Carta geológico-minera, ciudad del carmen e15-6, campeche y tabasco. 15/04/2018.

Zheng, J., Zheng, L., Liu, H. H., and Ju, Y. (2015). Relationships between permeability, porosity and effective stress for low-permeability sedimentary rock. *International Journal of Rock Mechanics and Mining Sciences (IJRMMS)*, 78:304–318. Online: https://bit.ly/2LWcA1F.

Zhong, W., Zhang, Y., Wu, Z., Yang, R., Chen, X., Yang, J., and Zhu, L. (2018). Health risk assessment of heavy metals in freshwater fish in the central and eastern north china. *Ecotoxicology and Environmental Safety (EES)*, 157:343–349. Online: https://bit.ly/2LYNG1i.

THRIPS (*Thysanoptera*) ASSOCIATED WITH PITAHAYA *Selenicereus undatus* (HAW.) D.R. HUNT. SPECIES, POPULATION LEVELS AND SOME NATURAL ENEMIES

Thysanoptera) ASOCIADOS CON LA PITAHAYA *Selenicereus undatus* (HAW.) D.R. HUNT. ESPECIES, NIVELES POBLACIONALES, DAÑOS Y ALGUNOS ENEMIGOS NATURALES

Ketty Meza[1] , María Cusme[1] , José Velasquez[2] and Dorys Chirinos*[1]

[1] *Faculty of Agronomic Engineering, Universidad Técnica de Manabí. Av. Urbina y Che Guevara, 130105, Portoviejo, Ecuador.*
[2] *Sanidad Vegetal, Agrocalidad, 130802, Manta, Ecuador.*

*Corresponding author: dchirinos@utm.edu.ec

Abstract

The pitahaya, *Selenicereus undatus* (Haw.) D.R. Hunt (Cactaceae) is a species whose fruit is appetizing for its appearance and flavor, which has increased its demand in the international market. Ecuador has increased its planting reaching 1108 ha. This crop could be affected by pests, such as thrips, whose effects on pitahaya are unknown. During the period February - June 2019, a field study was carried out in the province of Manabí, Ecuador, with the aim of identifying the species of thrips, estimating population levels on the plant, organs (flower bud, flowers, fruits), as well as, determine the percentage of damage and the associated predators. Thrips species and populations were analyzed using the Kruskal-Wallis H test (P<0.05). Thrips populations (P <0.05) were correlated with rainfall and a regression analysis was performed between the latter and the percentage of damage to fruits. The most abundant species was *Frankliniella occidentalis* (Pergande). Populations ranged from 0.3 to 6.0 individuals per plant, which were not correlated with rainfall. The thrips showed a marked preference for flowers. The regression model [Y = 1.87 + 1.04 (X), R^2 = 0.83, P <0.05] showed an increase in fruit damage as a function of thrips populations. Four taxa of predatory arthropods were observed. As far as knowledge goes, this represents the first study on species, population levels, damage from thrips and predators associated with pitahaya.

Keywords: Cactaceae, dragon fruit, damage, population level, pest.

Resumen

La pitahaya roja, *Selenicereus undatus* (Haw.) D.R. Hunt (Cactaceae) es una especie cuya fruta es apetecible por su apariencia y sabor lo que ha aumentado su demanda en el mercado internacional. Ecuador ha incrementado su siembra alcanzando 1108 ha. Este cultivo podría ser afectado por plagas, como los trips, cuyos efectos sobre pitahaya se desconocen. Durante el período febrero-junio 2019, se realizó un estudio de campo en la provincia de Manabí, Ecuador, con el objetivo de identificar las especies de trips, estimar niveles poblacionales sobre la planta, órganos (botón floral, flores, frutos), así como, determinar el porcentaje de daño y los depredadores asociados. Las especies de trips y las poblaciones fueron analizadas mediante la prueba H de Kruskal-Wallis (P<0,05). Se correlacionaron las poblaciones de trips (P<0,05) con las precipitaciones y se realizó un análisis de regresión entre éstas últimas y el porcentaje de daños en frutos. La especie más abundante fue *Frankliniella occidentalis* (Pergande). Las poblaciones se presentaron entre 0,3 a 6,0 individuos por planta, las cuales no estuvieron correlacionadas con las precipitaciones. Los trips mostraron una marcada preferencia hacia las flores. El modelo de regresión [Y = 1,87 + 1,04(X), R^2 = 0,83, P<0,05] mostró un incremento de los daños en los frutos en función de las poblaciones de trips. Cuatro taxones de artrópodos depredadores fueron observados. Hasta donde llega el conocimiento este representa el primer estudio sobre especies, niveles poblacionales, daños de trips y depredadores asociados con la pitahaya.

Palabras clave: *Cactaceae*, fruta de dragón, daños, niveles poblacionales, plaga.

Orcid IDs:
Ketty Meza: http://orcid.org/0000-0002-9970-4651
Maria Cusme: http://orcid.org/0000-0001-5793-622X
José Velasquez: http://orcid.org/0000-0001-9886-746X
Dorys Chirinos: http://orcid.org/0000-0001-8125-5862

1   Introduction

Pitahaya, Selenicereus undatus (Haw.) D.R. Hunt (Cactaceae) is a perennial species, native from America. It is consumed as a fresh fruit, and it is valued for its unique appearance, flavor and nutritional properties, which has influenced the increase in its demand in the international market (Le Bellec et al., 2006; Montesinos Cruz et al., 2015). In Ecuador this crop has increased rapidly in recent years, reaching an estimated of 1108 ha in 2017, of which approximately 200 ha have been planted in provinces of the Ecuadorian coast, among these Manabí, with a national yield of 7.6 Tm.ha^{-1} (MAG, 2017).

As with other agroecosystems, the production of pitahaya species could be affected by phytosanitary problems caused by pest arthropods, as observed in yellow pitahaya *Selenicereus megalanthus* (K. Schum. ex Vaupel) Moran (Medina and Kondo, 2012; Salazar Restrepo, 2012; Kondo et al., 2013), other *Selenicereus species* (Ramírez-Delgadillo et al., 2011), and red pitahaya or dragon fruit (Choi et al., 2013). Thrips species (*Thysanoptera*) have been referred to as important pests in several fruit trees, such as grape, *Vitis vinifera L.* (Vitaceae) (Mujica et al., 2007), avocado, *Persea americana Mill.* (Lauraceae) (Cambero et al., 2010), mango *Mangifera indica L.* (Anacardiaceae) (Aguirre et al., 2013) and guava, *Psidium guajava L.* (Myrtaceae) (Pérez Artiles et al., 2009), which indicate that they could also affect the cultivation of red pithaya, *S. undatus.*

Although thrips can infest flowers and floral buds, the most significant damage is in the fruits is because when feeding on fruits, causing deformations in the epicarp (Aguirre et al., 2013; Denmark and Wolfenbarge, 2013). The increase in the fruit size also increases the size of the lesions, causing brown scars that range from very small to large, depending on the severity of the damage. These deformations decrease the quality of the fruit, which induces farmers to perform frequent sprays of chemical insecticides, which are economically, ecologically and socially unsustainable. Despite this, there is little research that support the incidence of thrips species on pitahaya crop, *S. undatus.* In this matter, the literature reported is the research by Kumar et al. (2012) who conducted a survey in South Florida to determine the fruit crops with more thrips, *Scirtothrips dorsalis* (Hood) (Thysanoptera: Thripidae), and found pitahaya *S. undatus* among the main hosts of this thrips species, without mentioning the population levels achieved by the insect in the crop.

The increment of the crop production in a country must be accompanied by adequate scientific-technological support for sustainability purposes. One of the relevant aspects to be considered is the study of arthropods that may affect the crop production, hence to implement measures for the sustainable management. Due to the limited knowledge of the incidence of thrips species in this crop, this research aimed to study the species present in red pitahaya *S. undatus*, and to estimate the population levels achieved by the plant, reproductive organs (floral buds, flowers and fruits), the damage and occurrence of associated arthropod predators related to thrips.

2   Materials and methods

2.1   Field

This research was carried out during February- June 2019, in a 2000 m^2 parcel of 3.5-year-old red pitahaya, within a planting of 20 ha located in La Estancilla, Tosagua, Rocafuerte (coordinates X: 568479 and Y: 990287), Province of Manabí, whose life area corresponds to a very Dry Tropical Forest according to Holdridge. The study had a descriptive, field and laboratory methodology, where thrips species, population levels per plant and organ, lesions, as well as the presence of some natural enemies were observed. The area was managed without the use of pesticides that could have affected the development of thrips populations in the plant.

For the sampling, 20 plants were marked by collecting at random two floral buds, two flowers and two fruits for each. The floral buds were placed in waterproof plastic bags (25×25 cm, width $\times$ height). An A4 white cardboard was placed under each flower, and the flower was delicately squeezed so that the trips would fall on the cardboard. Subsequently, the specimens were obtained with the help of a fine brush and placed in an eppendorf tube containing 75% of ethyl alcohol. For the fruits, those about approximately one week old, which were placed individually, were taken to the plastic bags described above. The floral buds and fruits were refri-

gerated in iceboxes at $10°C$ at the Plant Health Laboratory of the Agency of Phyto and Zoosanitary Regulation and Control (Agrocalidad), in Manta, Zone 4, province of Manabí for their counting and identification. Thrips populations per plant are the result of the sum of the observed populations between floral buds, flowers and fruits. Samples were taken once a week, for a total of 15 samples.

2.2 Laboratory

In the laboratory, floral buds and fruits were observed under a stereoscope with 10 to 100X, counting the number of individuals per organ, and for their counting these were placed in a Petri capsule containing 75 % ethyl alcohol by using a fine brush. The flower specimens collected in the field were placed in Petri dishes for their counting. Then, the specimens were separated into genus or species. Previously, individuals were placed in *KOH* for two hours to discolor them to better observe the body structures of the insect. Subsequently, three washes with distilled water were performed and finally glycerin was placed and they were proceeded to be mounted on slides using Hoyer solution as a culture medium (Anderson, 1954). The dishes were dried on the stove at $50°C$ for 24 hours and the borders of the slides were sealed with clear enamel. The taxonomic key of Mound et al. (2009) was used for the identification of the thrips species. After the counting, the percentage of abundance was calculated using Equation 1

$$\% = \frac{\# \text{ individuals per specie or gender}}{\text{Total of individuals}} \times 100 \quad (1)$$

The severity of the damage was estimated weekly on ten physiologically mature fruits by assigning a visual randomized scale, assigning degrees based on deformations or scars in the pericarp relative to the fruit area: Degree 0: without damage, Degree 1: 1 to 5 % damage, Degree 2: 6 to 25 %, Degree 3: 26 to 50 %, Degree 4: 51 to 75 %, Degree 5: 76 to 100 %. The number of fruits was counted on each scale, which calculated the damage percentage, using the Equation 2 referred by Rivas et al. (2017). Where g is damage scale, f is number of fruits on the scale, N is the number of evaluated fruits and G is maximum scale set.

$$\% \text{ damage} = \frac{g \times f}{N \times G} \times 100 \quad (2)$$

In the case of predators, those anthropods that fed on the trips were observed in the same plant, then were obtained each week with an insect vacuum cleaner for their further evaluation. For conducting the identification, the reference collection of the Agroquality Laboratory was used, which was complemented by the diagnostic characteristics referred by Najera-Rincón and Souza (2010). The specimens of thrips and natural enemies were included in the Entomological Collection of Agroquality, Manta, Ecuador.

2.3 Data analysis

The variables: percentage of abundance of thrips species and number of thrips per organ were compared with the Kruskal-Wallis H test (P<005). A correlation analysis was conducted between the number of thrips and the monthly rainfall obtained from INAMHI (2019) (P<0.05). A regression analysis was also performed between the percentage of fruit damage and the populations obtained per plant (P<0.05). Statistical analyses were carried out with the Infostat program (2018).

3 Results

3.1 Identification and abundance of species

The characteristics that correspond to each species or genus observed in this research are presented in Figures 1-3. A total of 866 specimens were collected during this study, identified as the western thrips of flowers, *Frankliniella occidentalis* (Pergande) (Thysanoptera: Thripidae) (Figure 1) the most abundant species, followed by the thrips, *Strepterothrips sp.* (Thysanoptera: Phlaeothripidae) (Figure 2) and bean thrips, *Caliothrips fasciatus* (Pergande) (Thysanoptera: Thripidae) (Figure 3) as the least abundant species (Table 1), with no significant differences between the last two.
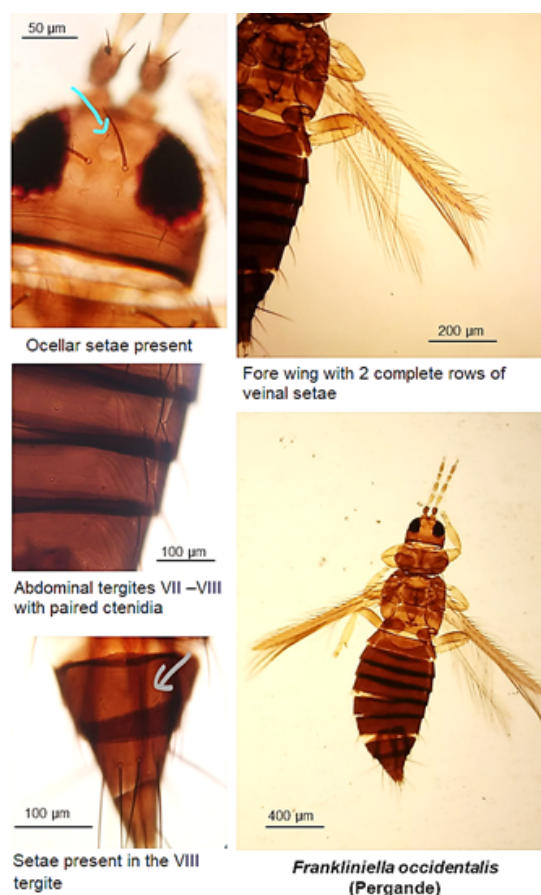
Figure 1. *Franklinilella occidentalis* (Pergande) (Thysanoptera: Thripidae)

Table 1. Abundance of thrip species by pitahaya plant, *Selenicereus undatus* (Haw.) D.R. Hunt in field conditions, Rocafuerte, Manabí. Period February- June 2019.

Species	Percentage of abundance (%)
Franklinella occidentalis	91.2 a
Strepterothrips sp.	8.2 b
Caliothrips fasciatus	0.3 bc

Means ± standard mean error. Means with equal letters do not differ significantly. Mean comparisons were made with Kruskal-Wallis test. H=23.49, P<0.05.

3.2 Population levels and damage

Thrips populations detected at the beginning of the study were low, ranging from 0.5 to 2.0 individuals per plant in the first five samplings (February-March, Figure 4), increasing during the first three weeks of April, in which the largest populations were detected, reaching their peak at the sixth sampling (six individuals per plant). After this period, populations decreased to levels inferior to a specimen per plant. These low populations at the beginning of the study agreed with high rainfall (96-114 mm) (Figure 4) and subsequently high populations (April) were associated with lower precipitation. However, towards the end of the study (late April- June) there was less rainfall and the populations were low. A non-significant correlation was found (r: 0.14; P>0.05), between thrips populations and precipitations registered during the research.
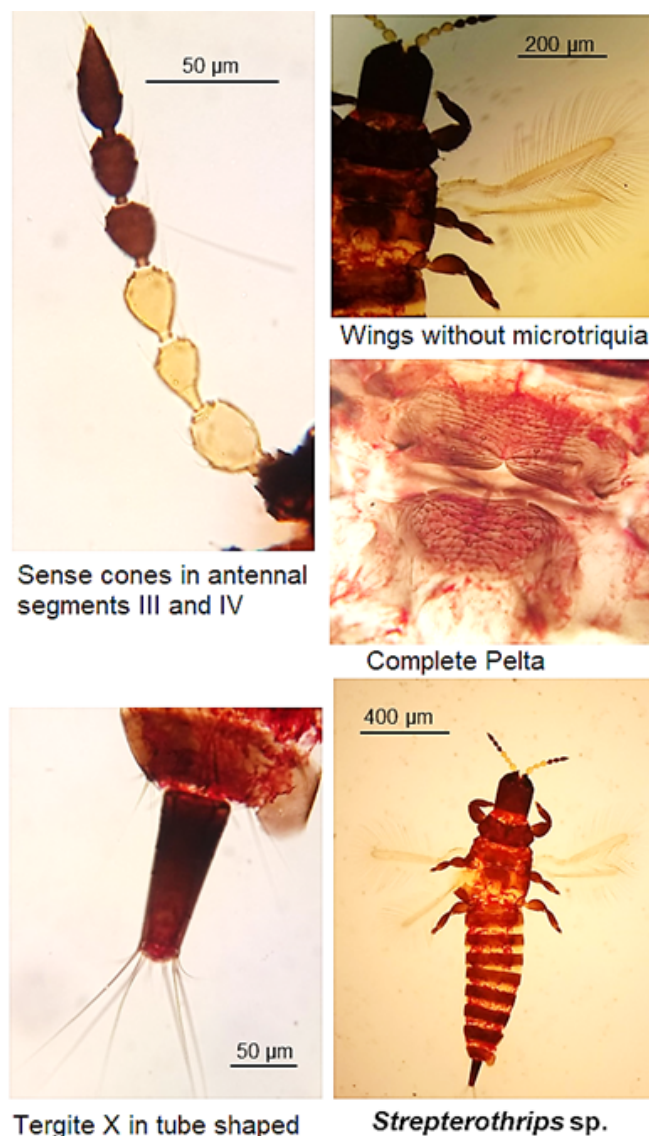
Figure 2. *Streterothrips sp.* (Pergande) (Thysanoptera: Phlaeothripidae).

When analyzing populations in the reproductive organs of pitahaya during the research, the highest number of thrips was found on the flowers (Figure 5B), which resulted into different populations on flower buds and fruits (Table 2). Flowers were present in the plant in greater abundance in April and the highest populations were detected on this organ, and at the end of the trial there were no flowers and the populations declined abruptly (Figure 5B). On floral buds, there were two population peaks in April (7 and 9 individuals) and these ranged from 0 to 1 (Figure 5A) in the rest of the samples.

In fruits, the populations were lower than the floral buds, reaching maximum values of 3 to 4 individuals in the last two weeks of March and the first week of April (Figure 5C). Despite these numerical differences between floral buds and fruits, populations of thrips on these organs did not differ significantly (Table 2, P <0.05).

The calculated simple regression model shows that the increase in the damage percentage of fruits (Y) is based on the increase in thrips populations (X), with a significant (P <0.05) and high determination coefficient (R^2 : 0,83) (Figure 6). Figure 6 also shows that the least fruit damage was about 2% and the estimated maximum value was around 8%. Using the equation, it was estimated that a population of 18 thrips would get 20% of damage and with 47 trips, there would be 50% damage on fruits.

Table 2. Average number of thrips per pitahaya plant, *Selenicereus undatus* (Haw.) D.R. Hunt, in field conditions, Rocafuerte, Manabí. Period February- June 2019.

Organ	Number of individuals
Floral bud	1.8 ± 0.2 b
Flowers	2.5 ± 0.3 a
Fruits	1.1 ± 0.1 b

Means with equal letters do not differ significantly. Mean comparisons were done using Kruskal-Wallis test. H= 8.06; P <0.05.
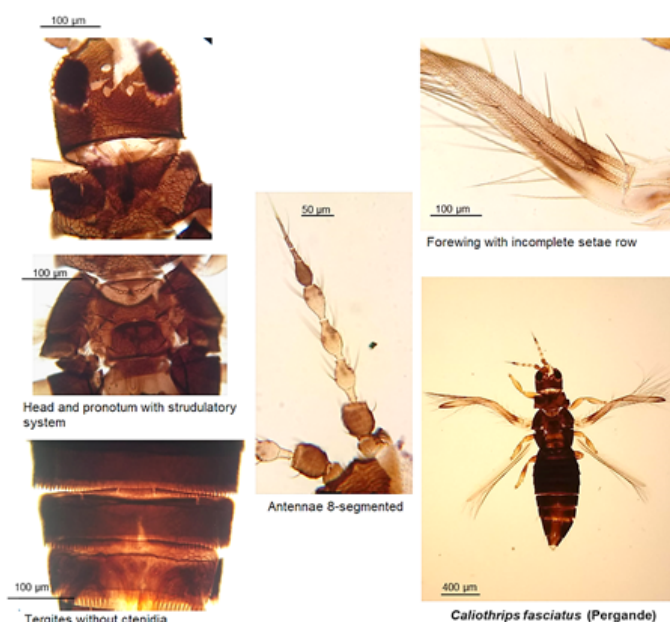
Figure 3. *Caliothrips fasciatus* (Pergande) (Thysano ptera: Thripidae).

3.3 Predators

Four taxa of natural enemies were detected: a species of undetermined chrysopid (Neuroptera: Chrysopidae), *Zelus sp.* (Hemiptera: Reduviidae), *Orius insidiosus* (Say) (Hemiptera: Anthocoridae) and an unidentified species of spider (Aranae: Salticidae) (Table 3). The abundance of these natural enemies differed significantly (P<0.05). Thus, *Chrysopidae* and *Zelus sp.* were significantly superior, being O. insidiosus the least abundant species (Table 3).

Figure 4. Population levels of Thrips on pitahaya, *Selenicereus undatus* (Haw.) D.R. Hunt, and precipitation. Rocafuerte municipality, Manabí. Period from February to June, 2019.

Table 3. Abundance of natural thrips enemies per pitahaya plant, *Selenicereus undatus* (Haw.) D.R. Hunt, under field conditions, Rocafuerte, Manabí. Period February- June 2019.

Natural enemy	Abundance (%)
Neuroptera: Chrysopidae	27.0 a
Zelus sp.	27.0 a
Aranea: Salticidae	24.3 ab
Orius insidiosus	21.7 b

Means ± standard mean error. Means with equal letters do not differ significantly. Mean comparisons were done using Kruskal-Wallis test. H= 22.01; P>0.01.

4 Discussion

4.1 Identification of species

The results obtained show that *F. occidentalis* was the most abundant species. It is a polyphagia insect which is able to feed on more than 250 species of plants distributed in 60 botanical families (Reitz, 2009). This species of thrips has a high capacity to develop resistance to insecticide applications, consequently, ecological aspects and population levels must be well known to manage the damage of this insect (Reitz, 2009). Herein lies the importance to know the species present in a crop, i.e., if determined that the species is resistant to insecticides it is necessary to look for other control alternatives in case they represent damage to it.

The second species detected belongs to the genus *Strepterothrips*. The described species of this genus mainly feeds on fungi (Mound and Tree, 2015). In Ecuador, *Strepterothrips floridanus* (Hood) and *Strepterothrips sp.*, were reported in Galapagos

Island as part of a survey made in the area and whose specimens are in the Collection of Terrestrial Invertebrates at the Charles Darwin Research Station (Hoddle and Mound, 2011). *Caliothrips fasciatus*, the least abundant species, is from North America and is particularly associated with plants belonging to the Fabaceae family, whose adults sometimes hide within the navels of some fruit trees such as orange, where they can cause damage (Rugman-Jones et al., 2012). It is possible that the preference of thrips for other hosts species explains the low abundance detected in red pitahaya during this research.

4.2 Population levels and damage

Several studies that evaluated aspects related to thrips in other crops show different results between the populations obtained, levels of damage and their relation to climatic conditions. Thus, low populations obtained in this research with *S. undatus* agree with those found by Thongjua et al. (2015), in mango in Thungsong, Thailand, observing no correlation between climatic conditions

and thrips populations, *Scirtothrips dorsalis* Hood. Likewise Aguirre et al. (2013) carried out a research in two production cycles (2009 and 2010) in Castamay, Campeche, Mexico, due to the ignorance of the species associated with mango, as well as their population fluctuation and levels of damage, observing very low populations (amplitude: 0.00 - 0.35 individuals per leaf) that were not associated with climatic conditions and did not significantly affect the fruit production.

In contrast, in a study conducted in Nayarit, Mexico to determine the population fluctuation of thrips in squash, *Cucurbita moschata L.* (Cucurbitaceae), high population peaks of various species were found (upper level: 50 individuals in a week) associated with low rainfall, concluding that the absence of rainfall favors the increase of population densities of the thrips on the crop (Valenzuela-García et al., 2010). A marked preference for thrips to be placed in the flowers was observed, which could be directly related to the fact that more than 90% of the observed individuals belonged to the species *F. occidentalis*, which is known by its preference for this reproductive organ (Reitz, 2009) especially towards light-colored flowers (Arce-Flores et al., 2014), as the case of the red pitahaya, whose flower is white.
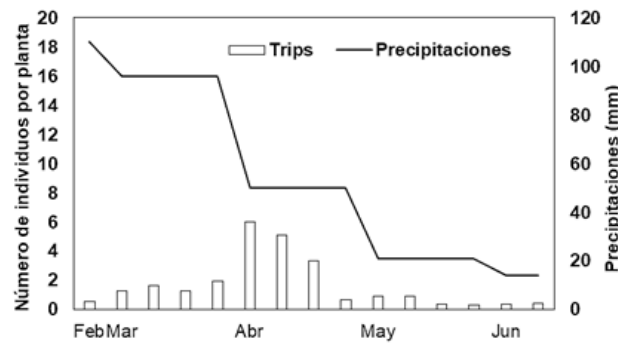

Figure 5. Population levels of thrips on pitahaya plants, *Selenicereus undatus* (Haw.) D.R. Hunt, and precipitation. Rocafuerte, Manabí. Period February-June 2019.

Figure 6. Regression equation between trip populations (X) and observed damage in fruits (Y) in pitahaya plants, *Selenicereus undatus* (Haw.) D.R. Hunt, under field conditions, Rocafuerte, Manabí. Period February- June 2019.

The increase in population densities of several thrips species has been referred to, associated with the presence of flowers for other crops, which agrees with these results (Urías-López et al., 2007; Palomo et al., 2015; García-Escamilla et al., 2016). Duran Trujillo et al. (2017) in a research carried out on a mango plantation in Guerrero, Mexico, found that the high populations of several *Frankliniella* species were mainly favored by the phenological state of flowering. Mujica et al. (2007), in a study conducted in Uruguay in white grape vineyards, detected high populations of F. occidentalis at the time of flowering.

Regarding the fruit damage, a population density of 47 thrips per plant is required to achieve 50% of damage. This is similar to what Sengonca et al. (2006) estimated for populations of *F. occidentalis* on nectarine, *Prunus persica L.* (Rosaceae) where populations of 50 individuals in flowers were associated with 37.5% of non-marketable fruits. In contrast, in an avocado study with greenhouse thrips, *Heliothrips haemorrhoidalis* (Bouché) was estimated only two thrips per plant, with 40% of damage on leaves or fruits (Larral et al., 2018).

4.3 Predators

The predators detected represent biological control factors for various pests in other crops. Rocha et al. (2015) states that the survey of natural enemies is the basis for determining their role in regulating pest populations. Given the increased resistance to insecticides shown by some thrips species, among

these, *F. occidentalis*, the use of biological controllers is being evaluated as a management alternative.

Chrysopidae species have been relevant in some studies. Laboratory and greenhouse research conducted with several species of Chrysopidae suggests its effectiveness in the control of *F. occidentalis* in cucumber, *Cucumis sativus L.* (Sarkar et al., 2019). The mortality of thrips individuals ranged from 40 to 90% when they were preyed upon by third-urging larvae from *Chrysoperla pallens* (Rambur) under laboratory conditions (Shrestha et al., 2013). Predatory bugs of the genus *Zelus*, which were abundant, have been referred to as an important biological controller of thrips associated with lemon, *Citrus aurantifolia* Swingle (Miranda-Salcedo and Loera-Alvarado, 2019) and with bean *Phaseolus vulgaris L.* (Blanco and Leyva, 2013). Spiders (Aranea) also represent biological control agents of several phytophagia species and their role as thrips mortality factors has been mentioned in some research (Rocha et al., 2015; Medina and Kondo, 2012).

Although *O. insidiosus* was not abundant, in other studies it has constituted a primary biological control agent. **?** pointed this species as a relevant biological controller of thrips, which feed on all stages (nymphs and adults). Anthocoridae species (Hemiptera: Anthocoridae), including those of the genus *Orius*, which are the main predators of thrips in Chiapas, Mexico and Florida, United States (Rocha et al., 2015).

5 Conclusions

Frankliniella occidentalis (Pergande) *Strepterothrips sp.* and *Caliothrips fasciatus* (Pergande), were detected in red pitahaya *Selenicereus undatus* (Haw.) D.R. Hunt, being F. occidentalis the most abundant with more than 90% of the total individuals. Flowers seem to be more attractive for the identified thrip species, which use them as elements of sheltering and feeding.

At least 47 thrips individuals are required to achieve 50% of damage in red pitahaya fruits *S. undatus*. Natural enemies represent an essential component as natural biological control agents of these phytophages. As far as this study is known, this research represents the first identification report of thrip species, population levels, damage and their relation to some natural enemies in the of red pitahaya.

Financial support and sponsor

References

Aguirre, L., Miranda, M., Urías, M., Orona, F., Almeyda, I., Johansen, R., and Tucuch, M. (2013). Especies de trips (thysanoptera) en mango, fluctuación y abundancia. *Revista Colombiana de Entomología*, 39(1):9–12. Online: https://bit.ly/2E6yJd6.

Anderson, L. (1954). Hoyer's solution as a rapid permanent mounting medium for bryophytes. *The bryologist*, 57(3):242–244. Online: https://bit.ly/3gWAU1g.

Arce-Flores, J., Martínez, López-Martínez, V., and García-Gaona, Á. (2014). Fluctuación poblacional y distribución de frankliniella occidentalis (pergande)(thysanoptera: Thripidae) en nardo en morelos, méxico. *Acta agrícola y pecuaria*, 1(1):37–42. Online: https://bit.ly/3asQaAB.

Blanco, Y. and Leyva, Á.. (2013). Las arvenses y su entomofauna asociada en el cultivo del frijol (phaseolus vulgaris, l.) posterior al periodo crítico de competencia. *Avances en Investigación Agropecuaria*, 17(3):51–65. Online: https://bit.ly/2E04FQD.

Cambero, C. J., Johansen, N. R., Retana, S. A., García, M. O., Cantú, S. M., and Carvajal, C. C. (2010). Thrips (thysanoptera) del aguacate (persea americana) en nayarit, méxico. *Revista Colombiana de Entomología*, 36(1):47–51. Online: https://bit.ly/3axWtTp.

Choi, K., Yang, J., Park, Y., Kim, S., Choi, H., Lyu, D., and Kim, D. (2013). Pest lists and their damages on mango, dragon fruit and atemoya in jeju, korea. *Korean journal of applied entomology*, 52(1):45–51. Online: https://bit.ly/347dRgv.

Denmark, H. A. and Wolfenbarge, D. O. (2013). Redbanded thrips, selenothrips rubrocinctus (giard) (insects: Thysanoptera: Thripidae). In *Department of Entomology and Nematology, UF/IFAS Extension.* Florida Department of Agriculture and Consumer Services, Division of Plant Industry, Online: https://bit.ly/31iWyaQ.

Duran Trujillo, Y., Otero-Colina, G., Ortega-Arenas, L., Arriola Padilla, V., Mora-Aguilera, J., Damián-Nava, A., and García-Escamilla, P. (2017). Evaluación de insecticidas para el control de trips y ácaros de plagas de mango (mangifera indica l.) en tierra, guerrero, méxico. *Tropical and Subtropical Agroecosystems*, 20(3):381–394. Online: https://bit.ly/3kTNnoG.

García-Escamilla, P., Duran-Trujillo, Y., Lázaro-Dzul, M., Vargas-Madríz, H., and Acuña-Soto, J. (2016). Manejo de trips (frankliniella spp.) en mango (mangifera indica l.) a base de azufre en veracruz, méxico. *Entomología Agrícola*, 3:441–444. Online: https://bit.ly/2PTWZ4O.

Hoddle, M. and Mound, L. (2011). Thysanoptera of the galápagos islands. *Pacific Science*, 65(4):507–513. Online: https://bit.ly/2Cv36cy.

INAMHI (2019). Red de estaciones meteorológicas e hidrológicas. Technical Report Consultado el 01 octubre 2019. Online:https://bit.ly/3iKeNf0, Instituto Nacional de Meteorología e Hidrología.

Kondo, T., Quintero, E., Medina, J., Imbachi-López, J., and Manrique-Burbano, M. (2013). *Tecnología para el manejo de pitaya amarilla Selenicereus megalanthus (K. Schum. ex Vaupel) Moran en Colombia*, chapter Insectos plagas de importancia económica en el cultivo de pitaya amarilla., pages 65–77. Produmedios, Bogotá, Colombia.

Kumar, V., Seal, D., Kakkar, G., McKenzie, C., and Osborne, L. (2012). New tropical fruit hosts of scirtothrips dorsalis (thysanoptera: Thripidae) and its relative abundance on them in south florida. *The Florida Entomologist*, 95(1):205–207. . Online: https://bit.ly/3iMWFBf.

Larral, P., Ripa, R., Funderburk, J., and Lopez, E. (2018). Population abundance, phenology, spatial distribution and a binominal sampling plan for heliothrips haemorrhoidalis (thysanoptera: Thripidae) in avocado. *Florida Entomologist*, 101(2):166–171. Online: https://bit.ly/3aCnchS.

Le Bellec, F., Vaillant, F., and Imbert, E. (2006). Pitahaya (hylocereus spp.): a new fruit crop, a market with a future. *Fruits*, 61(4):237–250. Online: https://bit.ly/3g6vMGC.

MAG (2017). Boletin situacional de pitahaya. Technical Report Electrónico consultado 29 de agosto del 2019. Online:https://bit.ly/3gXwSWt, Ministerio de Agricultura y Ganadería.

Medina, J. and Kondo, T. (2012). Listado taxonómico de organismos que afectan la pitaya amarilla, selenicereus megalanthus (k. schum. ex vaupel) moran (cactaceae) en colombia. *Ciencia y Tecnología Agropecuaria*, 13(1):41–46. Online: https://bit.ly/2PYu0g5.

Miranda-Salcedo, M. A. and Loera-Alvarado, E. (2019). Fluctuacóón poblacional de enemigos naturales de trips (thysanoptera: Thripidae) asociados a limón mexicano (citrus aurantifolia swingle) en michoacán. *Entomología Mexicana*, 6:151–155. Online: https://bit.ly/3h7wNzy.

Montesinos Cruz, J. A., Rodríguez-Larramendi, L., Ortiz-Pérez, R.and Fonseca-Flores, M. A., Ruíz Herrera, G., and Guevara-Hernández, F. (2015). Pitahaya (hylocereus spp.) un recurso fitogenético con historia y futuro para el trópico seco mexicano. *Cultivos Tropicales*, 36:67–76. Online: https://bit.ly/311XmAH.

Mound, L., Moritz, G., Morris, D., and Goldarazena, A. (2009). Pest thrips of the world — visual and molecular identification of pest thrips, cd-rom. *Florida Entomologist - FLA ENTOMOL*, 92:530–530.

Mound, L. A. and Tree, D. J. (2015). Fungus-feeding thysanoptera: Phlaeothripinae of the idiothrips genus-group in australia, with nine new species. *Zootaxa*, 4034(2):325–341. Online: https://bit.ly/2Qb8Mfj.

Mujica, M. V., Scatoni, I. B., Franco, J., Nuñez, S., and Bentancourt, C. M. (2007). Fluctuación poblacional de frankliniella occidentalis(pergande)(thysanoptera: Thripidae) en vitis vinifera l. cv. italia en la zona sur de uruguay. *Boletín de sanidad vegetal. Plagas*, 33(4):457–468. Online: https://bit.ly/2DP6gsz.

Najera-Rincón, M. B. and Souza, B. (2010). *Insectos benéficos. Guía para su identificación*. México, Michoacan.

Palomo, L. A. T., Martinez, N. B., Johansen-Naime, R., Napoles, J. R., Leon, O. S., Arroyo, H. S., and Graziano, J. V. (2015). Population fluctuations of thrips (thysanoptera) and their relationship to the phenology of vegetable crops in the central region of mexico. *Florida Entomologist*, pages 430–438. Online: https://bit.ly/2FwtEeL.

Pérez Artiles, L., Díaz Tejeda, Y., Hernández Espinosa, D., and y Rodríguez Tapia, J. L. (2009). Nocividad producida por selenothrips rubrocinctus giard (thysanoptera: Thripidae) en frutales bajo tecnología de fincas integrales. *Citrifrut*, 26(1):49–51. Online: https://bit.ly/2Cvp0fM.

Ramírez-Delgadillo, J. J., Rodríguez-Leyva, E., Livera-Muñoz, M., Pedroza-Sandoval, A., and Bautista-Martínez, N.and Nava-Díaz, C. (2011). Primer informe de cactophagus spinolae (gyllenhal)(coleoptera: Curculionidae) en tres especies de hylocereus (cactaceae) en morelos, méxico. *Acta zoológica mexicana*, 27(3):863–866. Online: https://bit.ly/2Fnn5Lk.

Reitz, S. R. (2009). Biology and ecology of the western flower thrips (thysanoptera: Thripidae): the making of a pest. *Florida Entomologist*, 92(1):7–13. Online: https://bit.ly/3kKJQt3.

Rivas, F., Moreno, F., Rivera, G., Herrera, L., and Leiva, M. (2017). Incidencia, progresión e intensi-

dad de la pudrición del cogollo de elaeis guineensis jacq. en san lorenzo, ecuador. *Centro Agrícola*, 44(1):28–33. Online: https://bit.ly/3g47Svw.

Rocha, F. H., Infante, F., Castillo, A., Ibarra-Nuñez, G., Goldarazena, A., and Funderburk, J. (2015). Natural enemies of the frankliniella complex species (thysanoptera: Thripidae) in ataulfo mango agroecosystems. *Journal of Insect Science*, 15(1):114. Online: https://bit.ly/3iEZ5BU.

Rugman-Jones, P., Hoddle, M., Amrich, R., Heraty, J., Stouthamer-Ingel, C., and Stouthamer, R. (2012). Phylogeographic structure, outbreeding depression, and reluctant virgin oviposition in the bean thrips, caliothrips fasciatus (pergande)(thysanoptera: Thripidae), in california. *Bulletin of entomological research*, 102(6):698–709. Online: https://bit.ly/2CwigOL.

Salazar Restrepo, J. C. (2012). *Manejo fitorsanitario del cultivo de la pitahaya. Hylocereus megalanthus (K. Schum. ex Vaupel) Ralf Bauer. Medidas para la temporada invernal.* Produmedios, Bogotá.

Sarkar, S., Wang, E., Zhang, Z., Wu, S., and Lei, Z. (2019). Laboratory and glasshouse evaluation of the green lacewing, chrysopa pallens (neuroptera: Chrysopidae) against the western flower thrips, frankliniella occidentalis (thysanoptera: Thripidae). *Applied entomology and zoology*, 54(1):115–121. Online: https://bit.ly/3axJIrS.

Sengonca, C., Blaeser, P., Özden, Ö., and Kersting, U. (2006). Occurrence of thrips (thysanoptera) infestation on nectarines and its importance to fruit damage in north cyprus. *Journal of Plant Diseases and Protection*, 113(3):128–134. Online: https://bit.ly/2Ec1wwB.

Shrestha, G., Enkegaard, A., and Giray, T. (2013). The green lacewing, chrysoperla carnea: preference between lettuce aphids, nasonovia ribisnigri, and western flower thrips, frankliniella occidentalis. *Journal of insect science*, 13(1):94. Online: https://bit.ly/3atK5E5.

Thongjua, T., Thongjua, J., Sriwareen, J., and Khumpairun, J. (2015). Attraction effect of thrips (thysanoptera: Thripidae) to sticky trap color on orchid greenhouse condition. *Journal of Agricultural Technology*, 11(8):2451–2455. Online: https://bit.ly/2DPNvVW.

Urías-López, M. A., Salazar-García, S., and Johansen-Naime, R. (2007). Identificación y fluctuación poblacional de especies de trips (thysanoptera) en aguacate'hass' en nayarit, méxico. *Revista Chapingo Serie Horticultura*, 13(1):49–54. Online: https://bit.ly/2E9hO9P.

Valenzuela-García, R., Cambero-Campos, O., Carvajal-Cazola, C., Robles-Bermúdez, A., and Retana-Salazar, A. (2010). Fluctuación poblacional y especies de thrips (thysanoptera) asociados a calabaza en nayarit, méxico. *Agronomía mesoamericana*, 21(2):333–336. Online: https://bit.ly/2Y8nkR5.

Concordance between micological culture and cytopathology in the diagnosis of dermatophytosis in guinea pigs

Concordancia entre el cultivo micológico y la citopatología en el diagnóstico de dermatofitosis en cuyes

Renzo Venturo B. and Siever Morales-Cauti

Veterinary Medicine and Zootechnics Career, Universidad Científica del Sur. Carr. Panamericana Sur 19, Villa EL Salvador 15067, Lima, Perú.

*Corresponding author: sieverm@hotmail.com

Abstract

Dermatophytosis is a disease that affects the stratum corneum of the skin, hair and nails in guinea pigs, causing bad aspect of the carcass, affecting its commercialization and generating economic losses. For the study 189 samples of guinea pigs with dermatological lesions were collected in intensive breeding farms; the guinea pigs were analyzed by cytopathology and mycological culture in the Laboratory of Microbiology and Microscopy of Universidad Científica del Sur. The frecuency of dermatophytosis was $18.5 \pm 5.5\%$ by mycological culture and $43 \pm 7.1\%$ by cytopathology; according to the age stratum, the dermatophytosis frecuency was 0% / 0% in breeding, 25.6% / 62% in rearing, and 4.8% / 6% in reproductive guinea pigs by mycological culture and cytopathology, respectively. About the location of the lessions, a frequency of 0% / 0% was found in cages by both techniques, while for animals raised in pools a frequency of 26.5% / 61% was found by culture and cytopathology, respectively. The grade of congruity between these two tests was determined by the value of Kappa (κ) equal to 0.46. The result indicates that there is a moderate degree of association.

Keywords: Guinea pigs, dermatophytoses, mycological culture, cytopathology.

Resumen

La dermatofitosis es una enfermedad que afecta al estrato córneo de la piel, pelo y uñas de los cuyes, causando un mal aspecto en la carcasa, afectando su comercialización, y generando pérdidas económicas. Se colectaron 189 muestras de cuyes con lesiones dermatológicas en granjas de crianza intensiva; las cuales fueron analizadas mediante cultivo micológico y citopatología en el Laboratorio de Microbiología y Microscopía de la Universidad Científica del Sur. Se

halló una frecuencia de dermatofitosis de 18.5 ± 5.5% por cultivo micológico y 43 ± 7.1% por citopatología; según el estrato etario la frecuencia de dermatofitosis fue de 0% / 0% en lactantes, 25.6% / 62% en recría y 4.8% / 6% en reproductores, por cultivo micológico y citopatología, respectivamente. Según la ubicación de la lesión la frecuencia de dermatofitosis fue mayor en las regiones frontal y nasal, con 41.7% / 70% y 28.1% / 67%, por cultivo micológico y citopatología, respectivamente; en cuanto al tipo de instalación, se presentó una frecuencia de 0% / 0% en animales criados en jaulas, y 26.5% / 61% en animales de crianza en poza, por la técnica de cultivo micológico y citopatología, respectivamente. Al evaluar el grado de concordancia entre ambas técnicas se halló un valor de Kappa (κ) igual a 0.46, considerada moderada.

Palabras clave: Cuyes, dermatofitosis, cultivo micológico, citopatología.

Orcid IDs:

Renzo Venturo B.: http://orcid.org/0000-0003-2653-8477

Siever Morales-Cauti: http://orcid.org/0000-0002-5396-8889

1 Introduction

Guinea pig (*Cavia porcellus*) is a rodent mammal from the Andean region. This species is important because it represents a product with a great nutritional value for high Andean rural areas. In addition, it is highly rustic, with competitive advantages over other species, and with commercial and economic viability (Morales, 2013; Solórzano, 2014). Despite its rusticity, there are factors that can predispose guinea pig to various diseases, such as variations in temperature, humidity, air currents, high population density, among others (Morales-Cauti, 2018). Dermatophytosis is one of the diseases that most affect guinea pig; it is a dermatophyte fungal infection that affects the stratum corneal of the skin, hair and nails. It is caused by fungi of the genera *Trichophyton* and *Microsporum*, and is transmitted by contact between sick animals or through contaminated facilities or tools. The most commonly found dermatophyte in guinea pig is *Trichophyton mentagrophytes*, which usually manifests with clinical signs such as non-itchy diffuse flaking and alopecia in the nose, ears, face and/or limbs (White et al., 2016). This infection may be accompanied by a secondary bacterial infection, where the lesion is suppurative known as weeping eczema (Burke, 1994; Indranil, 2015).

There are two essential methods for the diagnosis of dermatophytosis: direct examination and mycological culture; however, there are other methods such as Wood lamp or dermatoscopy (Hnilica and Patterson, 2017; Moriello et al., 2017). Skin cytopathology is not commonly used for the diagnosis of dermatophytosis, but it is mentioned as a valid technique (Mendelsohn et al., 2006; Joyce and Vandis, 2007; Scurrel, 2011; Miller et al., 2013; Wiebe, 2015; Albanese, 2017). However, mycological culture is the standard gold test for the diagnose of dermatophytosis and it should be performed whenever the disease is suspected (Patel and Forsythe, 2008). *aburaud dextrose Agar* is a peptone medium supplemented with dextrose to promote fungal growth. While peptone works as a source of nitrogenous growth factors, dextrose provides an energy source for the growth of microorganisms, the medium is not selective for dermatophytes since there is no inhibition of saprophyte fungi, thus to modify it chloramphenicol must be added to inhibit gram-negative and positive bacteria (Sparkes et al., 1993).

Dermatophytes are identified macroscopically based on their growth rate, appearance, texture, surface color and reverse color (Indranil, 2015). For performing the microscopic examination, the colonies are transferred to a slide, using a tape or sterile swab. Lactophenol cotton blue is added since it highlights the appearance of the hyphae and conidia; for identifying it, hyphae, macroconidials and/or microconids should be searched (Helton and Werner, 2018). On the other hand, skin cytology is the second most common technique for diagnosing dermatological diseases. It consists of identifying bacterial or fungal organisms (yeasts) and evaluating the types of inflammatory cells, neoplastic cells or acantholytic keratinocytes found in the skin (Hnilica and Patterson, 2017). Findings that may suggest a dermatophytosis infection are the presence of neutrophils, macrophages, keratinocytes and acantholytic cells. The first two are the most commonly detected cells in skin lesion samples. This type of mixed inflammation is often associated with foreign bodies, fungal infections, mycobacteria infections, granulomas and other chronic injuries (Raskin and Meyer, 2015).

For a definitive diagnosis of dermatophytosis, septate hyphae and/or arthroconidia should be detected on the surface of these corneocytes (Gross et al., 2005; Albanese, 2017). Purple or blue hyphae and spores may be observed with a Diff Quick stain (Neuber and Nuttall, 2017). In Peru, studies on the use of cytopathology in the diagnosis of dermatophytosis have not yet been reported. For this reason, the purpose of this study is to find the concordance between the mycological culture technique and the cytopathological technique in the diagnosis of dermatophytosis in intensively reared guinea pigs, and determine their frequency according to their own characteristics, so that cytology can be established as a rapid diagnostic technique for this disease, establishing appropriate treatment and decreasing its impact on the producer.

2 Materials and Methods

2.1 Date and place of the research

This study was conducted from January to March 2018, with an average environmental temperature of 19,5°C and humidity of 87% (INEI, Instituto Na-

cional de Estadística e Informática, 2018). The skin samples collected for the diagnosis of mycosis were transported for their evaluation to the Microbiology and Microscopy Laboratory of the Faculty of Veterinary and Biological Sciences of Universidad Científica del Sur. Populations of guinea pigs from intensive breeding systems, from both sexes and different productive stages (infant, breeding, reproductive) were studied. The samples were taken from animals with skin lesions such as flaking and alopecia, using surface skin scraping and deep skin scraping techniques.

2.2 Sample size

In determining the sample size of the study, reference was taken from the research that determined dermatophytosis in guinea pigs at the headquarters of INIA (Celis, 1998), in which 93 % of prevalence was obtained; and the infinite population formula was used for this purpose. 189 samples were processed by opportunity and resource availability, and the distribution of which was as follows: Farm 1 (n=86), farm 2 (n=40), farm 3 (n=5) and farm 4 (n=73).

2.3 Obtaining of samples

The samples were collected using two techniques: surface skin scraping and deep skin scraping, mentioned by Bexfield et al. (2014). Surface scraping was performed for the mycological culture, while deep skin scraping for the cytology technique as bleeding helps to generate more contrast and facilitate the visualization of fungal structures alongside inflammatory cells of the lesion. The surface skin scraping was performed with a scalpel throughout the peripheral area of the lesion, taking scales and scabs. These were transported in sterile containers with a threaded lid for their processing in the laboratory. For the deep skin scraping, the surface of the skin continued to be scraped with the scalpel until capillary bleeding occurred. The sample was then transferred to a slide, and the sample was extended by passing one slide against another, using the squash technique (Valenciano and Cowell, 2014).

2.4 Citology processing

The slides with the samples were stained with the Diff Quick staining protocol. First they were immersed in the alcoholic fixer 3 times from 2 to 3 se-

conds at a time; then these were drained on filter paper; later, the samples were immersed in the basic red staining; and finally, in the purple acid staining during 8 seconds. They were then immersed in water to remove the excess of dye and were allowed to dry for 5 minutes (Albanese, 2017). The dyed and dried slides were observed under the microscope with a lens of 100X, in order to identify the types of existing cells and possible fungal organisms (Hnilica and Patterson, 2017). The samples considered positive were those that indicated the presence of hyphae and/or spores. Spores are small, rounded or oval structures with a clear pericellular halo. Hyphae were recognized for their peculiar bamboo branch shape, such as segmented linear filaments (Mendelsohn et al., 2006; Raskin and Meyer, 2015; Albanese, 2017).

2.5 Micologycal culture processing

Sabouraud Dextrose Agar medium with a 5.6 pH was used for the cultivation of the samples, to which chloramphenicol was added in a concentration of 50mg/dL. The samples were sown with the help of Falcon tubes containing the culture medium, in an inclined position or flute beak to avoid drying. Cultures were kept at a temperature of $22°C$ for 21 days, monitoring daily to observe the colony growth (Cuétara, 2007; Kraemer et al., 2012). Samples that on day 10 day had flat white, cottony or woolly colonies, golden edges with or without depressed center, and yellow orange or orange brown on the back (compatible with *M. canis*) were considered positive; as well as flat colonies with powdery texture, and cream color with white edges, white myceliums and pale yellow or brown on the back (compatible with *M. gypseum*); or flat colonies with a white or creamy powdery surface, and copper brown or dark red on the back (compatible with *T. mentagrophytes*) (Moriello, 2001; Miller et al., 2013). Colonies with other aspects were compared with an atlas of mycology to be considered positive or not to the diagnosis of dermatophytosis.

2.6 Microscopic identification

From the cultivated plates, the colonies were transferred to slides. Lactophenol cotton blue was used on the slides, and were then covered with tape. They were then observed under the microscope (Helton and Werner, 2018). Findings of fusiform

macroconidias of 6 or more segments with thick spiny walls (*M. canis*) were considered positive as well as findings of elliptical-shaped macroconidia with up to 6 segments and thin walls (*M. gypseum*); and findings of globose microconids with occasional presence of cigar-shaped macrochondicates with thin, smooth walls and sporadic spiral hyphae (*T. mentagrophytes*) (Miller et al., 2013). Kappa test was used to determine the concordance between the two techniques used, for which a 2×2 contingency table was prepared and is detailed below.

2.7 Interpretation of the results

The determination of Kappa's index, the STATA15.0 statistical package and qualitative interpretation based on the concordance force described by Altman (1990), were used and were qualified as: poor or weak for values lower than 0.40; moderate for values between 0.41 and 0.60; good between 0.61 and 0.80; and very good for values up to 1.13. The determination of the frequency of dermatophytes for each diagnostic technique was obtained from the concordance between the number of positive diagnoses versus the total number of animals evaluated.

3 Results and discussion

The overall frequency of dermatophytosis was 18.5 ± 5.5 % (35/189) by using the culture technique, while in the cytopathology technique, the overall frequency was 43 ± 7.1 % (81/189) (Table 1). The frequency for dermatophytosis in animals with lesions by the mycological culture method was 18.5 ± 5.5 %, contrasting with the values found by other authors using the same method in the country. Other authors report higher frequencies, between 50 and 95 % of dermatophytosis (Celis, 1998; Jara et al., 2003; Pineda et al., 2009). These high occurrences are due to the environmental factor, since dermatophytes, although ubiquitous, have a higher frequency in warm places and high relative humidity (Helton and Werner, 2018). On the other hand, the immunity of the host also has an influence which depends on the age, feeding and management of animals (Morales, 2013); so this can be circumstantial, and it might have multifactorial influence.

Various factors influence the degree of kappa index (κ) consistency for this study where diagnostic techniques such as mycological and cytological culture are used; these factors are age, gender, type of facilities, degree of training of the operating technicians responsible for obtaining sampling and the execution of diagnostic techniques (Table 2).

As for the frequencies of dermatophytosis per age group in this study using the mycological culture method, these were found to vary from 0 % in lactating animals to 25.6 % in breeding; these results were similar to those found by Jara et al. (2003), who reported that the breed had the highest percentage of positive animals. This is caused by the incomplete development of the immune system and the low concentration of fungistatic fatty acids present in the sebum parenciteRichardson2000, Patel2008. In addition, after puberty the aggressions between males begin, increasing stress and causing injuries that serve as an entry route to the fungus (Jara et al., 2003).

In relation to the location of the lesion, injuries in the nasal and frontal region were much more common, while lesions found on the back of the caudal back and limbs did not show dermatophytosis. This also agrees with Jara et al. (2003) where lesions in the periocular and nasal region were the most reported, while the extremities and back show the lowest frequency of dermatophytosis. In addition, Miller et al. (2013) describe that the most affected areas by dermatophytosis are the nasal, periocular, frontal and atrial area, and can only rarely spread to the lumbosacral area without affecting the limbs. Therefore, this location of injuries could be related to the behavior of the species, easing the contact with contaminated areas of the environment, favored by the moisture of these areas due to the feeding behavior of the species.

As for the type of facility, there is a higher frequency of dermatophytosis in animals raised in pools. Jara et al. (2003) in determining the humidity of intensively reared guinea pigs reported that the pools that stay wet for longer present more animals with dermatological lesions. Therefore, it is confirmed that the type of installation influences the presence or absence of moisture, ventilation and lighting, and potentially the presentation of dermatophytosis.

Table 1. Frequency of dermatophytosis in guinea pig intensively reared according to the sex, age, location of the injury, and type of facilities; by mycological culture and cytology (n=189).

	Total of animals	Positive animals (culture)*				Positive animals (cytology)*			
		n	%		± IC 95%	n	%		+ IC 95%
Sex									
Female	103	8	7.80%	±	5.20%	24	23.00%	±	8.10%
Male	86	27	31.40%	±	9.80%	57	66.00%	±	10.00%
Age									
Lactating	1	0	0.00%	±	0.00%	0	0.00%	±	0.00%
Breeding	125	32	25.60%	±	7.70%	77	62.00%	±	8.50%
Reproductive	63	3	4.80%	±	5.30%	4	6.00%	±	5.90%
Location of the injury									
Nasal	64	18	28.10%	±	11.00%	45	70.00%	±	11.20%
Frente	12	5	41.70%	±	27.90%	8	67.00%	±	26.60%
Atrial	5	1	20.00%	±	35.00%	3	60.00%	±	42.90%
Face	3	0	0.00%	±	0.00%	3	100.00%	±	0.00%
Medial	96	10	10.40%	±	6.10%	17	18.00%	±	7.70%
Caudal dorsum	4	0	0.00%	±	0.00%	1	25.00%	±	42.40%
Limbs	2	0	0.00%	±	0.00%	1	50.00%	±	69.30%
Periocular	3	1	33.30%	±	53.30%	3	100.00%	±	0.00%
Facilities									
Cage	57	0	0.00%	±	0.00%	0	0.00%	±	0.00%
Pool	132	35	26.50%	±	7.50%	81	61.00%	±	8.30%
TOTAL	189	35	18.50%	±	5.50%	81	43.00%	±	7.10%

* The concordance determination between both diagnosis techniques was 0.46 (moderate).

On the other hand, the frequency for dermatophytosis in animals with dermatological lesions diagnosed by the cytopathology method was higher compared to the mycological culture, with indices of $43 \pm 7.1\%$ of the animals evaluated. In relation to the frequencies of dermatophytosis per age group in this study, it is reported that these vary from 0% in infants to 62% in breeding. At the level of affec- ted areas, the highest frequency occurs in the nasal, frontal and atrial region with frequencies between 28.1% and 40.7% (Table 1). As for the type of facility, there is a dermatophytosis frequency of 62% in animals raised in pools, and 0% in animals raised in cages. Showing more sensitivity of this technique for the diagnosis.

Table 2. Proportion of concordance between mycological culture technique and cytology as a diagnosis of dermatophytosis in guinea pigs.

		Cytological technique		
		Negative	**Positive**	**Total**
Mycological culture technique	**Negative**	108	46	154
	Positive	0	35	35
	Total	108	81	189
				Kappa index = 0.46

The cytopathology technique is often used to determine the presence of etiological agents in dermatological lesions, because it is easy to perform, fast and it is minimally invasive; it is also not too expensive (Neuber and Nuttall, 2017); however, it is not widely used for this purpose. Within this technique, the best sampling method is that of adhesive tape. However, the amount of fungi found will de-

pend on the intensity of the infection (Albanese, 2017). On the other hand, although the staining of the slides with Diff Quick is very effective to visualize spores and/or hyphae, stains such as Schiff or Gomori allow to distinguish much better these fungal structures in histopathological slides (Albanese, 2017); however, the costs are higher. On the other hand, with regard to the sensitivity of the diagnosis of dermatophytosis, the frequency reported by the cytopathology technique was higher than that reported by the mycological culture, because the latter not only identifies dermatophytes but also tested positive for other fungal species, subsequently defined by mycological culture.

In the study of concordance between the two diagnostic techniques (Table 2), the mycological culture technique and cytopathology determined that a moderate concordance of 0.46 was found using the Kappa test (Altman, 1990), due to the difference between the frequencies reported with both techniques. Despite the false positives of the cytopathology technique, these other fungal species not only cannot be considered as contamination but could potentially be causing the dermatological lesions. In addition, this result represents the first concordance study between the two diagnostic techniques.

Finally, cytopathology could be used as a first-intentioned technique for the diagnosis of dermatomycosis in guinea pigs, and if positive, a definitive diagnosis by mycological culture is necessary.

4   Conclusions

EThe degree of concordance found between the mycological culture and the cytopathology techniques for detecting dermatophytosis in extensive reared guinea pigs is moderate (Kappa = 0.46).

The presence estimation of dermatophytosis in extensive reared guinea pigs was $18.5 \pm 5.5\%$ using the mycological culture method and $43 \pm 7.1\%$ using the cytopathology method.

Acknowlegment

References

Albanese, F. (2017). Cytology of skin tumours. In *Canine and Feline Skin Cytology*, pages 291–490. Online:https://bit.ly/2BHdrSu. Springer.

Altman, D. G. (1990). *Practical statistics for medical research*. CRC press, New York.

Bexfield, N., Lee, K., et al. (2014). *BSAVA guide to procedures in small animal practice*. Number Ed. 2. British Small Animal Veterinary Association.

Burke, T. (1994). *Kirk's Current Veterinary Therapy*. Saunders, Missouri.

Celis, E. (1998). Detección de dermatomicosis en cuyes criados en baterías y pozas en la sede central del inia-lima. Tesis de médico veterinario, Universidad Nacional Hermilio Valdizán, Huúnuco.

Cuétara, M. S. (2007). Procesamiento de las muestras superficiales. *Revista Iberoamericana de Micología*, 4:1–12. Online:https://bit.ly/33gpRMD.

Gross, T., Ihrke, P. J., Walder, E. J., and Affolter, V. K. (2005). *Skin Diseases of the Dog and Cat: Clinical and Histopathologic Diagnosis*. Oxford.

Helton, K. and Werner, A. . (2018). *Small animal dermatology*. Wiley –Blackwell, Iowa.

Hnilica, K. and Patterson, A. (2017). *Small Animal Dermatology: a color atlas and therapeutic guide*. Saunders, Missouri.

Indranil, S. (2015). *Veterinary Micology*. Springer, Nueva Delh.

INEI, Instituto Nacional de Estadística e Informática (2018). Temperatura promedio anual, según departamento.

Jara, M., Muscari, J., and Chauca, L. . (2003). Dermatofitosis en cuyes (cavia porcellus) de granjas tecnificadas de la costa central, provincia de lima - perú. In *XXVII Reunión de la Asociación Peruana de Producción Animal*, Lima.

Joyce, S. and Vandis, M. (2007). *Clinical exposures: canine dermatophyte infection*. Veterinary Medicine 360.

Kraemer, A., Mueller, R. S., Werckenthin, C., Straubinger, R. K., and Hein, J. (2012). Dermatophytes in pet guinea pigs and rabbits. *Veterinary microbiology*, 157(1-2):208–213. Online:https://bit.ly/2P1CIK4.

Mendelsohn, C., Rosenkrantz, W., and Griffin, C. E. (2006). Practical cytology for inflammatory skin diseases. *Clinical techniques in small animal practice*, 21(3):117–127. Online:https://bit.ly/3f3QLJG.

Miller, W., Griffin, C., and Campbell, K. (2013). *Small animal dermatology*. Mosby, Missouri.

Morales, S. (2013). La sanidad en sistemas de crianza comercial de cuyes. In *XXXVI Reunión Científica Anual. Lima*. Asociación de Producción Animal. Online:http://bit.ly/31CuqOh.

Morales-Cauti, S. (2018). La sanidad en sistemas de crianza comercial de cuyes. In *Lima. XLI Reunión Científica Anual*. Asociación de Producción Animal. Online:http://bit.ly/31CuqOh.

Moriello, K. (2001). Diagnostic techniques for dermatophytosis. *Clinical techniques in small animal practice*, 16(4):219–224. Online:https://bit.ly/3jSpDki.

Moriello, K. A., Coyner, K., Paterson, S., and Mignon, B. (2017). Diagnosis and treatment of dermatophytosis in dogs and cats. clinical consensus guidelines of the world association for veterinary dermatology. *Veterinary Dermatology*, 28(3):266–e68. Online:https://bit.ly/3g9uc7N.

Neuber, A. and Nuttall, T. (2017). *Diagnostic techniques in veterinary dermatology*. Oxford.

Patel, A. and Forsythe, P. (2008). *Small animal dermatology*. Saunders, London.

Pineda, C., Camiloaga, S., and Zuñiga, M. (2009). Frecuencia de hongos dermatofitos en la crianza de cobayos (cavia porcellus) en la provincia de huánuco. *Investigación Valdizana*, 3(1):5–8. Online:http://bit.ly/2H92ZlE. .

Raskin, R. and Meyer, D. (2015). *Canine and Feline Cytology: a Colour Atlas and Interpretation Guide*. Saunders, Missouri.

Scurrel, E. (2011). Kerion dermatophytosis in a cocker spaniel.

Solórzano, J. (2014). *Crianza, producción y comercialización de cuyes.* Lima.

Sparkes, A., Gruffydd-Jones, T., Shaw, S., Wright, A., and Stokes, C. (1993). Epidemiological and diagnostic features of canine and feline dermatophytosis in the united kingdom from 1956 to 1991. *The Veterinary Record*, 133(3):57–61. Online:https://bit.ly/3jV8E0K.

Valenciano, A. and Cowell, R. (2014). *Cowell and Tyler´s Diagnostic cytology and hematology of the dog and cat.* Elsevier, Missouri.

White, S. D., D., S.-M. G., and Paul-Murphy, J.and Hawkins, M. G. (2016). Skin diseases in companion guinea pigs (cavia porcellus): a retrospective study of 293 cases seen at the veterinary medical teaching hospital, university of california at davis (1990–2015). *Veterinary dermatology*, 27(5):395–e100. Online:https://bit.ly/2P9aNYB.

Wiebe, V. (2015). *Drug therapy for infectious diseases of dog and cat».* Oxford.

Metal content evaluation in soils and edible tissues of *Allium fistulosum L.* on crops near the Tungurahua volcano

Evaluación del contenido de metales en suelos y tejidos comestibles de *Allium fistulosum L.* cultivado en zonas cercanas al volcán Tungurahua

Jorge Briceño*[1] , Evelyn Tonato[1], Mónica Silva[1], Mayra Paredes[1] and Arnaldo Armado[2]

[1] Laboratorry of functional foods. Faculty of Science, Food Engineering and Biotechnology. Universidad Técnica de Ambato. Campus Huachi, Av. Los Chasquis y Río Payamino, CP. 180206, Ambato, Ecuador.
[2] Environmental, chemistry, Biology Research Center. Scientific and Technological Faculty. Universidad de Carabobo, Naguanagua (2005), Carabobo, Venezuela.

*Corresponding author: jbriceno@uc.edu.ve

Abstract

The Tungurahua volcano, located in the eastern mountain range of Ecuador, since its reactivation in 1999 has had several phases of volcanic activity, which have produced gas, ash and lava emissions. These emissions release a large amount of metals to nearby soils that are currently used for agricultural purposes. Metal pollution can cause serious problems for human health; while other metals are necessary as nutrients in most agricultural crops. In this investigation, the metal content in agricultural soils of the Quero canton was evaluated, as well as its bioavailability and content in the culture of *Allium fistulosum L.*, in order to obtain information on the impact of potentially polluting metals (cadmium, lead, nickel, strontium, cobalt, copper and zinc) and nutrients (potassium, magnesium, iron and manganese) on crops. For the estimation of total metals in soil an acid digestion was performed; for bioavailable metals an extractant mixture (EDTA-Triethanolamine-$CaCl_2$, pH 7) was used and for the branch onion a calcination followed by acid digestion was carried out. The quantification of the metals was carried out by flame atomic absorption spectroscopy or graphite furnace. The results showed that the metal content, both in the soil samples and in the branch onion, was below the maximum values allowed in the local regulations for all the metals studied. In addition, the intake of the metal by the branch onion was independent of the bioavailable fraction.

Keywords: Cadmium, copper, metal intake, bioavailable metal, branch onion.

Resumen

El volcán Tungurahua, ubicado en la cordillera oriental de Ecuador, desde su reactivación en 1999 ha entrado en varias fases de actividad volcánica, produciendo emisiones de gas, cenizas y lava. Estas emisiones liberan una gran cantidad de metales a suelos cercanos que, en la actualidad, se emplean con fines agrícolas. La contaminación por metales puede provocar graves problemas para la salud humana; mientras que otros metales son necesarios como nutrientes, en la mayoría de los cultivos agrícolas. En esta investigación, se evaluó el contenido de metales en suelos agrícolas del cantón Quero, su biodisponibilidad y el contenido en el cultivo de *Allium fistulosum L.*, con la finalidad de obtener información sobre el impacto de metales potencialmente contaminantes (cadmio, plomo, níquel, estroncio, cobalto, cobre y cinc) y nutrientes (potasio, magnesio, hierro y manganeso) sobre los cultivos. Para la estimación de metales totales en el suelo se realizó una digestión ácida; para metales biodisponibles se empleó una mezcla extractante (EDTA-Trietanolamina-*CaCl$_2$*, pH 7) y para la cebolla de rama se realizó una calcinación seguida de digestión ácida. La cuantificación de los metales se realizó mediante espectroscopia de absorción atómica (EAA) de llama o de horno de grafito. Los resultados mostraron que el contenido de metales, tanto en las muestras de suelo como en cebolla de rama, estaba por debajo de los valores máximos permitidos en las normas locales para todos los metales estudiados; además, la ingesta del metal por la cebolla de rama fue independiente de la fracción biodisponible.

Palabras clave: Cadmio, cobre, ingesta de metal, metal biodisponible, cebolla de rama.

Orcid IDs:
Jorge Briceño: http://orcid.org/0000-0002-0692-1228
Evelyn Tonato: http://orcid.org/0000-0002-1707-4298
Mónica Silva: http://orcid.org/0000-0001-8887-1553
Mayra Paredes: http://orcid.org/0000-0001-9320-9177
Arnaldo Armado: http://orcid.org/0000-0003-4670-0339

1 Introduction

The Tungurahua volcano, located in the eastern mountain range of Ecuador, has been into different phases of volcanic activity since its activation in 1999, with gas, ash and lava emissions (Battaglia et al., 2019). These emissions release a large amount of metals to nearby soils that are currently used for agricultural purposes. Heavy metal contamination in agricultural soils can create serious human health problems, because many edible plant species can absorb large amounts of potentially toxic metals from the soil. The metal intake through the consumption of contaminated food can lead to malformations, neuronal dysfunctions and even death (Rai et al., 2019).

While heavy metals such as cadmium, lead, nickel, cobalt, copper and zinc are considered potentially toxic (Tóth et al., 2016), for plants, animals and even humans (Rai et al., 2019), other metals such as potassium, magnesium, iron and manganese, are necessary for the nutrition of plants and agricultural crops in general. It is important to evaluate the content of metals in soils and crops, since soil composition is one of the factors influencing the transfer of trace elements in the soil-plant chain as part of the biochemical cycle (Kabata-Pendias, 2004; Kabata-Pendias and Sadurski, 2004; Tóth et al., 2016). In addition, knowing the metal content makes it possible to show that the nutrient content is suitable for cultivation, and that potentially polluting heavy metals are below permissible limits, according to national and international environmental regulations.

Onion (*Allium fistulosum L.*) is grown in the Quero canton (Choumert-Nkolo and Phélinas, 2019), especially near Tungurahua Volcano. Therefore, there is the need to evaluate the content of metals that could have been expelled in the latest ash emissions in 2016 (Battaglia et al., 2019). In this investigation, the content of some metals in agricultural soils in the Quero canton, their bioavailability and content in the cultivation of *Allium fistulosum L.* were evaluated in order to obtain information on the possible impact of metals on crops, taking into account that metals such as cadmium, lead, nickel, strontium, cobalt, copper and zinc, may be potential pollutants; and metals such as potassium, magnesium, iron and manganese act as macro and micronutrients for the crop.

2 Materials and methods

2.1 Soil sampling area and onion

The soil and onion samples were selected from a plot of 3 884 m^2 located at 3 185 m.a.s.l in the Quero canton, 12 km from the Tungurahua volcano and 29 km from the Chimborazo volcano. Figure 1 shows its geographic location (A) and its subdivision into five similar transects for sampling (B).

2.2 Selection and preservation of samples

Soil and onion samples were collected in November 2018 near the ash catchment zone of the Tungurahua volcano. For the sampling, the zigzag method was used on a plot at approximately 5 meters of distance, and 10-30 cm of deep were dug, taking approximately 1-2 kg of soil. For the onion, a cluster in its final stage of growth was cut from the same places where the soil sample was obtained. The samples were moved in clean and properly labeled polyethylene bags. The entire sampling process was carried out within 5 months.

The soil sample underwent a drying process at room temperature, it was grounded and sifted with a mesh No. 14, and the onion was washed with distilled water to remove visible dirt and the edible portion was taken for analysis. Subsequently, it was subjected to a convection drying at 40 $°C$ for 24h, it was grounded and sifted (Faithfull et al., 2005) and was properly stored until performing the analysis of the metals.

2.3 Physicochemical parameters

The moisture percentage for soil samples was determined by weight loss on a stove, using the method 93.06-37.1.10 (AOAC, 2006). Soil organic matter was determined in samples dried in a stove at 105 $°C$, by ignition loss at $450°C$ for 10 h using a flask NABERTHERM LT 15/12/B180 (Cargua Catagña et al., 2017). The pH and electrical conductivity were determined in distilled water (Kazlauskaitė-Jadzevičė et al., 2014), 1:2.5 w/v ratio by using a potentiometer METTER TOLEDO SEVENCOMPACT PH/ION and a THERMO SCIENTIFIC ORION VERSASTAR conductimeter, respectively. For the onion samples,

the moisture content was determined using an infrared balance METTER TOLEDO HX 2014 MOISTURE ANALYZER, using 3 g of sample with working condition of $150°C$ and with drying criterion of 1 mg/50 seconds.
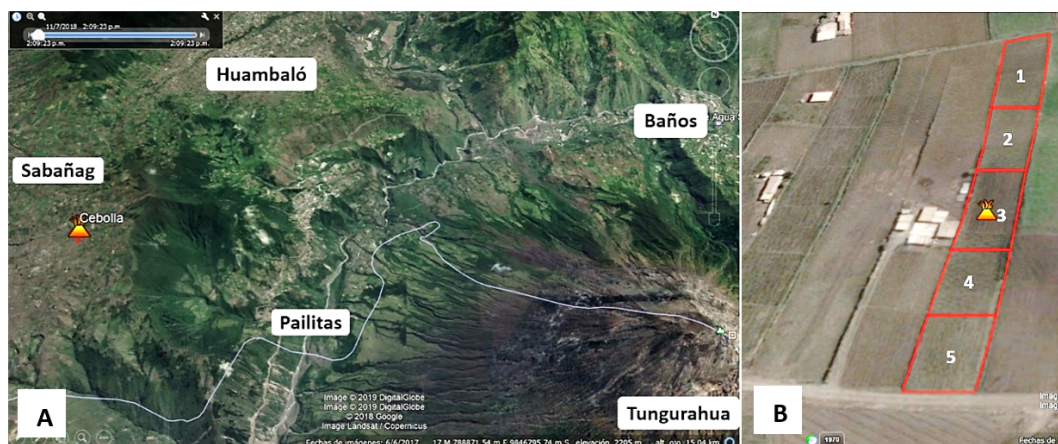

Figure 1. (A) Geographical location of the sampled plot. (B) Subdivision and sampling points. Source: Google Earth, 2019

2.4 Extraction of total and bioavailable metals in soil samples

For the estimate of the total fraction of each metal in the soil, digestion was performed with *agua regia* concentrated HNO_3 and concentrated HCl in 1:3 v/v ratio) (Sungur et al., 2014); 0.5 g of soil was weighted by triplicate on an analytical balance and agua regia was added in a ratio of 1:10 w/v to $90°C$ by 2 h with magnetic agitation, subsequently it was filtered and gauged at 25 mL with HNO_3 0.14 M.

For the estimation of the bioavailable fraction of each metal, an extractant mixture prepared with EDTA 0.05M, triethanolamine 0.1 M and calcium chloride dihydrate 0.01M adjusted to pH was used: 7 (Khan et al., 2019). The extraction was performed in a ratio of 1:2 soil / extracting mixture, agitating it for 30 minutes, it was subsequently centrifuged at 4500 rpm for 10 min, the supernatant was filtered by gravity and graduated to 50 mL with HNO_3 0.14 M (Golia et al., 2008).

2.5 Extraction of metals in onion samples

Onion samples were submitted to calcination at $450°C$, followed by acid digestion. The ashes resulting from the determination of organic matter were taken and 0.50 mL of *HCl* and 0.25 mL of concentra-

ted HNO_3 were added, then were left to stand for 15 min and werefiltered with Nylon microfilters of 13 mm in diameter and with pore size of 0.45 μm, were gauged with 25 mL with HNO_3 0.14 M.

2.6 Determination of metals using EAA

The determination of metals was carried out using an atomic absorption spectrophotometer with PG Intruments line source model AA500, using the electrical conditions recommended by the manufacturer for each metal. The instrument is equipped with flame atomizers and graphite furnace; a D_2 deuterium lamp was used to correct non-specific absorbance and an AUTO SAMPLER PG Intruments model AS500 was used for the introduction of liquid samples into the atomization system. Single-element standards (AccuStandart) were used to obtain daily calibration curves for each element. The concentration of cobalt, strontium, lead, nickel and cadmium was determined with the graphite furnace using argon 5.0 grade of 99.99% of purity (Linde Ecuador S.A.) during the pyrolysis stage and with stopped flow during atomization. Similarly, potassium, magnesium, manganese, copper, iron and zinc were determined with 2.5 grade of acetylene air flame and purity of 99.5% (Linde Ecuador S.A.). In all two cases, the determination of

the metal content was made by direct comparison of the signal of each element versus the calibration obtained for each metal. All samples were processed by triplicate, including a white interleaved between each sample. The quality of the data was verified by measuring a separately prepared calibration point with other certified reference material to determine the veracity of the method.

2.7 Bioavailability factor, β

The typical measurement of the total content of the metal in the soil is not always suitable for assessing its mobility or availability (Rieuwerts, 2007). In this sense, a bioavailability factor β, determined by Equation 1, was established to evaluate the bioavailable fraction and to verify that the metal content is independent from the total content of the same metal in the soil. With the value set, the metal absorbed

by the plant could be evaluated (Khan et al., 2015).

$$\beta = \frac{Metal_{bioavailable}}{Metal_{Total}} \quad (1)$$

3 Results and discussion

3.1 Physicochemical parameters of the soil

The soil samples were evaluated based on national reference values (Table 1) according to the Secretariat of Environment and Natural Resources (SEMARNAT). The results obtained from the soil characterization are presented in Table 2. The pH was below 5, thus the sampling sector is strongly acid as specified in SEMARNAT (2003); these conditions favor the solubility of metallic elements, thus allowing better assimilation by plants (Kabata-Pendias and Sadurski, 2004; Tangahu et al., 2011).

Table 1. Reference values reported for the classification of soils. Values taken from SEMARNAT (2003).

Property	Classification	Value
pH	Stronly acid	< 5
	Moderate acid	$5.1 - 6.5$
	Neutral	$6.6 - 7.3$
	Partly alkaline	$7.4 - 8.5$
	Stronly alkaline	> 8.5
Electric conductivity [dS/m]	Negligible salinity effects	< 1.0
	Slightly saline	$1.1 - 2.0$
	Moderate saline	$2.1 - 4.0$
	Saline soil	$4.1 - 8.0$
	Very saline	$8.1 - 16.0$
	Stronly saline	> 16.0
Organic matter [%]	Very low	< 4
	Low	$4.1 - 6.0$
	Medium	$6.1 - 10.9$
	High	$11.0 - 16.0$
	Very high	>16.1

As for the found values of electrical conductivity, the soils analyzed are considered to have negligible salinity effects and the values of the organic matter content were very low according to SEMARNAT (2003). However, these conditions have allowed an easy development of the plant, so it was

evident at the time of sampling, probably by the incorporation of rice shell residues into the soil by farmers as an attempt to improve the properties of the soil (Park et al., 2011).

The result of a low pH soil low in organic matter

Table 2. Characterization of the soil studied.

Points	pH	EC [dS/m]	OM [%]	Humidity [%]
1	4.96 (0.06)	0.163(0.002)	2.9 (0.2)	20.4 (2.0)
2	4.88 (0.03)	0.160(0.002)	2.4 (0.1)	18.8 (0.3)
3	4.73 (0.06)	0.238(0.002)	2.6 (0.9)	17.4 (0.6)
4	4.36 (0.04)	0.525(0.003)	2.5 (0.2)	17.5 (1.2)
5	4.93 (0.04)	0.200(0.001)	3.0 (0.2)	20.4 (1.7)

pH: Hydrogen potential, EC: electrical conductivity, OM: organic matter. The average is displayed and the standard deviation for n = 3 is shown in parentheses.

increases the bioavailability of metals for the plant due to the lack of formation of organometallic complexes, making it impossible for metals to be absorbed by the root of the plant that is in direct contact with the soil (Tangahu et al., 2011; Bravo Realpe et al., 2014; Bornø et al., 2019). On the other hand, the humidity for the collected agricultural soil samples were between 17.4 and 20.4 %, which is typical to the climate of the area and the conditions of the harvesting day.

3.2 Moisture and ash content in onion

In onion samples, the humidity and ash parameters were from 90.63 to 91.70 % and 5.17 to 6.06 %, respectively. In general, the moisture content is consistent with a review conducted by Mitra and Rao (2012) of 91.20 %, while the ash content was similar to those obtained by Bello et al. (2013) who reported values up to 11.46 %. However, these properties are of minimal control since they are influenced by climatic and soil conditions, conditions of transport and storage of the product during the post-harvest.

3.3 Metal content in the soil and onion

The metal content was compared to reference values according to national and international regulations. For the specific case of onion, no legislation regulating the metal content was found; however, the value corresponding to items similar to those analyzed was taken as a reference. Table 3 shows the values of various legislations for food and soils obtained from the MAE.

The results obtained from the metal content in soil samples for soluble fractions in *agua regia* (totals), the soluble fraction in the extracting mixture (bioavailable) and onion samples are expressed as quantity of metal in fresh mass (Table 4). The discussion of the results was based on the total content, the bioavailable fraction and the value found in onion for each metal.

The cadmium content (total 0.09-0.13 mg/kg and bioavailable 0.0218-0.049 mg/kg) for soil samples was found within the environmental quality standards established for soils, according to the MAE (values below 0.5 mg/kg). The results obtained for cadmium are within the reported values (0.07–1.35 mg/kg) in New Zealand soils (Cavanagh et al., 2019); however, they are lower than those reported in soils of a petrochemical area (0.25–1.50 mg/kg) in Sardinia, Italy (Cortis et al., 2016) and in sediments of Texcoco Lake (0.64–2.28 mg/kg), located at the east of the Trans-Mexican Volcanic Belt (Sedeño-Díaz et al., 2020). In another sediment study of Caviahue Lake, Argentina, affected by Copahue volcano fluids, cadmium values were below the detection limit (Cabrera et al., 2015).

As for the Cd content in the edible portion of onion (0.0188-0.030 mg/kg) it was comparable to another variety of New Zealand onion with reported values of 0.007- 0.05 mg/kg (Cavanagh et al., 2019). In addition and according to the laws consulted, the samples were found in all cases below the established limits of the cadmium content (0.1 mg/kg for the European Union, Australia, Codex Alimentarius and 0.03 mg/kg for Russia).

Table 3. Quality criteria of the soil and vegetables. Adapted from Diaz. (2014).

Metal	Soil MAE [mg/Kg]	Food products [mg/kg]						
		UE	Australian law	Brazilean law	Codex Alimentarius	Finland	Russia	Soth Africa
Cd	0.5	0.1	0.1	1	0.1		0.03	0.05
		Root vegetables, tubers and yound stems	Leaf/ Root vegetables and tubers	Other food except juices, alcoholic drinks, and fishing products	Stem and root vegetables	-	Vegetables/ fruits	Fruits and vegetables
Co	10	-	-	-	-	-	-	-
Cu	30	-	-	5	-	10	-	5
				Fresh		Vegetables		Juices of vegetables, fruits and nectars
Ni	20	-	-	5	-	-	-	-
				Other food except juices, alcoholic drinks and hidrogenated products				
Pb	25	0.3	0.1	0.5	0.1	1	0.5	0.1
		Vegetables	Vegetables (except Brassica)	Vegetables	Roots and tubers tubérculos	Potato, cucumber, natsudaidai (Pulp), peach, strawberry and grape.	Vegetables/ fruits	Fruits and other vegetables
Zn	60	-	-	-	-	-	-	5
								Juices of vegetables, fruits and nectars
Fe, K, Mg, Mn, Sr		-	-	-	-	-	-	-

The lead content (total 0.64-1.28 mg/kg and bioavailable 0.25-0.29 mg/kg) for the soil did not exceed 25 mg/kg, remaining within the environmental quality standards established in accordance with the MAE, and below those found by Arnalds et al. (2007) for Italian volcanic soils that report values up to 3.420 mg/kg. In addition, the Pb content in onion (0.040-0.058 mg/kg) in all cases was lower than the limits established under the legislation consulted (0.3 mg/kg for the European Union, and 0.1 mg/kg for Australia, Codex Alimentarius and South Africa).

Table 4. Soil metal content and edible tissue of *Allium fistulosum L.*

Metal	Soil content (mg/kg)		Content in edible tissue of *Allium fistulosum L.* (mg/kg)
	Total	Bioavailable	
Cd	0.09 -0.13	0.0218 – 0.049	0.0188 – 0.030
Pb	0.64 – 1.28	0.25 – 0.29	0.040-0.058
Ni	13.9-18.6	0.9-1.8	5.1-6.9
Co	5.8-9.0	0.22-0.34	0.085-0.12
Sr	7.4-19.5	0.83-1.24	0.84-0.95
Cu	14.8-21.6	4.8-6.2	0.44-0.61
Zn	72.5-88.7	4.4-7.0	5.0-6.16
K	95-601	58-148	652-829
Mg	1217-3217	84-96	128-147
Fe	6462-7850	246-289	8.6-10.3
Mn	55-73	6.7-8.3	1.43-1.61

As for the nickel content (total 13.9-18.6 mg/kg and bioavailable 0.9-1.8 mg/kg) the soil did not exceed 20 mg/kg, remaining within the environmental quality standards established according to the MAE, being lower than those found by Arnalds et al. (2007) for Italian volcanic soils with values up to 101 mg/kg. Moreover, the values obtained (5.1 to 6.9 mg/kg) for the Ni content in the edible tissue of onion were above the established limits, in accordance with the legislation consulted (5 mg/kg for Brazil); however, it should be emphasized that the categorization is not specific to the onion.

The cobalt content (total 5.8-9.0 mg/kg and bioavailable 0.22-0.34 mg/kg) in soil did not exceed 10 mg/kg, remaining within the environmental quality standards established in accordance with the MAE, and it was consistent with the cobalt content reported for European volcanic soils with a maximum of 33 mg/kg (Arnalds et al., 2007) and agricultural soils on the São Miguel island, with average values from 1.66 to 13.9 mg/kg (Linhares et al., 2019). As for the content of Co in the edible portion of the onion, between 0.085 and 0.12 mg/kg was found (the legislation consulted does not indicate Co limit values).

In relation to the strontium content in soil (total 7.4-19.5 mg/kg and bioavailable 0.83-1.24 mg/kg) and in onion (0.84-0.95 mg/kg), no comparison was found with any legislation; however, higher values have been reported in other works, e.g. study of strontium accumulation by native plants grown on Gumuskoy mining soils, and values between 22.60 and 691.80 mg/kg were reported in soils and mean levels of Sr were 163.65 and 163.93 mg/kg for roots and shoots, respectively of the plants studied (Sasmaz and Sasmaz, 2017), and also, in Volcanic Minerals in Chaco Canyon, New Mexico with maximum values of 254 mg/kg (Tankersley et al., 2018).

The copper content (total 14.8-21.6 mg/kg and bioavailable 4.8-6.2 mg/kg) in soils did not exceed 30 mg/kg, being within environmental quality standards according to the MAE and below those reported for Italian volcanic soils with values up to 565 mg/kg (Arnalds et al., 2007); however, as a nutrient it was found at very high levels (>5 mg/kg). Moreover, the content of Cu in onion (0.44 to 0.61

mg/kg) was low, being below the established limits, in accordance with the legislation consulted (5 mg/kg for Brazil and South Africa, and 10 mg/kg for Finland).

The total zinc content obtained (72.5-88.7 mg/kg) exceeded 60 mg/kg, being outside the environmental quality standards according to the MAE; although the bioavailable fraction (4.4-7.0 mg/kg) is below that limit and below those reported for Italian volcanic soils with values of up to 2.550 mg/kg (Arnalds et al., 2007). As a nutrient, it is at very high levels (>20 mg/kg), and its bioavailability goes from average (2-5 mg/kg) to high (5-20 mg/kg). Moreover, the content of Zn in onion (5.0-6.16 mg/kg) was found above the reference value (5 mg/kg in accordance with South African legislation) for vegetable, fruit and nectar juices. No reference values of onion or some other vegetables were found.

Potassium content (total 95-601 mg/kg and bioavailable 58-148 mg/kg) in soils was very high as a nutrient; however, although there are no environmental rules regulating its content, it is below what is reported in other works; for example, there are values of up to 3,500 mg/kg of potassium in soils in an industrial location in Italy (Cortis et al., 2016). As for the content of onion, it resulted between 652 and 829 mg/kg. Importantly, the recommended potassium intake is between 90-120 mmol/day in adults to reduce blood pressure and the risk of cardiovascular disease, stroke and coronary heart disease in adults (WHO, 2012).

Magnesium content (total 1217-3217 mg/kg and bioavailable 84-96 mg/kg) in soils was high, resulting in very high bioavailability levels (>8 cmol/kg); although there are no regulations that restrict its content. Average Mg values of 29,052 mg/kg have been reported in Lake Texcoco sediments (Sedeño-Díaz et al., 2020). While the magnesium content in onion was between 128 and 147 mg/kg, the recommended daily intake for magnesium is varied, depending on age and sex with values between 30 and 420 mg to regulate muscle function, protein formation, bone growth, and others (NIH, 2016).
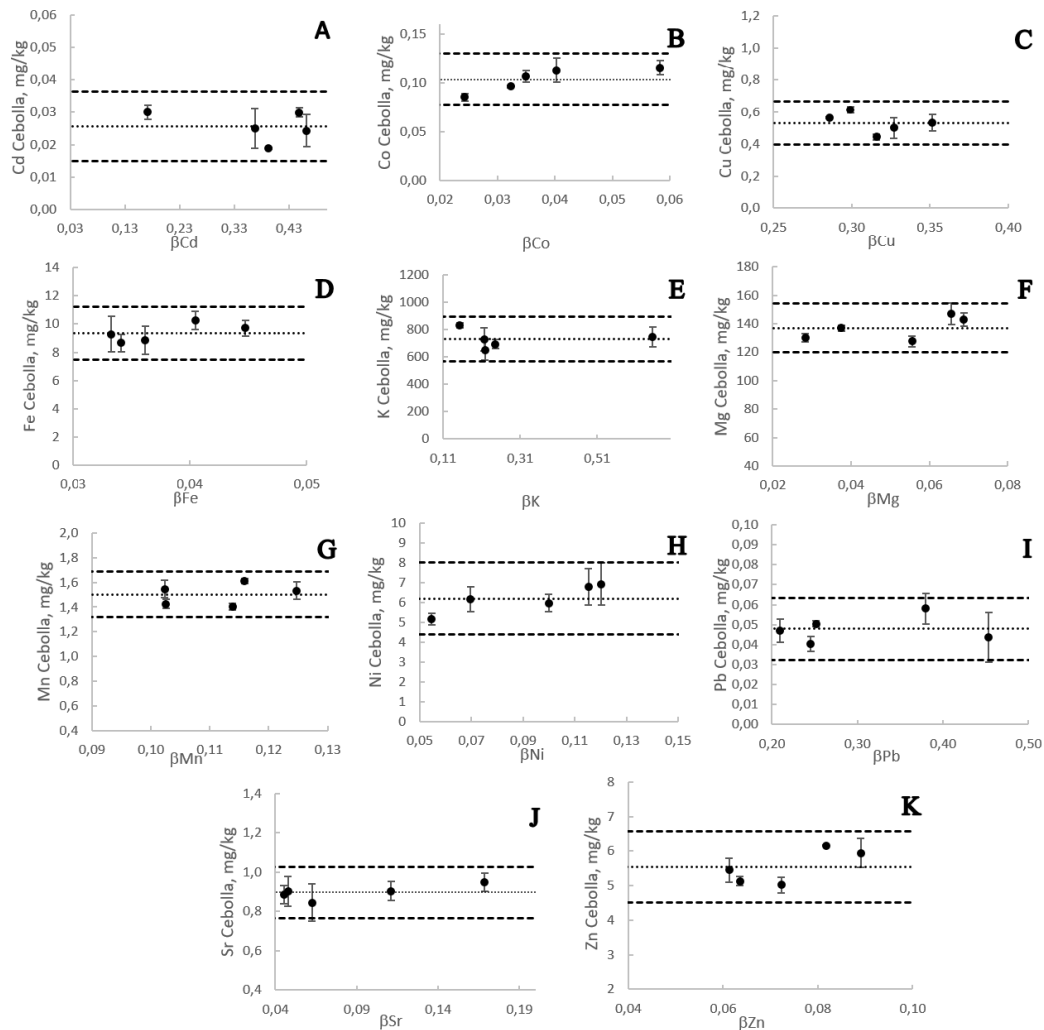
Scientific paper / Artículo científico
Soil sciences

Briceño, J., Tonato, E., Silva, M., Paredes, M. and Armado, A.

Figure 2. Metal absorption by onion based on the bioavailable fraction in the soil.

The iron content (total 6 462-7 850 mg/kg and bioavailable 246-289 mg/kg) in the soil as a nutrient was very high (>200 mg/kg), however, these high concentrations are common in most agricultural soils, without this representing negative effects. As an example, studies may be cited in sediments from a lake in Mexico (averages of 14 428 mg/kg) and in soils close to an industrial area in Italy with up to 3 200 mg/kg (Cortis et al., 2016). While the iron content in onion was found from 8.6 to 10.3 mg/kg, above reported values of 0.84 to 2.47 (Vilanova et al., 2008) and within those reported by Bello et al. (2013) up to 40 mg/kg in the estimated bulb with 90 % of humidity.

The manganese content (total 55-73 mg/kg and bioavailable 6.7-8.3 mg/kg) as a nutrient in the soil is considered high (50-100 mg/kg), although its bioavailability was low (2-10 mg/kg). These values are lower than those reported by Linhares et al. (2019) for agricultural soils in six volcanic areas of the island of São Miguel (1 782.50 ± 108.98). While the manganese content in onion was found between 1.43 and 1.61 mg/kg. No legislation was found to regulate manganese content in soils or food. For most of the metals studied, it was observed that they were within the maximum values set out in the standards consulted, aligned with the results obtained in a study of metals in pineapple and pitahaya grown in the vicinity of the Masaya volcano in Ni-

caragua.

3.4 Bioavailability factor, β

Figure 2 shows the influence of the bioavailable fraction of the metal in the soil on the absorption of the metal by onion. The fine dashed line represents the average of the obtained metal values in onion and in the environment; the thick dashed lines represent the upper and lower limits determined as the average 1.96 (corresponding to the z value for 95 % confidence) times the standard deviation.

The absorption of metal in the onion samples analyzed had an independent correlation of the bioavailable fraction in the soil, and in all cases it was lower than the total concentration of the same metal in the soil. This behavior observed in Figure 2 shows that onion is not a metal-accumulating plant since it exclusively absorbs necessary amounts of its nutrients from the soil. Unlike other plants such as *Brassica napus* that has been investigated its role in the recovery of soils contaminated with metals and Diesel by rhizoremediation (Lacalle et al., 2018) or vetiver (Vetiveria zizanioides) which is used for phytoremediation for its metal bioaccumulation properties (Chen et al., 2004; Almeida et al., 2019; Shabbir et al., 2019). Possibly these results could be because onion is short-cycle, which limits its exposure to metals for extended periods. It has been mentioned that plants absorb metals to varying degrees, depending on the plant species and metal exposure (Intawongse and Dean, 2006; Khan et al., 2015).

4 Conclusions

The studied soil collected in an area affected by the ashes of Tungurahua volcano was strongly acidic, with negligible salinity effect and low organic matter content. The content of potentially polluting metals (cadmium, lead, nickel, strontium and cobalt), in soil and onion of the Quero canton, is below the regulations consulted. The content of nutrient metals (potassium, manganese, magnesium, iron, copper and zinc) was found at adequate levels, in no case deficiency was found.

The bioavailability of metals in soils near the Tungurahua volcano allowed to determine that the intake of metal by onion was independent of the bioavailable fraction of metal in the soil for all metals studied.

Acknowledgement

References

Almeida, A., Ribeiro, C., Carvalho, F., Durao, A., Bugajski, P., Kurek, K., Pochwatka, P., and Jóźwiakowski, K. (2019). Phytoremediation potential of vetiveria zizanioides and oryza sativa to nitrate and organic substance removal in vertical flow constructed wetland systems. *Ecological Engineering*, 138:19–27. Online:https://bit.ly/3gICrYg.

AOAC (2006). Official methods of analysis proximate analysis and calculations moisture (m) fruits, vegetables, and their products - item 107. In *Association of Analytical Communities*, volume Reference data: Method 934.06 (37.1.10); NFNAP; WATER.

Arnalds, Ó., Bartoli, F., Buurman, P., García-Rodeja, E., Óskarsson, H., and Stoops, G. (2007). *Soils of volcanic regions in Europe*.

Battaglia, J., Hidalgo, S., Bernard, B., Steele, A., Arellano, S., and Acuña, K. (2019). Autopsy of an eruptive phase of tungurahua volcano (ecuador) through coupling of seismo-acoustic and so2 recordings with ash characteristics. *Earth and Planetary Science Letters*, 511:223–232. Online:https://bit.ly/2W7wKLF.

Bello, M., Olabanji, I., Abdul-Hammed, M., and Okunade, T. (2013). Characterization of domestic onion wastes and bulb (allium cepa l.): fatty acids and metal contents. *International Food Research Journal*, 20(5):2153–2158. Online:https://bit.ly/3fhgwqJ.

Scientific paper / Artículo científico

Soil sciences

Briceño, J., Tonato, E., Silva, M., Paredes, M. and Armado, A.

Bornø, M., Müller-Stöver, D., and Liu, F. (2019). Biochar properties and soil type drive the uptake of macro-and micronutrients in maize (zea mays l.). *Journal of Plant Nutrition and Soil Science*, 182(2):149–158. Online:https://bit.ly/2ZWJcPt.

Bravo Realpe, I., Arboleda Pardo, C. A., and Martín Peinado, F. J. (2014). Efecto de la calidad de la materia orgánica asociada con el uso y manejo de suelos en la retención de cadmio en sistemas altoandinos de colombia. *Acta Agronómica*, 63(2):1–14. Online:https://bit.ly/3gNvR2Q.

Cabrera, J., Temporetti, P., and Pedrozo, F. (2015). Trace metal partitioning and potential mobility in th e naturally acidic sediment of lake caviahue, neuquén, argentina. *Revista Clínica Las Condes*, 26(2):217–222. Online:https://bit.ly/3g4YSpT.

Cargua Catagña, F., Rodríguez Llerena, M., Damián Carrión, D., Recalde Moreno, C., and Santillán Lima, G. (2017). Analytical methods comparison for soil organic carbon determination in andean forest of sangay national park-ecuador. *Acta Agronómica*, 66(3):408–413. Online:https://bit.ly/321hjIN.

Cavanagh, J. A. E., Yi, Z., Gray, C. W., Munir, K., Lehto, N., and Robinson, B. H. (2019). Cadmium uptake by onions, lettuce and spinach in new zealand: Implications for management to meet regulatory limits. *Science of the total Environment*, 668:780–789. Online:https://bit.ly/3iO1vip.

Chen, Y., Shen, Z., and Li, X. (2004). The use of vetiver grass (vetiveria zizanioides) in the phytoremediation of soils contaminated with heavy metals. *Applied Geochemistry*, 19(10):1553–1565. Online:https://bit.ly/3fiLQpf.

Choumert-Nkolo, J. and Phélinas, P. (2019). Natural disasters, land and labour. *European Review of Agricultural Economics*, 47(1):296–323. Online:https://bit.ly/2CnRiso.

Cortis, P., Vannini, C., Cogoni, A., De Mattia, F., Bracale, M., Mezzasalma, V., and Labra, M. (2016). Chemical, molecular, and proteomic analyses of moss bag biomonitoring in a petrochemical area of sardinia (italy). *Environmental Science and Pollution Research*, 23(3):2288–2300. Online:https://bit.ly/2W9MQUS.

Diaz., A. (2014). Metales pesados. Technical report, Secretaria de Estado de Comercio, Valencia.

Faithfull, N. T., T, N., and Ferrando Navarro, A. C. (2005). Métodos análisis quiímico agriícola: manual praáctico. acribia. Accessed: 19 August 2019.

Golia, E. E., Dimirkou, A., and Mitsios, I. K. (2008). Influence of some soil parameters on heavy metals accumulation by vegetables grown in agricultural soils of different soil orders. *Bulletin of environmental contamination and toxicology*, 81(1):80–84.

Intawongse, M. and Dean, J. R. (2006). Uptake of heavy metals by vegetable plants grown on contaminated soil and their bioavailability in the human gastrointestinal tract. *Food additives and contaminants*, 23(1):36–48. Online:https://bit.ly/302bpnT.

Kabata-Pendias, A. (2004). Soil-plant transfer of trace elements—an environmental issue. *Geoderma*, 122(2-4):143–149. Online:https://www.sciencedirect.com/science/article/abs/pii/S0016706104000084.

Kabata-Pendias, A. and Sadurski, W. (2004). Trace elements and compounds in soil. *Elements and their compounds in the environment: Occurrence, analysis and biological relevance*, pages 79–99. Online:https://bit.ly/3iRFZcB.

Kazlauskaitė-Jadzevičė, A., Volungevičius, J., Gregorauskienė, V., and Marcinkonis, S. (2014). The role of ph in heavy metal contamination of urban soil. *Journal of Environmental Engineering and Landscape Management*, 22(4):311–318. Online:https://bit.ly/2DvLcXj.

Khan, A., Khan, S., Khan, M., Aamir, M., Ullah, H., Nawab, J., Rehman, I., and Shah, J. (2019). Heavy metals effects on plant growth and dietary intake of trace metals in vegetables cultivated in contaminated soil. *International journal of Environmental Science and Technology*, 16(5):2295–2304. Online:https://bit.ly/38VdQgk.

Khan, A., Khan, S., Khan, M. A., Qamar, Z., and Waqas, M. (2015). The uptake and bioaccumulation of heavy metals by food plants, their effects on plants nutrients, and associated health risk: a review. *Environmental Science and Pollution Research*, 22(18):13772–13799. Online:https://bit.ly/327Vmrx.

Lacalle, R., Gómez-Sagasti, M. T., Artetxe, U., Garbisu, C., and Becerril, J. M. (2018). Brassica napus has a key role in the recovery of the health of soils contaminated with metals and diesel by rhizoremediation. *Science of The Total Environment*, 618:347–356. Online:https://bit.ly/2WrshUr.

Linhares, D., Pimentel, A., Borges, C., Cruz, J., Garcia, P., and dos Santos Rodrigues, A. (2019). Cobalt distribution in the soils of são miguel island (azores): From volcanoes to health effects. *Science of The Total Environment*, 684:715–721. Online:https://bit.ly/2Zih2iP.

Mitra, J.and Shrivastava, S. and Rao, P. S. (2012). Onion dehydration: a review. *Journal of food science and technology*, 49(3):267–277. Online:https://bit.ly/38Mbpwg.

NIH (2016). ¿Qué es el magnesio? ¿Para qué sirve? Online: https://bit.ly/3ausdZH.

Park, J., Choppala, G. k., Bolan, N., Chung, J. W., and Chuasavathi, T. (2011). Biochar reduces the bioavailability and phytotoxicity of heavy metals. *Plant and soil*, 348(1-2. Online:https://bit.ly/3fjXbVW):439.

Rai, P.and Lee, S. S., Zhang, M., Tsang, Y. F., and Kim, K. (2019). Heavy metals in food crops: Health risks, fate, mechanisms, and management. *Environment International*, 125:365–385. Online:https://bit.ly/3iQAWcq.

Rieuwerts, J. S. (2007). The mobility and bioavailability of trace metals in tropical soils: a review. *Chemical Speciation and Bioavailability*, 19(2):75–85. Online:https://bit.ly/3frUzWk.

Sasmaz, M. and Sasmaz, A. (2017). The accumulation of strontium by native plants grown on gumuskoy mining soils. *Journal of Geochemical Exploration*, 181:236–242. Online:https://bit.ly/2ZkvYwP.

Sedeño-Díaz, J. E., López-López, E., Mendoza-Martínez, E., Rodríguez-Romero, A. J., and Morales-García, S. S. (2020). Distribution coefficient and metal pollution index in water and sediments: Proposal of a new index for ecological risk assessment of metals. *Water*, 12(1):29. Online:https://bit.ly/3ei4Brr.

SEMARNAT (2003). Acuerdo que establece las reglas de operación para el otorgamiento de pagos del programa de servicios ambientales hidrológicos. viernes, 3, 6-23. sgr. (2014). programa de prevención y mitigación para reducir el riesgo por diferentes amenazas. Technical report, Secretaría de Medio Ambiente y Recursos Naturales.

Shabbir, A., Khan, M., Ahmad, B., Sadiq, Y., Jaleel, H., and Uddin, M. (2019). Vetiveria zizanioides (l.) nash: A magic bullet to attenuate the prevailing health hazards. In *Plant and Human Health, Volume 2*, pages 99–120. Online:https://bit.ly/2ZUdlic. Springer.

Sungur, A., Soylak, M., and Ozcan, H. (2014). Investigation of heavy metal mobility and availability by the bcr sequential extraction procedure: relationship between soil properties and heavy metals availability. *Chemical Speciation and Bioavailability*, 26(4):219–230. Online:https://bit.ly/3020RFp.

Tangahu, B. V., Sheikh Abdullah, S. R., Basri, H., Idris, M., Anuar, N., and Mukhlisin, M. (2011). A review on heavy metals (as, pb, and hg) uptake by plants through phytoremediation. *International Journal of Chemical Engineering*, 2011. Online:https://bit.ly/3fqux5C.

Tankersley, K. B., Huff, W. D., Dunning, N. P., Owen, L. A., and Scarborough, V. L. (2018). Volcanic minerals in chaco canyon, new mexico and their archaeological significance. *Journal of Archaeological Science: Reports*, 17:404–421. Online:https://bit.ly/2AP6RJ2. 17(November 2017).

Tóth, G., Hermann, T., Da Silva, M. R., and Montanarella, L. (2016). Heavy metals in agricultural soils of the european union with implications for food safety. *Environment international*, 88:299–309. Online:https://bit.ly/3ekqQNE.

Vilanova, M., Zamuz, S., Tardáguila, J., and Masa, A. (2008). Descriptive analysis of wines from vitis vinifera cv. albariño. *Journal of the Science of Food and Agriculture*, 88(5):819–823. Online:https://bit.ly/3elNQfd.

WHO (2012). Guideline: Potassium intake for adults and children. Technical report, World Health Organization.

Point of view/ Punto de vista

EPIDEMIOLOGY

ABYA YALA | UNIVERSIDAD POLITÉCNICA SALESIANA

CORONAVIRUS IN ECUADOR: AN OPINION FROM THE ACADEMIA

CORONAVIRUS EN ECUADOR: UNA OPINIÓN DESDE LA ACADEMIA

Santiago Guerrero[iD]

Genetic and Genomic Research Center, Medicine Faculty, Eugenio Espejo, Universidad UTE. Av. Mariscal Sucre and Av. Mariana de Jesús, Building I, 2nd floor, 170129 Quito, Ecuador

*Corresponding author: sxguerrero@gmail.com

Abstract

This is the third time that a zoonotic coronavirus has infected various human populations. This new virus, classified as SARS-CoV-2 (*severe acute respiratory syndrome coronavirus 2*), is the causative agent of the new pandemic outbreak called COVID-19 (*coronavirus disease 2019*). The international research carried out around this new outbreak was so effective that shortly thereafter the genome of the virus, its biology and its main epidemiological aspects were determined. To date, 1962 positive cases of SARS-CoV-2 have been reported in Ecuador, situation that has caused great concern among Ecuadorian academics and society. Thus, in this opinion article, the main research carried out internationally on the SARS-CoV-2 will be detailed, the importance of the Academia in healthcare decision-making will be discussed and the role of fundamental research to hold a possible outbreak in Ecuador will be mentioned.
Keywords: coronavirus, SARS-CoV-2, COVID-19, Ecuador.

Resumen

Esta es la tercera vez que un coronavirus zoonótico ha podido infectar diversas poblaciones humanas. Este nuevo virus, clasificado como SARS-CoV-2 (*severe acute respiratory syndrome coronavirus 2*), es el agente causal de la epidemia denominada COVID-19 (*coronavirus disease 2019*). La investigación internacional realizada en torno a este nuevo brote fue tan eficaz que en poco tiempo ya se conocía el genoma del virus, su biología y sus principales aspectos epidemiológicos. En Ecuador se han reportado hasta la fecha 1962 casos positivos de SARS-CoV-2, situación que generó una gran preocupación por parte de la sociedad y la Academia ecuatoriana. Por lo tanto, en este artículo de opinión se detallarán las principales investigaciones realizadas sobre el SARS-CoV-2 a nivel internacional, se discutirá sobre la importancia de la Academia en la toma de decisiones sanitarias y se pondrá en perspectiva el papel de la investigación fundamental para la contención de un posible brote en Ecuador.
Palabras clave: coronavirus, SARS-CoV-2, COVID-19, Ecuador.

Orcid ID:

Santiago Guerrero: https://orcid.org/0000-0003-3473-7214

1   Introducción

"Another Decade, another Coronavirus" is the heading of the editorial published by Stanley Perlman in the prestigious journal "The New England Journal of Medicine". Indeed, this is the third time that a zoonotic coronavirus has infected various human populations. Like SARS-CoV (*severe acute respiratory syndrome coronavirus*) in 2002-2003 and MERS-CoV (*Middle East respiratory syndrome coronavirus*) in 2012, this new virus, called SARS-CoV-2 (*severe acute respiratory syndrome coronavirus 2*) was also transmitted from animals to humans (Perlman, 2020).

Coronaviruses can cause viral upper respiratory tract infections (URTIs) in a wide variety of domestic and wild animals, as well as in humans. These viruses were not considered highly pathogenic to humans until the SARS-CoV outbreak occurred in Guangdong Province, China. Coronaviruses circulating before this outbreak only caused mild infections in immunocompromised people. Ten years after SARS-CoV, another highly pathogenic zoonotic coronavirus (MERS-CoV) emerged in Middle Eastern countries. The latter was transmitted directly from camels to humans, while SARS-CoV was transmitted from civets sold in markets; both viruses are believed to have originated in bats (Perlman, 2020).

There are currently more than 200 serologically different viral types that cause URTIs. The symptoms of URTIs depend on the nature of the virus, but it is mostly affected by the age, physiological state and immune response of the host. Thus, depending on these factors, URTIs can go unnoticed (asymptomatic) until death. The main agents that cause URTIs in humans are rhinoviruses ($30-50\%$ of cases), followed by coronaviruses ($10-15\%$), influenza viruses ($5-10\%$) and other lower-incidence viruses such as adenovirus, human respiratory syncytial virus, among others (Eccles, 2005).

The great viral diversity makes it difficult to detect URTIs and develop diagnostic methods at the time of a new outbreak. For example, the SARS-CoV outbreak appeared in November 2002 but it was not until April 2003 that the virus genome was identified thanks to an international collaboration of 13 laboratories from 10 countries (Cui et al., 2019). Once the genome of the virus has been determined, the real-time RT-PCR (real time *reverse transcription polymerase chain reaction*) is used to amplify a specific region of the virus and identify it at the molecular level.

The molecular identification of the virus and the study of its biology and epidemiology is of great importance to stop an outbreak as well as for drug development and public health policies aimed at preventing the spread of this type of virus. Hence, this opinion article will detail the main research carried out on SARS-CoV-2 at the international level, discuss the importance of the Academia in health decision-making and put into perspective the role of main research to the containment of a possible outbreak in Ecuador.

2   SARS-CoV-2: identification, epidemiology and treatment

SARS-CoV-2 is the causative agent of the new outbreak called COVID-19 (*coronavirus disease 2019*) originated in Wuhan, China. The first cases were reported at the end of December 2019 by Chinese authorities to the World Health Organization (WHO). Research to determine the causative agent of COVID-19 was so thorough that, by January 7, 2020, scientists at the Shanghai Clinical Center for Public Health, associated with Fudan University, identified the pathogen responsible for COVID-19 and it was genomically characterized (Liu et al., 2020).

The genetic sequence of SARS-CoV-2, shared with the public through the GISAID initiative (*Global Initiative on Sharing All Influenza Data*), enabled the rapid development of diagnostic tests using the real time RT-PCR technique worldwide. Thus, by 17 January 2020, scientists from Charité University in Berlin shared the detection protocol with WHO and made positive controls available worldwide through the *Global European Virus Archive* (EVAg). Subsequently, scientists from Hong Kong, Japan, China, Thailand and the United States, associated with universities and public institutes, shared their screening protocols to WHO from January 23 to January 28, 2020 (Corman et al., 2020b). Currently, 133 partial or complete sequences of the virus are now available at the GenBank (https://www.ncbi.nlm.nih.gov/genbank/).

At the clinical-epidemiological level, the largest study published to date conducted by the China CDC (*Chinese Center for Disease Control and Prevention*), analyzed 72 314 patient records: 44 672 (61,8 %) confirmed cases, 16 186 (22,4 %) suspected cases, 10 567 (14,6 %) clinically diagnosed cases and 889 asymptomatic cases (1,2 %). Among confirmed cases, 1 023 died resulting in a mortality rate of 2,3 %. Although the mortality rate is low, it increases to 8 % in individuals aged 70-79 years and to 14 % in patients over 80 years old; these patients also had pre-existing conditions, such as hypertension, cardiovascular disease and diabetes. In addition, this study found that 80,9 % of infections are classified as mild, 13,8 % as severe, and only 4,7 % as critical. With respect to previous outbreaks, SARS-CoV infected 8 096 individuals in 29 countries, killing 774 people (mortality rate: 9,6 %), while MERS-CoV infected 2 494 people in 27 countries, causing 858 victims (mortality rate: 34,4 %) (Huang et al., 2020; Liu et al., 2020).

Currently, several institutes and research centers along with biotech companies are developing possible vaccines against SARS-CoV-2. Research in this field also advanced in leaps and bounds. In this way, just weeks after the publication of the SARS-CoV-2 genome, scientists associated with the National Institute of Allergy and Infectious Diseases (USA) and the University of Texas managed to solve the glycoprotein S structure of this virus. This protein is involved in the entry of the virus into the host cells and its structure is key to the development of vaccines, therapeutic antibodies and diagnostic methods (Wrapp et al., 2020).

Another strategy to fight the virus is to use developed antivirals to treat other infections. In this regard, Jinyintan Hospital in Wuhan is conducting a randomized controlled trial to treat patients diagnosed with COVID-19. This trial aims to test the effectiveness of a combination of lopinavir and ritonavir, medicines already used to treat HIV (Huang et al., 2020). These compounds inhibit protease, an enzyme used by both HIV and coronaviruses for the processing of new viral particles. Previously, in 2004, a study showed that such combination may have a positive clinical effect in patients infected with a strain similar to SARS-CoV-2. However, the study did not randomize patients to receive the combina-

tion or a placebo, which is a priority for a controlled trial. In addition, two other trials are ongoing to test the efficacy of remdesivir in 760 people with COVID-19 in China. This compound showed great efficacy against several coronaviruses *in vitro* and *in vivo*, including SARS-CoV and MERS-CoV (Cohen, 2020). Currently, China has more than 80 clinical trials running or pending on possible treatments for COVID-19 (Maxmen, 2020).

3 Situation in Ecuador

1962 positive cases of SARS-CoV-2 and 62 deaths have been reported to date in Ecuador (30-march-2020). During the first days of the epidemic, Ecuador's Ministry of Public Health (MSP) announced on January 26, 2020 the presence of a suspected case of COVID-19. It was a 49-year-old Chinese citizen with the symptomatology associated with this disease: high temperature ($39°C$), cough with greenish phlegm, chest pain and signs of severe renal and respiratory failure (Figure 1) (MSP, Ministerio de Salud Pública del Ecuador, 2020).

To diagnose the case, the MSP sent the samples for their analysis to the *Centers for Disease Control and Prevention* (CDC) located in Atlanta, USA. According to official reports issued on January 29 and February 1, 2020, Ecuador had not yet received the results of the CDC; however, it was not until February 4 that the MSP ruled out the presence of SARS-CoV-2 based on the results presented by the CDC. Finally, the Chinese citizen died on 7 February presenting symptoms of hepatitis B and pneumonia (Figure 1) (MSP, Ministerio de Salud Pública del Ecuador, 2020). While waiting for the results by the CDC, the MSP also announced that the *National Institute of Public Health Research* (INSPI) has the necessary reagents for the identification of future suspected cases (Figure 1). This institute has the National Influenza and Other Respiratory Viruses Reference Center, a WHO-accredited organization for testing possible cases of SARS-CoV-2 (MSP, Ministerio de Salud Pública del Ecuador, 2020).

Weeks later, on February 29, 2020, the MSP reported the first case of COVID-19 (Figure 1). She was an Ecuadorian citizen residing in Spain who entered the country on February 14 from José Joaquín de Olmedo Airport. Subsequently, out of the

177 citizens who were in the epidemiological area with respect to the first case, 1962 have tested positive for SARS-CoV-2 (MSP, Ministerio de Salud Pública del Ecuador, 2020). Worthy of note, diagnosis of the first case ocurred 5 days after admission to the hospital and 13 days after arrival to Ecuador (MSP, Ministerio de Salud Pública del Ecuador, 2020).
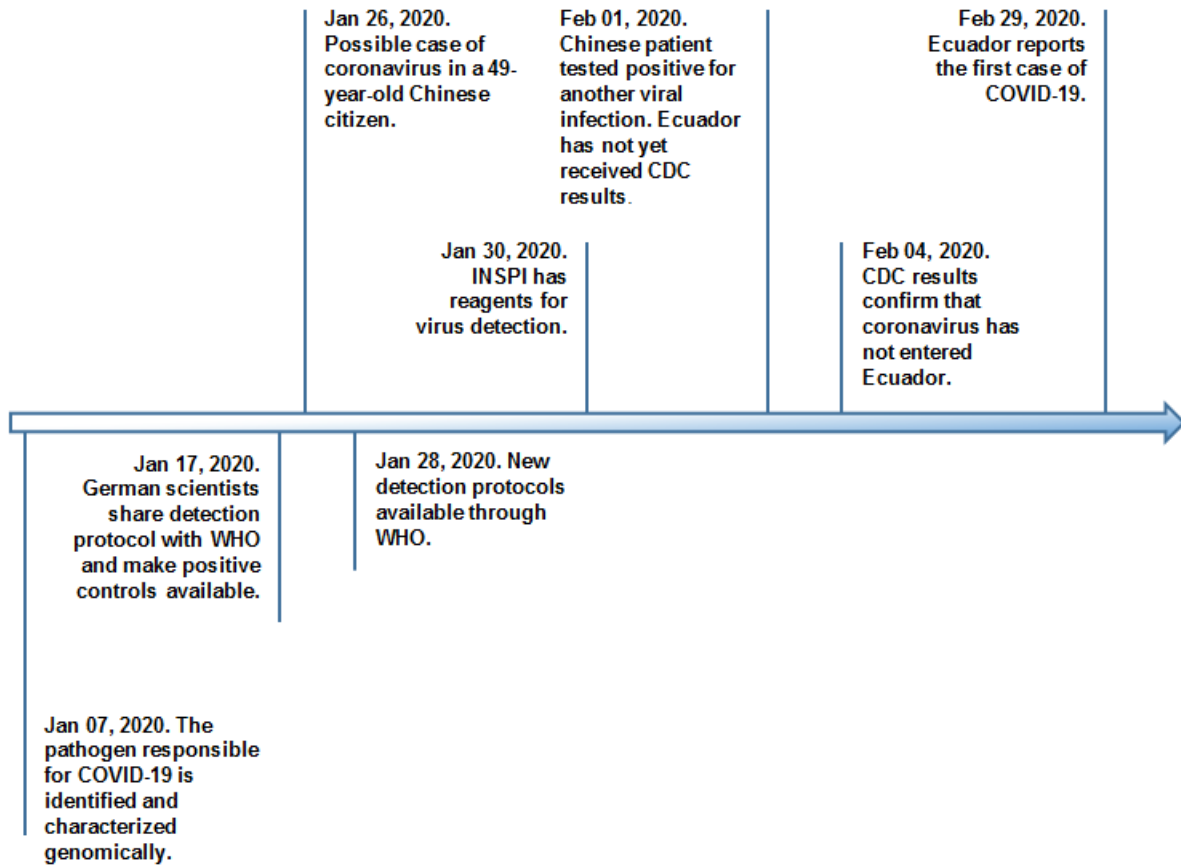
Jan 26, 2020. Possible case of coronavirus in a 49-year-old Chinese citizen.

Feb 01, 2020. Chinese patient tested positive for another viral infection. Ecuador has not yet received CDC results.

Feb 29, 2020. Ecuador reports the first case of COVID-19.

Jan 30, 2020. INSPI has reagents for virus detection.

Feb 04, 2020. CDC results confirm that coronavirus has not entered Ecuador.

Jan 17, 2020. German scientists share detection protocol with WHO and make positive controls available.

Jan 28, 2020. New detection protocols available through WHO.

Jan 07, 2020. The pathogen responsible for COVID-19 is identified and characterized genomically.

Figure 1. Main events occurring in Ecuador and internationally on the detection of SARS-CoV-2 in the early days of the epidemic.

4 Perspectives for Ecuador

International research on this new outbreak was so effective that in just months the causal agent of COVID-19 was discovered, its biology— highlighting its genome and the structure of glycoprotein S^- and its epidemiology. The research progressed to such an extent that there are 80 pending or running clinical trials on possible treatments for this disease. In addition, several institutes and research centers, in collaboration with the industry, are developing potential vaccines. This has been achieved in large terms by close collaboration between university research groups, public research centers and biotech companies.

In Ecuador, it is essential that the Academia, through its accredited institutions, e.g. *Academia Ecuatoriana de Ciencias* (AEC) or consolidated research groups, work closely with the State to generate fundamental and applied research in issues of national importance. In this way, Ecuador could generate a more effective response for an epidemic outbreak containment. This is supported by WHO recommendations for the formation of *Emergency Operations Centers* (EOCs) for health decision-making. EOCs, made up by several entities including the Academy, manage the response to a wide variety

of dangerous situations, such as natural disasters, chemical spills, outbreaks, etc (Balajee et al., 2017).

Unlike other countries, Ecuador has not published any scientific reports on the positive cases of SARS-CoV-2 circulating in the country. To generate an effective health response, it is essential that the MSP publish clinical cases of COVID-19 in specialized journals. Clinical case reports present the lowest evidence within the scale of scientific research and are considered as the first source of information at the medical level (Pineda-Leguízamo et al., 2018). Thus, based on these reports, primary care physicians will be able to better assess future suspected cases in Ecuador. In addition, the genetic identification of SARS-CoV-2 types present in Ecuador will help to implement containment protocols more effectively, because the virus evolved into two types: L and S, called based on their genetic variants. The L type is more aggressive and it transmits faster than S (Tang et al., 2020). In Ecuador, it is still unknown which strain infected patients diagnosed with COVID-19. At the international level, this type of research has been carried out thanks to close collaboration between the Academia and the State.

On the other hand, Ecuador is home to a surprising number of endemic species that inhabit a wide variety of ecosystems. With regard to bats, the main reservoir of coronaviruses, the Museum of Zoology of the Pontifical Catholic University of Ecuador (Pontificia Universidad Católica del Ecuador) has recorded 176 species of bats in the country (Brito et al., 2019). A study published in 2013, led by Christian Drosten, who published the German protocol for SARS-CoV-2 detection (Corman et al., 2020a), found a great diversity of coronavirus in neotropical bats sampled in Costa Rica, Panama, Ecuador and Brazil. However, out of 1 868 collected samples, only 62 (26 species represented) were obtained in Ecuador and no samples tested positive for coronavirus (Corman et al., 2013). This highlights the need to study the diversity of coronavirus in Ecuador to determine geographical areas that may be at high risk of zoonotic outbreaks. Indeed, the most effective way to prevent these outbreaks is to identify these areas and maintain the barriers between natural reservoirs and civilization.

To conduct this type of research, Ecuador needs a diversification of research groups that develop specific lines of study, such as coronaviruses or other zoonotic viruses. However, according to World Bank data (https://www.bancomundial.org/), Ecuador spends only 0,44 % of *gross domestic product* (GDP) in research. Other Latin American countries, such as Argentina and Brazil, allocate 0,53 % and 1,2 %, respectively. The difference is significant with more developed countries: China, 2,11 % and The United States 2,7 %. With adequate funding and focused on the country's research priorities, Ecuador will not only be able to cope with any zoonotic outbreak but also participate in international research.

References

Balajee, S., Pasi, O. G., Etoundi, A. M., Rzeszotarski, P., Do, T. T., Hennessee, I., and Mounts, A. W. (2017). Sustainable model for public health emergency operations centers for global settings. *Emerging Infectious Diseases*, 23(13):Online: https://bit.ly/2WRMOlI.

Brito, J., Camacho, M. A., Romero, V., and Vallejo, A. F. (2019). Mamíferos del ecuador. versión 2019.0. Museo de Zoología, Pontificia Universidad Católica del Ecuador (February 25, 2020). Online:https://bit.ly/2y5WrmA.

Cohen, J. (2020). Can an anti-hiv combination or other existing drugs outwit the new coronavirus? Science. Online: https://doi.org/10.1126/science.abb0659.

Corman, V., Bleicker, T., Brünink, S., Koopmans, M., Zambon, M., Peiris, M., and Drosten, C. (2020a). Diagnostic detection of 2019-ncov by real-time rt-pcr. resreport 2, Charité Virology, Berlin, Germany.

Corman, V., Landt, O., Kaiser, M., Molenkamp, R., Meijer, A., Chu, D., Bleicker, T., Brünink, S., Schneider, J., Schmidt, M. L., Mulders, D., Haagmans, B. L., Van der Veer, B., Van den Brink, S., Wijsman, L., Goderski, G., Romette, J. L., Ellis, J., Zambon, M., Peiris, M., and Drosten, C. (2020b). Detection of 2019 novel coronavirus (2019-ncov) by real-time rt-pcr. *Euro surveillance : bulletin Europeen sur les maladies transmissibles = European communicable disease bulletin*, 25(3):2000045. Online:https://bit.ly/39gJH9z.

Corman, V., Rasche, A., Diallo, T., Cottontail, V., Stoecker, A., Dominguez Souza, B., Corrêa, J., Carneiro, A., Franke, C., Nagy, M., Metz, M., Knörnschild, M., Kalko, E., Ghanem, S., Sibaja-Morales, K., Salsamendi, E., Spínola, R., Herrler, G., Voigt, C., and Drexler, J. (2013). Highly diversified coronaviruses in neotropical bats. *Journal of General Virology*, 94:1984–1994. Online:https://bit.ly/2wE42sg.

Cui, J., Li, F., and Shi, Z. L. (2019). Origin and evolution of pathogenic coronaviruses. *Nature Reviews Microbiology. Nature Publishing Group*, 17(3):181–192. Online:https://bit.ly/3aniJOW.

Eccles, R. (2005). Understanding the symptoms of the common cold and influenza. *Lancet Infectious Diseases*, 5(11):718–25. Online: https://bit.ly/2Uiilf8.

Huang, C., Wang, Y., Li, X., Ren, L., Zhao, J., Hu, Y., and Cao, B. (2020). Clinical features of patients infected with 2019 novel coronavirus in wuhan, china. *The Lancet*, 395(10223):497–506. Online: https://bit.ly/2y8T0eV.

Liu, Z., Bing, X., and Za Zhi, X. (2020). The epidemiological characteristics of an outbreak of 2019 novel coronavirus diseases (covid-19) in china. *Lancet*, 41(2):145–151. Online:https://doi.org/10.3760/cma.j.issn.0254--6450.2020.02.003.

Maxmen, A. (2020). More than 80 clinical trials launch to test coronavirus treatments. *Nature*, 578(7795):347–348. Online:https://bit.ly/3braEsM.

MSP, Ministerio de Salud Pública del Ecuador (2020). Comunicados oficales del ministerio de salud pública del ecuador.

Perlman, S. (2020). Editorial: Another decade, another coronavirus. *New England Journal of Medicine*, pages 1–2: Online:https://doi.org/10.1056/nejme2001126.

Pineda-Leguízamo, R., Miranda-Novales, G., and Villasis-Keever, M. (2018). La importancia de los reportes de casos clínicos en la investigación. *Revista Alergia México*, 65(1):92. Online:https://doi.org/10.29262/ram.v65i1.348.

Tang, X., Wu, C., Li, X., Song, Y., Yao, X., Wu, X., Duan, Y., Zhang, H., Wang, Y., Qian, Z., Cui, J., and Lu, J. (2020). On the origin and continuing evolution of SARS-CoV-2. *National Science Review*.

Wrapp, D., Wang, N., Corbett, K. S., Goldsmith, J. A., Hsieh, C.-L., Abiona, O., and McLellan, J. S. (2020). Cryo-em structure of the 2019-ncov spike in the prefusion conformation. *Science*, 367(6483):1260–1263. Online:https://bit.ly/2Ju8f4N.